Zeitschrift: IABSE reports = Rapports AIPC = IVBH Berichte
Band: 42 (1983)

Rubrik: Theme D1: Consequences of collision without means to their reduction

Theme D1

Consequences of Collision without Means to their Reduction

Conséquences de collisions en l'absence de dispositifs de protection

Folgen eines Zusammenstoßes ohne Vorbeugemaßnahmen

Leere Seite
Blank page
Page vide

Hydrodynamic Aspects of Ships Colliding with Fixed Structures

Aspects hydrodynamiques de la collision de navires avec des structures fixes

Hydrodynamische Aspekte bei Schiffskollisionen mit stationären Objekten

J. J. BLOK
Naval Architect
Netherlands Ship Model Basin
Wageningen, the Netherlands

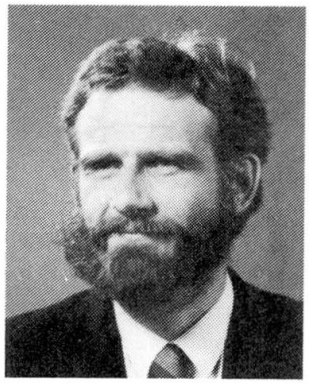

Jan J. Blok, born in 1947, received his masters degree in naval architecture from the Technical University Delft. He joined the staff of the Ocean Engineering Division of the Netherlands Ship Model Basin as a project manager and holds responsibility for experimental and computational projects.

J. N. DEKKER
Civil Engineer
Netherlands Ship Model Basin
Wageningen, the Netherlands

Jaap N. Dekker, born in 1943, got his masters degree in civil engineering at the Technical University Delft. After four years' work on a university laboratory he joined the staff of the Ocean Engineering Division of the Netherlands Ship Model Basin as project manager and is responsible for experimental and computational projects.

SUMMARY

A ship impact against an elastic structure carries a certain added mass of water with it, the quantification of which is crucial in the design. The magnitude of this hydrodynamic added mass is influenced by: vessel size, shape, draught, underkeel clearance, spring characteristic of the obstacle and collision mode. The paper describes a series of experiments to study the added mass during impact. Results are of interest to ship-to-ship collisions and to fender design. The resulting added mass values appear to be higher than the expected and frequently used design values.

RÉSUMÉ

Le choc d'un navire contre une construction élastique s'accompagne d'une certaine masse d'eau, dont la quantification est capitale pour une étude. L'importance de cette masse hydrodynamique ajoutée est fonction de la taille du navire, de sa forme, du tirant d'eau, de la profondeur sous la quille, de l'élasticité de l'obstacle, et du mode de collision. Un programme d'essais a été entrepris pour étudier la masse ajoutée pendant l'impact. Les résultats sont intéressants pour les collisons entre navires et pour la conception des défenses. Les valeurs réelles de la masse ajoutée sont plus élevées que celles fréquemment utilisées dans les calculs.

ZUSAMMENFASSUNG

Ein Schiff, das auf ein elastisches Objekt prallt, nimmt eine gewisse zugefügte Wassermasse mit sich mit, deren Festlegung während des Entwurfes wichtig ist. Die Größe dieser hydrodynamischen zugefügten Masse wird beeinflußt von: Schiffsgröße, Form, Tiefgang, Bodenfreiheit, Federkonstante des Hindernisses und Kollisionsart. Experimente zur Untersuchung der zugefügten Masse während des Aufpralls werden beschrieben. Die Resultate sind in Hinsicht auf Schiff-gegen-Schiff-Kollisionen und Fenderentwürfe interessant. Die gefundenen Werte liegen höher als erwartet und sind auch größer als die gewöhnlich benutzten Entwurfswerte.

1. INTRODUCTION

When a ship approaches a jacket, a jetty or some other structure, the amount of kinetic energy present will in most cases be absorbed by elastic or plastic deformation of usually some fendering system. The most common way to obtain the design loads on the structures and fendering systems is to estimate this amount of kinetic energy of the ship. For this estimation some assumptions have to be made. The biggest ship approaching the structure is selected and the maximum speed at which and the mode under where contact is made, is usually taken. When a ship with a certain approaching speed will be decelerated, also a certain amount of water, which is moving along with the ship, has to be decelerated. This means that the mass to be taken into account for the kinetic energy is not only the mass of the ship; there is a certain additional mass, the so-called hydrodynamic added mass.

The most common practice is that a constant amount of added mass is applied to the ship's mass, independent of all factors affecting it; see Saurin [19] and Vasco Costa [21] and [22]. Thoresen [20] takes possible eccentricities into account during collision. Giraudet [11] accounts for underkeel clearance only. In recent years the possibility of an accidental collision between a ship and an offshore platform has drawn considerable attention ([6], [10], [16], [17] and [18]), in which basically the structural aspects were considered.

An advanced computer program, dealing with all mentioned parameters affecting the added mass, has been developed at N.S.M.B. This program was presented at the OTC by Van Oortmerssen in 1974, [15]. The data presented in this paper are a result of an extensive model test program for further investigation and validation of the computer program. Another goal of the experiments was to supply potential designers with more test results in order to support their designs.

Parts of the results of this large test series have already been presented in papers contributed to the 1979 and 1983 OTC Conferences, [1] and [2].

2. CURRENT DESIGN PRACTICE

2.1 Basic equations

The current practice in the design calculations and dimensioning of fendering systems and flexible structures is almost invariably based on energy considerations [8], [12], [13] and [14]. In these it is assumed that the loss of kinetic energy of the ship is transformed into an equal amount of energy absorbed by the fender or structure, i.e.:

$$W = \tfrac{1}{2} M_v . V_0^2 \qquad \ldots\ldots\ldots\ldots\ldots\ldots\ldots\ldots\ldots\ldots\ldots\ldots\ldots\ldots (1)$$

in which:
W = work done by the fender
M_v = virtual mass of the ship, which is the sum of the ship's mass and the hydrodynamic added mass
V_0 = initial velocity of the ship on hitting the fender.

Whatever the design of the fender, the work done by the fender can be written as:

$$W = \int_{s(t_0)}^{s(t_1)} F.ds \qquad \ldots\ldots\ldots\ldots\ldots\ldots\ldots\ldots\ldots\ldots\ldots\ldots\ldots\ldots (2)$$

in which:
F = reaction force exerted by the fender
s = deflection of the fender
t_0 = instant of hitting the fender
t_1 = instant when the maximum deflection is attained.

Equation (1) is strictly valid for the situation where all the kinetic energy is absorbed, such that during the slowing down process no other modes of motion develop than the one present. That means that all kinetic energy is supposed to be absorbed when the fender deflection has reached its maximum.

2.2 Practical implementation

For the more complicated cases, in which yawing starts to develop during the slowing down process, the kinetic energy is never to reach zero at the point of maximum fender deflection; see Vasco Costa [21] and [22]. Equation (2) offers the possibility to determine the magnitude of the absorbed energy of the fender over the first part of the impact. This is independent of the shape of the fender characteristic. (Relation between load and deflection).

The most common formulation of the energy equation, (see [3], [19] and [21]), taking the various effects into account is:

$$W = \tfrac{1}{2}\, M.V_0^2.C_M.C_E.C_S \quad \ldots\ldots\ldots\ldots\ldots\ldots\ldots\ldots\ldots\ldots\ldots\ldots\ldots\ldots (3)$$

in which:

M = mass of the ship

C_M = coefficient of added mass

C_E = coefficient of eccentricity, accounting for the position of the point of contact relative to the ship's centre of gravity. It boils down to a reduction of the energy to be absorbed, since:
$C_E = 1$ for impact aside of the centre of gravity and
$C_E \approx 0.5$ for impact at one quarter ship's length from the fore or aft perpendicular.

C_S = coefficient of deformation, taking the elastic hull deformation into account. If 10 per cent of the energy is absorbed by the hull the fender need only take 90 per cent, hence:
$C_S = 0.9$.

It will be shown in the sequel that these assumptions can be grossly in error. As already suggested by the above expression the added mass is associated with a sway motion even if the ship has a certain rate of yaw before and after hitting the fender. In so far as the authors are aware no information is known to exist in which the added mass is split up into a coefficient pertaining to sway and another to yaw in a hydrodynamically sound way.

In [1] a review has been given of most of the values for C_M in use so far. They do not take into account all effects influencing the C_M magnitude. One of the results of the test series, as presented herein, is that the accepted and frequently used C_M values appear to be too low; a finding which is of direct consequence to the designers.

3. EXPERIMENTAL WORK

The most important aim of the test program was to gather as much as possible test data on the subject for the benefit of the practising engineer. A secondary purpose was the availability of reliable test data to validate a sophisticated N.S.M.B. developed computer program on this subject.

In order to cover realistic cases the test parameters had to be selected carefully. Also, the test set-up wherein the tests were done had to be very accurate and able to reproduce the test conditions and results precisely.

3.1 The test set-up

The tests were performed at a model scale of 1 to 75. A sketch of the test set-up is shown in Fig. 1. The structure, to which the fenders were connected, was completely transparent in order to avoid reflection from some quay wall. This

effect would produce lower values for the added mass coefficient, because a reflected wave would slow down the ship faster and as a result the measured peak load at the contact point would be lower.

The ship was connected to two endless wires by means of two electromagnetic couplings. By means of these wires the ship could be directed to the fender at a very precisely controlled heading and speed. Just before the moment of contact the ship was released of the wires, after which it was free to move in any mode of motion.

At the moment of impact, measurements were taken of: sway, surge, roll, yaw, roll rate, yaw rate, fender force and fender stroke.

3.2 The parameters

In order to gather data, corresponding to the most frequent situations in reality, the following selection of parameters was made:
- VLCC: 225,000 DWT, being one of the most popular sizes; see [7].
- Draught: full load, since the mass is then largest.
- Underkeel clearance: 20 per cent of the ship's draught.
- Fender characteristics: a linear relationship between deflection and reaction force, being 1600 kN/m, 4200 kN/m, 12000 kN/m and 20600 kN/m.
- Collision modes:
  Collision type 1: ship having a pure sway motion, hitting the fender at the midships.
  Collision type 2: ship having a pure sway motion, hitting the fender at 15, 20 and 30 per cent of its length forward of the midships.
  Collision type 3: ship's heading making an angle of 15 degrees with the final berthed position. Approach of the ship was a pure translation.
- Collision velocities: a range of velocities has been chosen, corresponding to 0.04 m/s up to 0.30 m/s for the full scale; see [3] and [4].

3.3 Analysis of the test results

For the analysis of the test results various principles from classic mechanics were invoked. These comprised the energy preservation law and the law of change of momentum.

Most concisely we can express the equations in the following form:

$$\int_{t_a}^{t_b} F(t).\cos\alpha.dt = C_{My}.M\{\dot{y}(t_b) - \dot{y}(t_a)\} \quad \ldots\ldots\ldots\ldots (4)$$

momentum equation for sway

$$\int_{s(t_a)}^{s(t_b)} F(t).ds = \tfrac{1}{2} C_{My}.M\{\dot{y}^2(t_b) - \dot{y}^2(t_a)\} \quad \ldots\ldots\ldots\ldots (5)$$

energy equation for sway

$$\int_{t_a}^{t_b} F(t).\overline{QG}.\cos\alpha.dt = C_{M\psi}.I_G\{\dot{\psi}(t_b) - \dot{\psi}(t_a)\} \quad \ldots\ldots\ldots\ldots (6)$$

momentum equation for yaw

For collision type 1, where before and after the impact solely a sideways sway motion existed, the first two equations were used. Both of them would yield a added mass coefficient for sway motion, which would not be exactly the same, see Section 5.1. For collision type 2 and 3 equation (5) could not be used anymore, since the energy would be distributed over all modes of motion, in particular, sway and yaw. The energy approach would give us more unknowns than equations. So for these cases the momentum approach remained and equations (4) and (6) were used. For collision type 2 the angle between ship and jetty was zero, so that cos α reduced to unity.

Each equation would give an added mass coefficient for any one test. This coefficient could be based on various time periods, depending on the choice of t_a and t_b. In the analysis three distinct time instants were defined, t_0 being the moment of impact, t_1 being the instant of maximum spring deflection and force and t_2 the instant of spring force being back to zero. These three points in time define three time periods which were all taken for the analysis, $t_0 - t_1$ being the most important as the added mass thus derived has a direct engineering application, while the others are of lesser importance.

4. ANALYTICAL WORK

4.1 Simple mass-spring system model

When a ship has a purely sideways motion and runs into a fender or other elastic structure exerting a force at the midships, the hydrodynamics associated with the arrested motion of the ship and the decelerated flow of the water around the ship are rather complicated. It would be interesting to see to what extent the motion of the ship, most dominantly sideways, can be predicted by a simple mathematical model and if the deflection of the fender and the exerted force can be predicted as well.

Suppose a ship with rigid body mass M and added mass coefficient C_{My} strikes an elastic structure with spring rate C at the origin of time t_0. We may illustrate this as done in Fig. 2. This single degree of freedom model can easily be solved. We may also suppose the ship to hit the fender at a point well forward of the midships as illustrated in Fig. 3. Solving the equations of motion we can evaluate the following:

maximum spring deflection: $$\hat{s} = V_0\sqrt{\frac{C_{My}.M.k^2}{C(a^2 + k^2)}} \quad \ldots\ldots\ldots\ldots (7)$$

maximum spring force : $$\hat{F} = V_0\sqrt{\frac{C_{My}.M.C.k^2}{(a^2 + k^2)}} \quad \ldots\ldots\ldots\ldots (8)$$

time to reach maximum : $$T_{01} = \frac{\pi}{2}\sqrt{\frac{C_{My}.M.k^2}{C(a^2 + k^2)}} \quad \ldots\ldots\ldots\ldots (9)$$

in which "a" represents the eccentricity distance and "k" stands for the radius of gyration in yaw. When we set "a" to zero the centric impact is obtained. It can be shown that the test results agree with these simple relations, see Section 5.

4.2 Linear mathematical model with fluid memory effect

The usual approach in ship motion theory is to use an equation of motion in the frequency domain, that takes the following form:

$$\{M + a_{yy}(\omega)\}\ddot{y} + b_{yy}(\omega)\dot{y} + C_{yy}.y = F_y(\omega) \quad \ldots\ldots\ldots\ldots\ldots\ldots (10)$$

This equation, in which all coefficients are frequency dependent, can only be solved for discrete frequencies, hence harmonic oscillations. This implies that, contrary to the looks of the equation, it is an algebraic equation rather than a differential equation.

In order to simulate time processes, like in the subject case, one needs a true differential equation in which the coefficients are constants and the time constitutes the sole independent parameter. Such an equation can be obtained by taking the Fourier transform of the above equation which leads to the following expression:

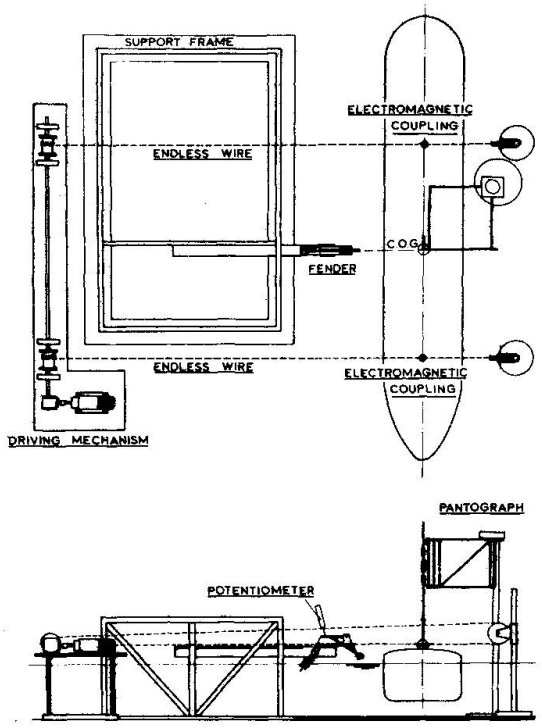

Fig. 1 Test set-up

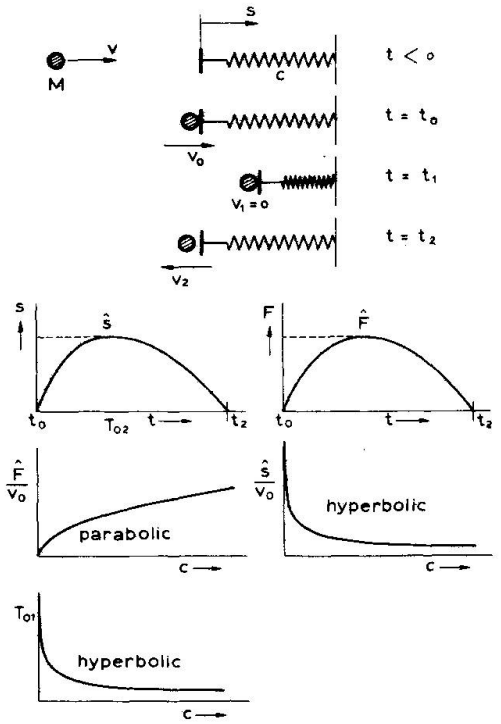

Fig. 2 Scheme and time histories for simple mass-spring system model for central impact

$$(M + M_{yy}).\ddot{y}(t) + \int_{-\infty}^{t} k_{yy}(t-\tau).\dot{y}(\tau).d\tau = F_y(t) \qquad \ldots\ldots\ldots\ldots\ldots (11)$$

This one degree of freedom model can be extended to more degrees of freedom as given by Cummins [5], Van Oortmerssen [15] and Fontijn [9]. This time domain model has been employed in the present study to check its applicability to the results of the model experiments and it is shown in the sequel that the results from experiments and computations agree fairly well, see Section 5.3.

5. DISCUSSION OF THE RESULTS

5.1 Some notes on the added mass coefficients

For the centric impact case there are basically two ways to obtain the added mass coefficient, namely through the use of the momentum equation or the energy equation. It has been observed that the C_{My} coefficients derived from both techniques do not correspond. As shown in the following expressions the C_{My} coefficients cannot be equal.

The loss of kinetic energy in the fluid can be written as:

$$\tfrac{1}{2}\{\rho \iiint \left(\frac{V_1(x,y,z)}{\dot{y}_0}\right)^2 dx\,dy\,dz - \rho \iiint \left(\frac{V_0(x,y,z)}{\dot{y}_0}\right)^2 dx\,dy\,dz\}\dot{y}_0^{\,2} \qquad \ldots\ldots (12)$$

Likewise the loss of fluid momentum in y-direction can be written as:

$$\{\rho \iiint \left(\frac{V_{y1}(x,y,z)}{\dot{y}_0}\right) dx\,dy\,dz - \rho \iiint \left(\frac{V_{y0}(x,y,z)}{\dot{y}_0}\right) dx\,dy\,dz\}\dot{y}_0 \qquad \ldots\ldots (13)$$

The terms within brackets represent a kind of lumped added mass, associated either with energy or with momentum; and it is clear that the two expressions are not the same.

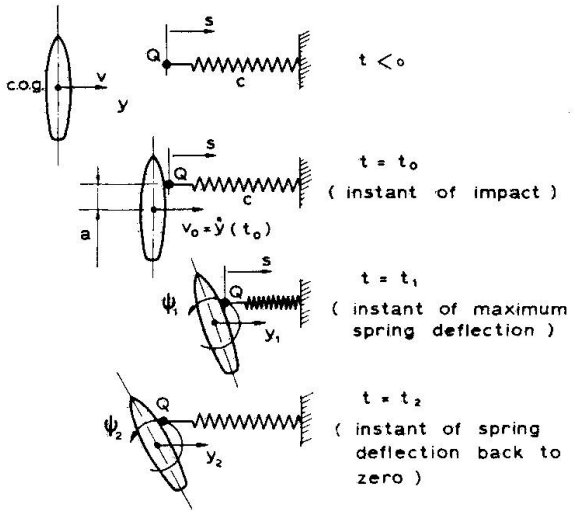

Fig. 3 Scheme for simple mass-spring system model for eccentric impact

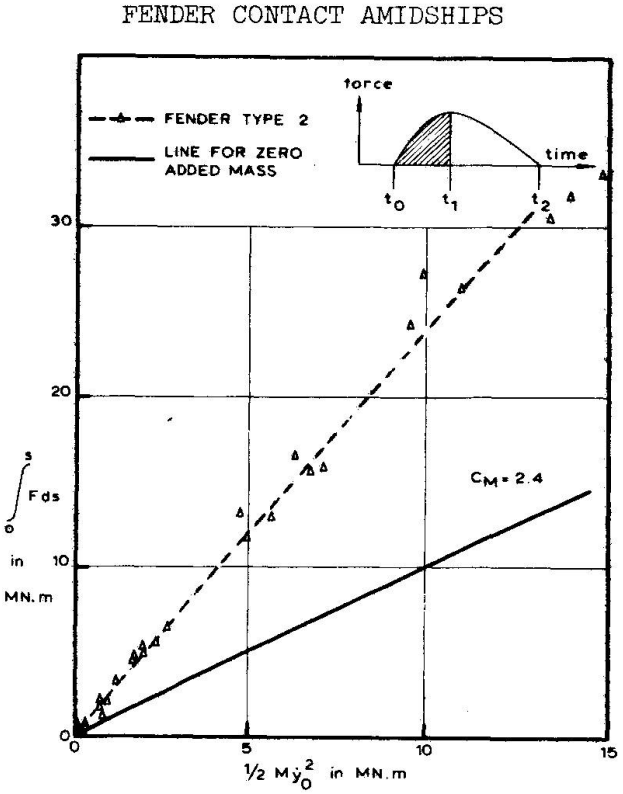

Fig. 4 Energy balance during compression phase

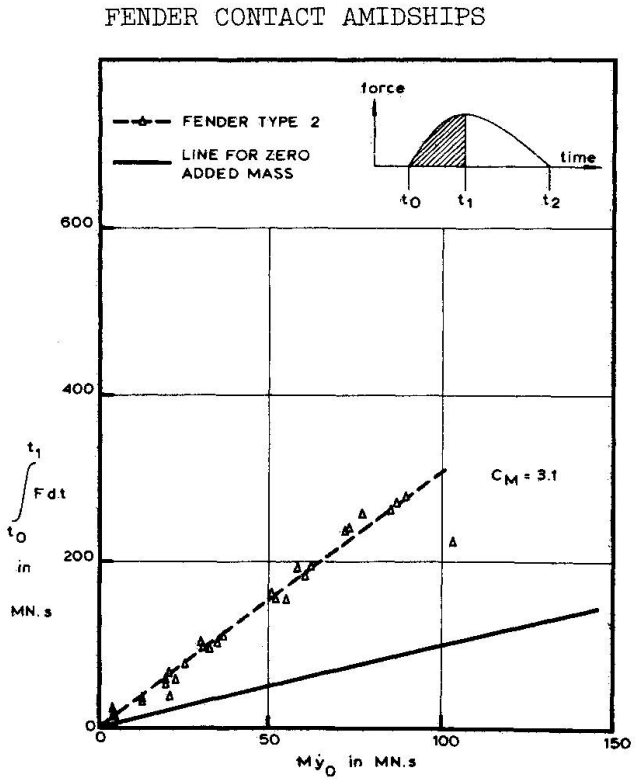

Fig. 5 Impulse versus change of momentum during compression phase

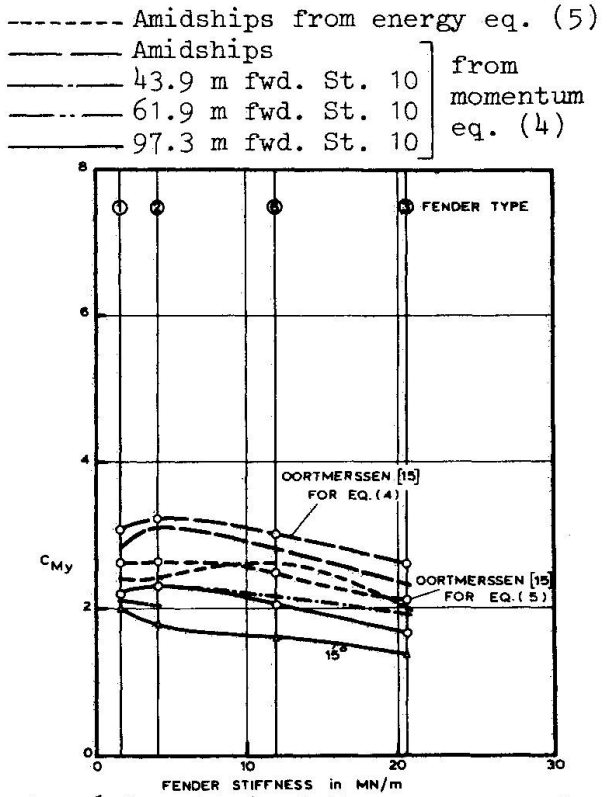

Fig. 6 C_{My} obtained from energy and momentum balance (eq. (5) and (4)) over compression phase

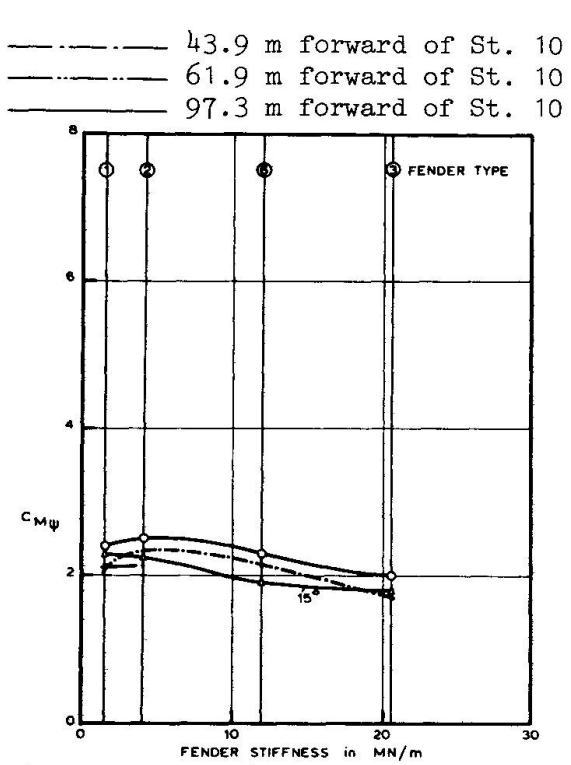

Fig. 7 $C_{M\psi}$ obtained from momentum balance (eq. (6)) over compression phase

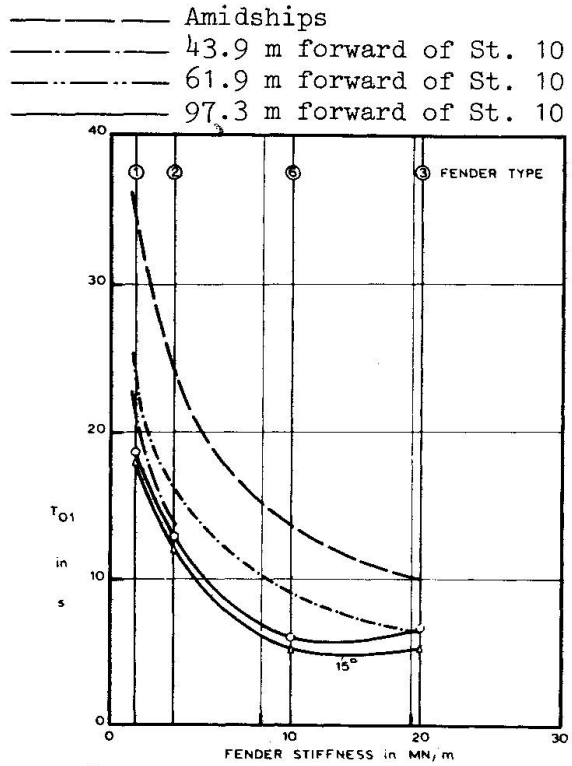

Fig. 8 Duration of ship-fender contact in compression phase

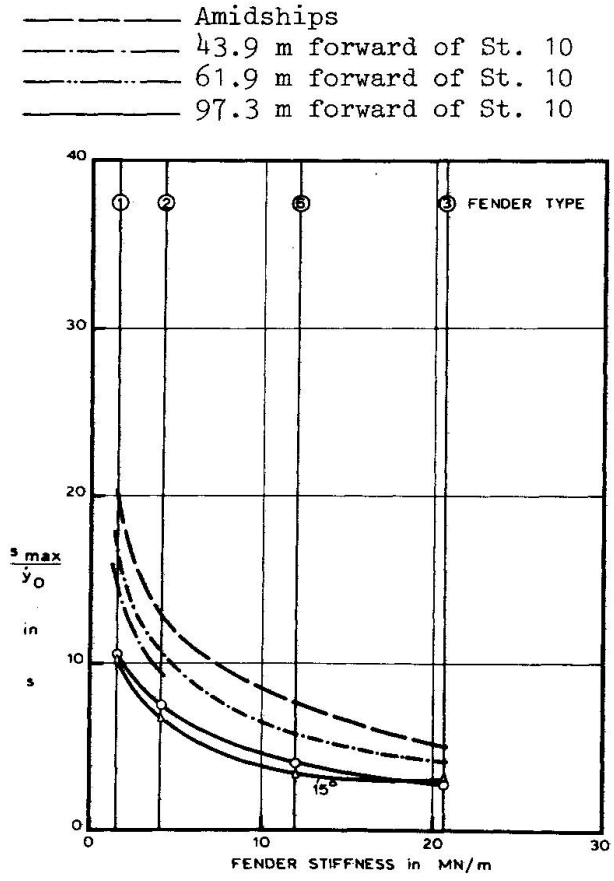

Fig. 9 Reduced maximum fender deflection

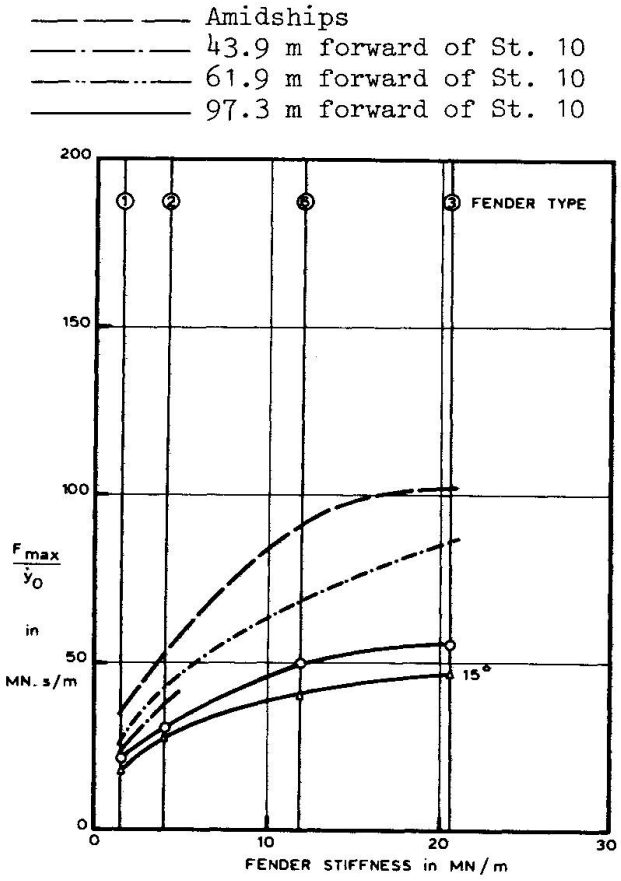

Fig. 10 Reduced maximum impact load

5.2 Discussion of the measured data

As outlined in Section 3.3, the derivations of the added mass coefficient can be done using the energy equation or the momentum equation. The results shown in Fig. 4 and 5 illustrate this point. The ensuing diagrams, Fig. 5 to 10 give in very concise form the total results of the whole test program, and they lead to the following observations. It is shown in Fig. 6 and 7 that as the fender point of contact moves further forward the added mass coefficients decrease. Theoretically there is no ground for this, but we can imagine that as the ship takes on an appreciable yaw angle the flow of water will be such that the sway and yaw added mass changes. Both the sway and yaw added mass coefficients are a function of the fender stiffness. In Fig. 8, 9 and 10 one can see that the shape of the curves corresponds fairly well to relations derived in Section 4.1.

5.3 Discussion on the comparison between test results and computations

The simple mathematical fitting model described in Section 4.1 agrees generally fairly well with the data, and is very instructive to gather some insight in the total impact event. However, this fit cannot predict the added mass value, so therefore a different model should be employed, as described in Section 4.2. That model gives a true time domain description of the total event, for instance the fender force as a function of time, which can then be analyzed in the same fashion as if it were a measurement result. This was done with regard to the sway added mass coefficient as shown in Fig. 6. The calculated added mass coefficient is indicated and it is clear that a close correspondence to the measured data exists.

It will be clear that a mathematical model of this kind can be used to advantage, for instance in the design stage of a jetty when due to the prevailing conditions there is little empirical data or experience to rely on.

6. EVALUATION

The results of the experiments presented herein and in [1] show the following:

- The added mass coefficients for sway and yaw are dependent upon the spring rate of the fender and on the characteristic of the fender's force-deflection curve, as is shown in [1].
- The maximum deflection of the fender decreases for increasing fender stiffness and for increasing eccentricity of the point of contact. The same applies to the characteristic time periods associated with the impact.
- The maximum force felt by the fender increases for increasing fender stiffness and decreases for greater eccentricity of the point of contact.
- The trend of these results can quite well be predicted by a simple mathematical model. However, the added mass coefficient can only be predicted by a sophisticated model in which due account is given to the fluid memory effect.

7. RECOMMENDED DESIGN PROCEDURE

It was stated in Section 3 that following the current design practice an added mass coefficient is to be selected applicable to the case. Usually, however, the designer takes a coefficient which has little if nothing to do with the subject case, and any dependency of the added mass coefficient on vessel size and shape, underkeel clearance, fender stiffness and characteristic and location of the point of contact on the ship's hull are eithr not rightly understood or considered of only marginal importance.

However, the present paper shows that these effects should not be left out of the design considerations. A simple mathematical model like the mass-spring system detailed in Section 4.1 can go a good way to explain the trends, but it takes a sophisticated mathematical model involving all the fluid memory effects

in order to accurately predict the added mass and the time history of the impact. In the design of jetties and berths for large ships, under conditions for which one has little recourse to existing data, such computations will yield the right data to be used in the design.

NOMENCLATURE

a	= $\overline{QG}$ = distance between C.O.G. and point of contact	s	= fender stroke
$a_{yy}(\omega)$	= added mass in sway	$\hat{s}$	= maximum fender deflection
$b_{yy}(\omega)$	= damping in sway	s_0	= $s(t_0)$
C	= spring rate	s_1	= $s(t_1)$
C_E	= coefficient of eccentricity	s_2	= $s(t_2)$
C_M	= coefficient of added mass	t	= time
C_{My}	= added mass coefficient in sway	t_a, t_b	= time instants
$C_{M\psi}$	= added mass coefficient in yaw	t_0	= time instant when the ship hits the fender
C_S	= coefficient of deformation	t_1	= time instant when fender deflection is maximum
C_{yy}	= spring rate in sway	t_2	= time instant when contact between ship and fender is lost
dx dy dz	= infinitesimal fluid element	T_{01}	= $t_1 - t_0$
$\hat{F}$	= maximum fender force	V	= speed
$F(s)$	= fender force as a function of deflection	V_0	= $V(t_0)$
$F(t)$	= fender force as a function of time	$\overline{V}(x,y.z)$	= local fluid velocity vector
$F_y(\omega)$	= external exciting force	$V_y(x,y,z)$	= local fluid velocity vector y-component
$F_y(t)$	= external driving force	$V_0(x,y,z)$	= $V(x,y,z)$ at $t = t_0$
G	= index to centre of gravity C.O.G.	$V_1(x,y,z)$	= $V(x,y,z)$ at $t = t_1$
I_G	= mass moment of inertia in yaw relative to C.O.G.	$V_{y0}(x,y,z)$	= $V_y(x,y,z)$ at $t = t_0$
$k_{yy}(t)$	= retardation function in sway	$V_{y1}(x,y,z)$	= $V_y(x,y,z)$ at $t = t_1$
k	= radius of gyration in yaw	W	= work
M	= ship's mass	y	= sway motion
M_a	= added mass	α	= angle of incidence between ship and fender
M_v	= virtual mass = $= M + M_a = C_{My}.M$	ρ	= fluid density
M_{yy}	= added mass in sway	ψ	= yaw motion
		ω	= circular frequency
$\overline{QG}$	= a = distance between C.O.G. and point of contact	τ	= dummy time variable

REFERENCES

1. BLOK, J.J. and DEKKER, J.N., On hydrodynamic aspects of ship collision with rigid or non-rigid structures, Proceedings of the Offshore Technology Conference 1979, Houston, Paper OTC 3664.
2. BLOK, J.J., BROZIUS, L.H. and DEKKER, J.N., The impact loads of ships colliding with fixed structures, Proceedings of the Offshore Technology Conference 1983, Houston, Paper OTC 4469.

3. BROLSMA, J.U. and OOSTERBAAN, J.W., Docking and mooring of a VLCC inside a harbour, Symposium on Shiphandling 1973, Wageningen, Netherlands, Publication No. 451, Netherlands Ship Model Basin, Wageningen, Netherlands.
4. BROLSMA, J.U., HIRS, J.A. and LANGEVELD, J.M., On fender design and berthing velocities, Proceedings of the 24th International Navigational Congress, Leningrad 1977, Permanent International Association of Navigational Congresses.
5. CUMMINS, W.E., The impulse response function and ship motions, Schiffstechnik, Heft 47, Juni 1962 (9. Band).
6. DONEGAN, E.M., Appraisal of accidental impact loadings on steel piled North Sea structures, Proceedings of the Offshore Technology Conference 1982, Houston, Paper OTC 4193.
7. FEARNLEY & EGERS CHARTERING CO., LTD., Some aspects of fleet trade, ports and off-hire of large tankers, January 1971 and the year 1970, Rådhustgt. 23 - Oslo 1 - Norway.
8. FISHER, J., Proceedings of the 24th International Navigational Congress, Leningrad 1977, Permanent International Association of Navigational Congresses.
9. FONTIJN, H.L., The berthing of a ship to a jetty, Journal of the Waterway, Port, Coastal and Ocean Division, May 1980.
10. FOSS, G. and EDVARDSEN, G., Energy absorbation during ship impact on offshore steel structures, Proceedings of the Offshore Technology Conference 1982, Houston, Paper OTC 4217.
11. GIRAUDET, P., Recherches expérimentales sur l'energie d'accostages des navires, Annales des Ponts et Chaussées - 1966 - II.
12. GIRGRAH, M., Practical aspects of dock and fender design, Proceedings of the 24th International Navigational Congress, Leningrad 1977, Permanent International Association of Navigational Congresses.
13. GRIM. O., Das Schiff und der Dalben, 288 Mitteilung der Hamburgischen Schiffbau-Versuchsanstalt, Schiff unf Hafen, 1955, H.9.
14. KIKUTAUI, H., IWAI, A. and OIKAWA, K., Some requirements for the design of seaberths from the view-point of ship handling, Proceedings of the 23rd International Navigational Congress, Ottawa 1973, Permanent International Association of Navigational Congresses.
15. OORTMERSSEN, G. VAN, The berthing of a large tanker to a jetty, Proceedings of the Offshore Technology Conference 1974, Houston, Paper OTC 2100.
16. OLIVERIA, J.G. DE, The behaviour of steel offshore structures under accidental collisions, Proceedings of the Offshore Technology Conference 1981, Houston, Paper OTC 4136.
17. PETERSEN. M.J. and PEDERSEN. P.T., Collisions between ships and offshore platforms, Proceedings of the Offshore Technology Conference 1981, Houston, Paper OTC 4134.
18. PETTERSEN, E. and JOHNSEN, K.R., New non-linear methods for estimation of collision resistance of mobile offshore units, Proceedings of the offshore Technology Conference 1982, Houston, Paper OTC 4135.
19. SAURIN, B.F., Berthing forces of large tankers, 6th World Petroleum Congress 1963, Frankfurt, Section VII, Paper 10.
20. THORESEN, C.A. and TORSET, P.O., Fenders for offshore structures, Proceedings of the 24th International Navigational Congress, Leningrad 1977, Permanent International Association of Navigational Congresses.
21. VASCO COSTA, F., The berthing ship, the effect of impact on the design of fenders and other structures, The Dock & Harbour Authority, May, June and July 1964.
22. VASCO COSTA, F., Dynamics of berthing impacts, NATO Advanced Study Institute on Analytical Treatment of Problems in the Berthing and Mooring of Ships, Wallingford, England, 7-16 May 1973.

Leere Seite
Blank page
Page vide

Effects of a Ship Collision with a Bridge

Effets de la collision d'un navire avec un pont

Auswirkungen einer Schiffskollision mit einer Brücke

Toivo ROIVAINEN
Project Manager
Oy Insinööritoimisto K. Hanson & Co.
Helsinki, Finland

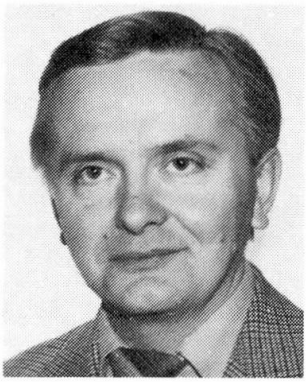

Toivo Roivainen, born 1946, graduated from the Kuopio Technical College (engineering) in 1971, and from the Helsinki University of Technology (MSc in Engineering) in 1982. Since 1971 Mr. Roivainen has been employed by Oy Insinööritoimisto K. Hanson & Co. (Consulting Engineers) as a construction designer and project manager.

Erkki TIKKANEN
Technical Director
Oy Insinööritoimisto K. Hanson & Co.
Helsinki, Finland

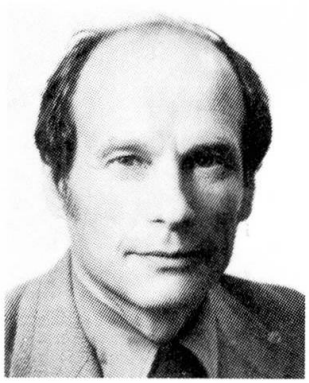

Erkki Tikkanen, born 1935, graduated from the Helsinki University of Technology (MSc in Engineering) in 1960. Since 1959 Mr. Tikkanen has been employed by Oy Insinööritoimisto K. Hanson & Co. (Consulting Engineers) as a construction designer, project manager and technical director.

SUMMARY

This study considers the after-effects of a hypothetical collision of a ship with the bridge connecting Lauttasaari with Salmisaari in Helsinki. Dynamic calculations for such a collision were carried out using a simple model having two lumped masses. The elasticity of the bridge and the reductions in rigidity caused by successive failures of the piers were also taken into account. The shear capacities of the bearings were found to be the most critical factors in the case of a collision. Lastly, an investigation was made as to how to reduce the possibility of further mishap which might result from such a collision.

RÉSUMÉ

L'étude s'intéresse aux conséquences d'une collision supposée d'un navire avec le pont reliant Lauttasaari et Salmisaari, à Helsinki. Des calculs dynamiques pour une semblable collision ont été effectués à l'aide d'un modèle simple faisant appel à deux masses distinctes. De même, il a été tenu compte de l'élasticité du pont et de la diminution de la rigidité du fait des défaillances successives des piles. La résistance au cisaillement des appuis est, selon cette étude, l'élement le plus important en cas de collision. Une étude a été menée sur la manière de réduire les conséquences d'un tel accident.

ZUSAMMENFASSUNG

Die Folgen einer hypothetischen Kollision eines Schiffes mit der Brücke zwischen Lauttasaari und Salmisaari in Helsinki werden untersucht. Unter Verwendung eines einfachen Modells aus zwei Massen wurden dynamische Berechnungen für eine solche Kollision vorgenommen. Die Elastizität der Brücke und die Minderung der Steifigkeit, die durch mehrfaches Versagen der Pfeiler verursacht wurde, ist ebenfalls berücksichtigt worden. Die Schubfestigkeit der Auflager stellte sich als kritischster Faktor im Fall einer Kollision heraus. Es wurde noch untersucht, wie die Folgen einer solchen Kollision verringert werden könnten.

1. PREFACE

1.1 General

In the year 1980, an accident took place in Sweden, at the Tjörnbro Bridge, where the entire bridge collapsed after a ship had crashed into the structures of the bridge. Apart from extensive economic damages, also several people were killed in the accident.

This incident attracted considerable attention among professionals of this field. Among others, the Town of Helsinki, the proprietor of the Lauttasaari bridge which also had been battered by ships a couple of times, decided to have a study made of the damages that would be caused by a possible collision. This study was prepared by Oy Insinööritoimisto K. Hanson & Co. (Consulting Engineers).

1.2 Bridge Site

The bridge is located in the town of helsinki between the Salmisaari and Lauttasaari districts, and it crosses a ca. 320 m wide strait in east-west direction. On the northern side of the bridge, in Salmisaari district, there is a power station to which coal is transported by sea through a gate in the bridge. The present bridge was built in 1967 as a result of an international design competition which was won by a Danish engineer, L. Steding-Jessen.

When approaching the bridge, the channel is very close to the Lauttasaari side bank. The water which is thus dammed between the bank and the ship, causes transverse flowings which make it difficult to steer the ship. In order to maintain manoeuvrability, the ship's speed cannot be decreased under 6 knots when sailing into bridge opening.

When the gate of the bridge is opened, traffic onto the bridge is prohibited by means of barriers located right next to the gate on both sides. Vehicles have, thus, free access to the stationary part of bridge when the barriers are lowered.

1.3 Bridge Construction

The base structure of the bridge consists of two rows of columns. The columns are supported partly by piled bases, partly by bases cast onto the rocks.

The spans of the bridge, starting from the Lauttasaari side, are:35.6, 56.6,

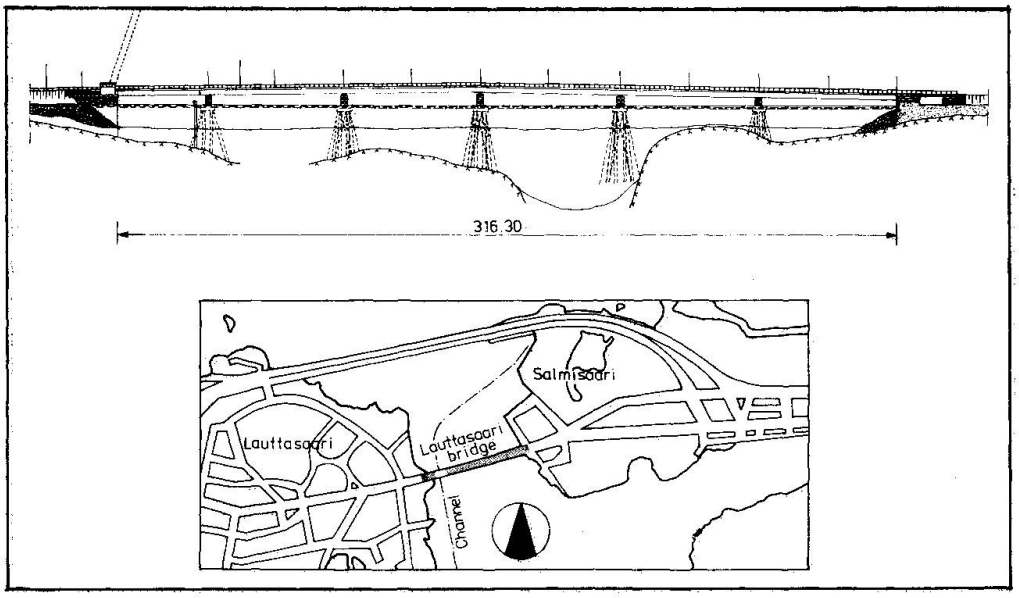

Figure 1. Side view of the bridge and map of the bridge site.

56.0, 56.6, 56.0 and 56.6 m (Figure 1). The gate whose machinery is located onto a ground support, is located in the opening at the Lauttasaari side. From the gate to the Salmisaari side bank, the bridge construction is of continuous composite beam. The 6-box cross section (Figure 2) is formed by a steel concrete cover, and 7 longitudinal main girders and a continuous base plate which are of steel.

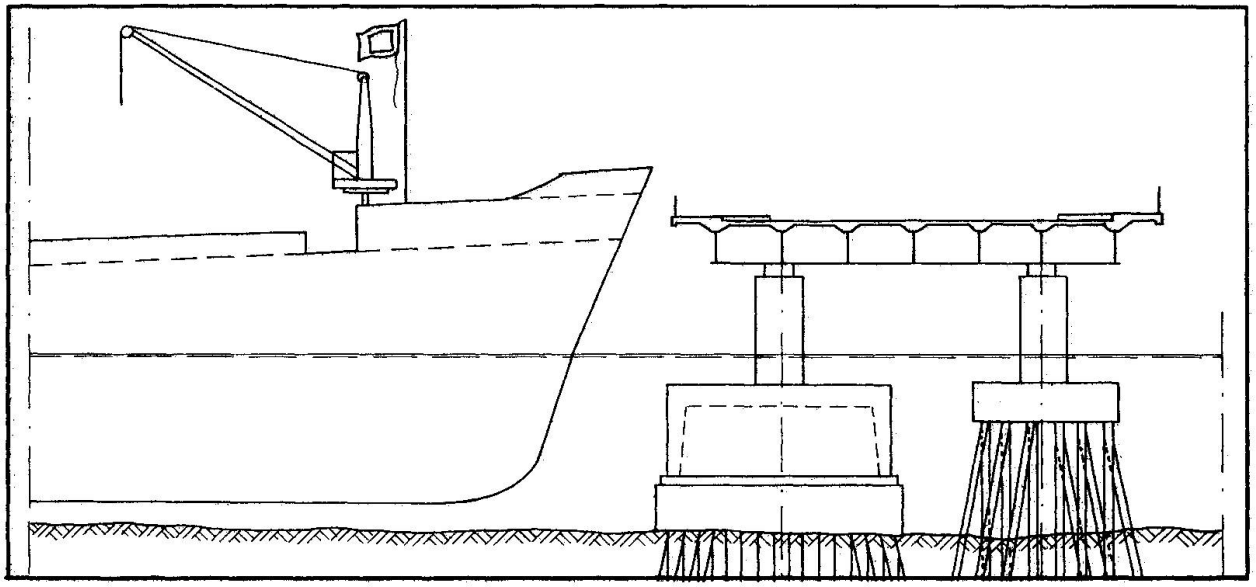

Figure 2. Bridge cross-section and the bow of a coal-carrying ship.

1.4 Aim of the Study

On the basis of preliminary research, it was decided to study a collision that would take place onto the stationary part of the bridge, in the area of the first span when counting from the gate opening (Figure 3). The ship's speed was set to the 6 knots required from point of view of manoeuvrability, and the load of the ship was set to the normal coal cargo amount, 12000 tons.

The aim was to find out the extensiveness of the damages to the bridge in a collision, the probable ways of breaking, as well as whether the damages and the risks to the vehicles could be minimized by, for example, traffic arrangements, protective structures or by stenghtening the bridge.

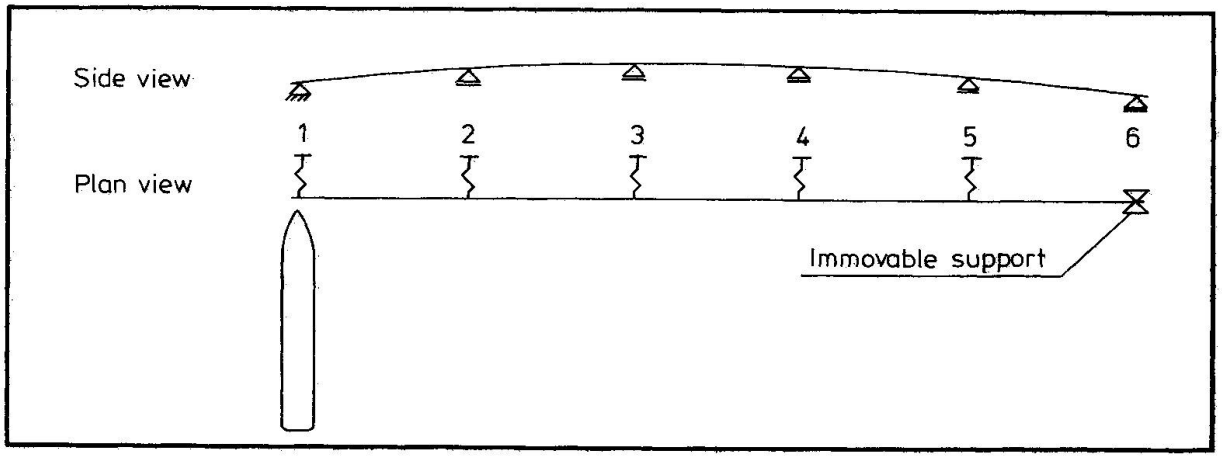

Figure 3. Construction model in a collision.

2. CALCULATION

2.1 General

In a collision, the ship and the bridge together form a system in which the ship pushes the bridge in front of it by its kinetic energy. The bridge's mass inertia and the supports, via the cover structure, counteract this motion. As the aim was to obtain a rough idea of the stresses imposed on the bridge in a collision, it was decided to use a system of two mass points. One of the masses would describe the ship, the other the bridge.

The connection between the two mass points was solved by using the Minorsky formula. This formula is well known in analysis of collisions between ships and is considered creditable owing to its straightforwardness. Its applicability has also been established in several collisions between ships (1, 2).

The connection of the bridge describing mass to its environment was described by a spring which contains the droop of the supports and the cover structure. The calculation of the spring constant was accomplished by a computer.

2.2 Components of the Model

2.2.1 Mass describing the ship (m_1)

The mass of the ship is ca. 5000 t and the weight of the load ca. 12000 t. As the vessel is moving in the direction of its longitudinal axis, the influence of the water moving with it corresponds to an increase of ca. 10% to the ship's mass. Thus, a numeric value of 18700 t was obtained for the mass m_1.

2.2.2 Mass describing the bridge (m_2)

The mass of the bridge was calculated to be 24.4 t/m. In the model, the bridge is described by a mass whose moment of inertia is the same as the moment of mass inertia of the cover structure. In this case, a value of 2330 t was calculated for the mass m_2 describing the bridge with respect to the eastern ground support which was supposed to be immovable.

2.2.3 Connection between the masses

The Minorsky formula describes the energy consumed in a collision into deformation of the structures. Converted into SI-units, it can be presented in the form:

$$E = 32.37 + 47.09\ R_T \qquad (1)$$

where E is the energy consumed (MNm) and R_T the amount of deformed steel (m^3).

The amount of steel of the bridge's cover structure is 0.091 m^3/m^2. As the bow of the ship is considerably sturdier than the 10...16 mm thick plate constructions of the bridge, it was supposed that deformation concentrate entire on the bridge. As, moreover, the ship's bow was simplified into a shape of a triangle (Figure 4), the following expression was obtained for the energy consumed in a deformation of the cover:

$$E(x) = 2.74\ x^2 + 32.37 \qquad (2)$$

where x is the penetration of the ship's bow into the bridge cover (m).

By derivation, the following expression is obtained for the force of contact:

$$P(x) = dE(x)/dx = 5.485\ x \qquad (3)$$

on the basis of which the studied connection can be described by a linear spring.

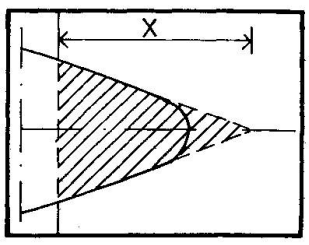

Figure 4.

2.2.4 Rigidity of the bridge

The bridge's rigidity characteristics were studied by using a grate model. In the model, each span was divided into four parts of equal length. The elasticity of the base structure was also taken into consideration. The most important parameters describing the bridge are:

- Moment of inertia of the cover construction with respect to the vertical axis $J_Y = 68.06\ m^4$
- Moment of torsional inertia $J_T = 2.47\ m^4$
- Moment of warping inertia $J_W = 26.34\ m^6$
- Rigidities of the supports in the ship's direction of motion varied between 123...182 MN/m

At the selected collision point, the rigidity of the bridge was: $k_2 = 143.8$ MN/m

As the calculation proceeded, it was established that the bearings of the bridge would seize as a result of a collision. For this reason, it was necessary to recalculate the rigidity of the bridge every time the displacement exceeded the displacement corresponding to the support's ultimate load.

There are two types of the bearings. The calculated seizing capacity of a stationary bearing is 1.13 MN and that of a roller bearing 0.61 MN. The capacity of a column with respect to a horizontal force at the bearing level is 3.1 MN.

2.3 Equations of Motion

Figure 5.
Masses and their connections

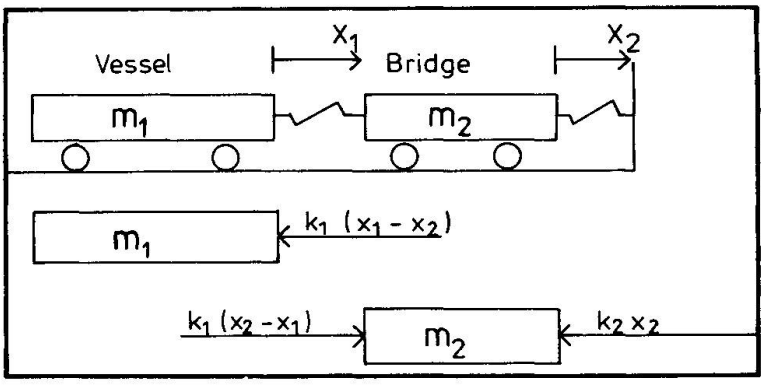

By means of the connections presented in Figure 5, the following equations of equilibrium are obtained:

$$\begin{cases} m_1\ddot{x}_1 + k_1(x_1-x_2) = 0 \\ m_2\ddot{x}_2 + k_1(x_2-x_1) + k_2x_2 = 0 \end{cases} \quad (4)$$

These equations can be presented in the form:

$$\ddot{X} + KX = 0 \quad (5)$$

When the friction forces F_μ, affecting at broken supports, are included into the model, the group of equations gets a form:

$$\ddot{X} + KX = F, \text{ where } F = \begin{bmatrix} 0 \\ F_\mu / m_2 \end{bmatrix} \quad (6)$$

By transforming K into diagonal matrix, we get:

$$\ddot{\Psi} + \Lambda\Psi = C \quad (7)$$

where:

$$\Psi = T^{-1}X \tag{8}$$

$$\Lambda = T^{-1}K\,T = \begin{bmatrix} \lambda_1 & 0 \\ 0 & \lambda_2 \end{bmatrix} \tag{9}$$

and

$$C = T^{-1}F \tag{10}$$

The solution of the group of equations (6) is:

$$\begin{aligned} \xi_i &= A_i \sin\omega_i t + B_i \cos\omega_i t + c_i/\omega_i^2 \\ \dot{\xi}_i &= \omega_i A_i \cos\omega_i t - \omega_i B_i \sin\omega_i t \\ \ddot{\xi}_i &= -\omega_i^2 A_i \sin\omega_i t - \omega_i^2 B_i \cos\omega_i t \end{aligned} \tag{11}$$

The factors Ai and Bi are obtained from the group of equations:

$$\begin{bmatrix} \sin\omega_i t_o & \cos\omega_i t_o \\ \omega_i \cos\omega_i t_o & -\omega_i \sin\omega_i t_o \end{bmatrix} \begin{bmatrix} A_i \\ B_i \end{bmatrix} = T^{-1} \begin{bmatrix} x_i(t_o) \\ \dot{x}_i(t_o) \end{bmatrix} - \begin{bmatrix} c_i(t_o)/\omega_i^2(t_o) \\ 0 \end{bmatrix} \tag{12}$$

When the $x_i(t_o)$ and $\dot{x}_i(t_o)$ are known.

2.4 Solution

The solution was calculated by proceeding in time in steps of 0.2 s, until the displacement of the mass x_2 describing the bridge, exceeded the precalculated displacement corresponding to the ultimate load of one of the supports. After the support had broken, a new rigidity value k_2 was used in the model as well as the friction force affecting the broken support. Calculation was proceeded with these values until the displacement corresponding to the breaking of the next support was achieved, etc.

In total, 4 phases (j) were calculated, during which the lateral rigidity of the bridge changed as is shown in Table 1.

The solution is presented in Figure 6. The contact force between the bridge and the ship developed as is shown in Figure 7. The ship's kinetic energy was divided onto the various components of the model as is shown in Table 2. The stresses imposed on the bridge were studied by means of the bridge's displacements. In the studies, the lateral displacement, the inertia forces and the changed position of the cover structure with respect to the seized supports, were taken into consideration. On the basis of the studies, it was found possible that the cover structure be not broken in a collision, but would move in front of the ship and finally collapse as a "rigid piece" after it has passed a certain critical position.

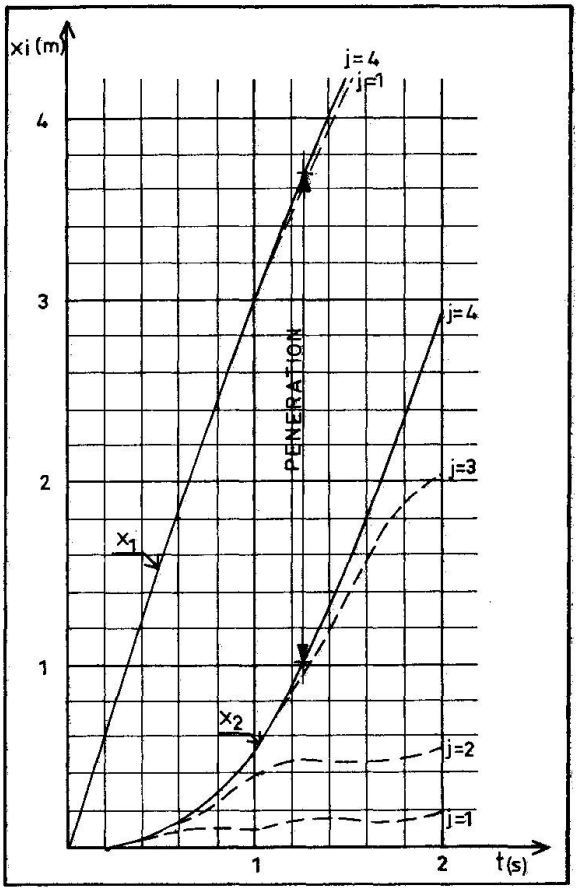

Figure 6. Solutions of the equations of motion

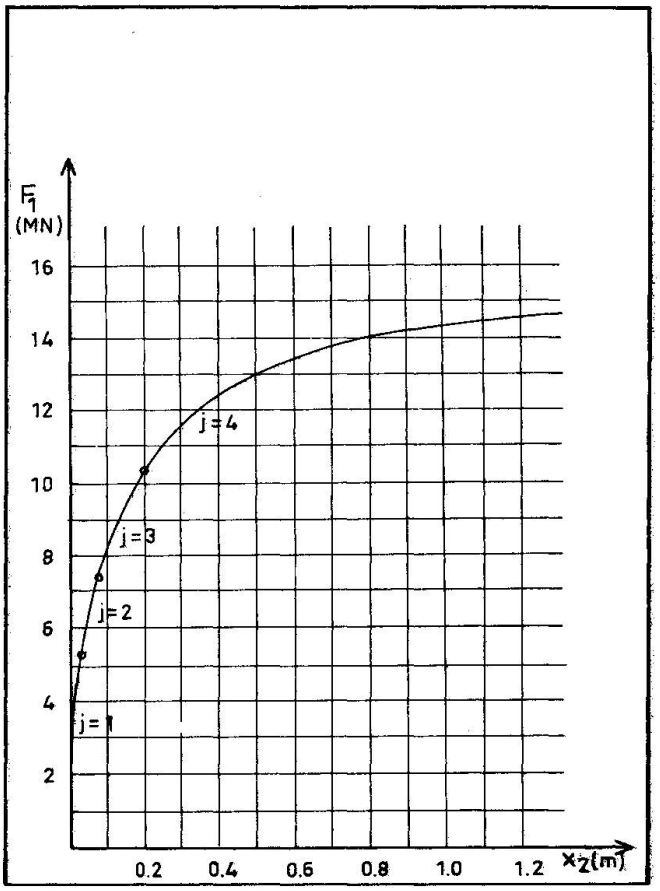

Figure 7. Curve of contact force - displacement

Table 1. Changes in the rigidity of the bridge as the supports are broken.

Phase	k_2	%	Notes
1	143.88	100	
2	34.53	24	as support 1 is broken
3	9.55	7	as support 2 is broken
4	3.97	3	as support 3 is broken

Table 2. Division of energy as a function of time

t	E_1	E_2	E_3	E_4	E_5	E_{tot}
0	89.04	0	0	0	0	89.04
0.335	86.18	0.05	2.72	0.07	0	89.02
0.465	83.70	0.17	5.00	0.14	0.05	89.06
0.700	77.50	0.73	9.96	0.32	0.55	89.06
1.000	67.51	2.50	15.90	0.81	2.33	89.05

E_1 = ship's kinetic energy
E_2 = bridge's kinetic energy
E_3 = work performed at contact point
E_4 = bridge's elastic deformation work
E_5 = work performed by friction forces

3. POSSIBLE MEASURES ON THE BASIS OF THE STUDY

3.1 Prohibiting collisions

In the studied case, the ship is being assisted by two tugs as it is sailed through the bridge opening. A more effective, but also more expensive way than the tugs to prevent collisions would be to use on the eastern side of the channel dolphins forming a sufficiently long guide-way. Depending on the bottom conditions, one possible solution could be application of protective ground structures on the eastern side of the channel. From the point of view of the ship, this solution is, however, obviously not as good as the use of dolphins. In the case we're discussing where the only risk of a collision is caused by the coal-carrying ships, transfer of the coal port onto the southern side of the bridge might be an applicable solution. If a suitable site could be found near enough, the coal could be transported to the power plant by means of a belt conveyor.

3.2 Traffic arrangements on the bridge

If we start by assuming that the probability of a collision cannot be sufficiently minimized, the risk to people can be decreased by prohibiting access to the bridge when a ship is approaching. In practice, this could be a accomplished by transferring the Salmisaari side barrier on a ground support. This arrangement is, however, difficult as due to the curved equalizing line of the bridge, the sight contact would be lost between the barrier and the bridge quard's cabin. Thus, using a barrier would make it necessary to employ eg. television equipment by means of which the bridge guard can check the situation at the barrier when making traffic arrangements.

3.3 Strengthening of the bridge

On the basis of the performed study, one can draw a conclusion that the bridge cannot be strengthened sufficietly to withstand a collision when the ship's speed is 6 knots and the ship's mass what was presumed in the study. By growing the seizing capacity of the bearings higher, to 3 MN, i.e. 4.4-fold of the original in average, the energy absorption of the support structures can be made ca. 19.5-fold.

3.4 Thoughts concerning bridge design

When considering design of new bridges, it can be noted that the lateral design loads are very small as compared with the forces created in ship collisions. As it is often necessary to design the groundwork of the bridges for ice loads, employment of stronger bearings could considerably increase the bridges capacity of carrying lateral loads. On the other hand, this would result in the damages spreading out to concern also the groundwork of the bridge in a collision. Factors affecting safety include, among others, straightness of the ship channel when approaching the bridge, spaciousness of the bridge openings, access of traffic to the bridge when a ship is approaching, effect of wind and water height on the ship, location of support and cover structures beyond the range of the ship, etc.

LITERATURE

1. OLNHAUSEN W., Påsegling av bropelare. Teknisk tidskrift 1966, Häfte 17.
2. WOISIN G., Design against collision. International Symposium on advances in marine technology. Norway, June 1979.
3. ROIVAINEN T., Laivan törmäyksen vaikutus siltaan (Effect of a collision of a ship to a bridge).Thesis, under supervision of Professor H. Paavola, Helsinki University of Technology, 1982.

Energy Absorption in Ship-Platform Impacts

Absorption de l'énergie dans les chocs navire - plate-forme

Energieabsorption bei Zusammenstößen zwischen Schiffen und Plattformen

Tore SØREIDE
Professor
Norwegian Inst. Technol.
Trondheim, Norway

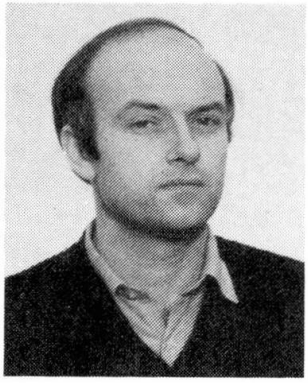

Tore Søreide, born 1948, got his civil engineering degree and dr.ing.degree at the Norwegian Institute of Technology. After three years in a consulting firm he is now professor in structural mechanics.

Jørgen AMDAHL
Naval Architect
Norwegian Inst. Technol.
Trondheim, Norway

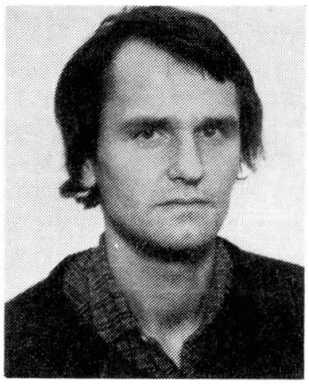

Jørgen Amdahl, born 1951, got his naval architecture degree at the Norwegian Institute of Technology. For three years he was at the research division of Det norske Veritas and is now studying for his dr.ing.degree.

SUMMARY
The paper deals with theoretical and experimental studies on ship-platform collision. General impact mechanics is presented together with a discussion on present design methods. A series of tests on models of platform bracing and bulbous bows is described with emphasis on load-deformation behaviour and the influence from impact velocity on the energy absorption capability.

RÉSUMÉ
L'article aborde certaines études théoriques et expérimentales portant sur les collisions navire - plate-forme. La mécanique générale des chocs est décrite et des commentaires sont faits sur les méthodes actuellement employées pour le projet. Une série d'essais a été pratiquée sur des modèles d'armature de plate-forme et de bouées en forme de bulbe. Une attention particulière est accordée au comportement de déformation en charge et à l'influence exercée par la vitesse du choc sur les capacités de l'absorption d'énergie.

ZUSAMMENFASSUNG
Der Artikel behandelt theoretische und experimentelle Untersuchungen von Zusammenstößen zwischen Schiffen und Plattformen. Allgemeine Aufprallmechanismen werden gemeinsam mit einer Erörterung über gegenwärtige Konstruktionsverfahren dargestellt. Eine Reihe von Tests mit Modellen von Plattformverstrebungen und Wulstbugen wird beschrieben, wobei der Schwerpunkt auf dem Lastverformungsverhalten und dem Einfluß der Aufprallgeschwindigkeit auf die Energieabsorptionseigenschaften liegt.

1. INTRODUCTION

Ship collisions with platforms have been identified as one of the possibly major hazards in connection with offshore oil activity. Statistics for world wide operation platforms during 1/1-70 to 31/12-80 indicate 9 cases with total or severe damage of the platform among 114 incidents with similar result [1]. At the same time many impact situations with minor consequences have been reported. As the number and size of vessels used in offshore operations (especially in the North Sea) increase, collision risk should be seriously considered in the design of platforms.

The event collision is characterized by the probability of occurrence and the inherent consequences. The two factors must be related to each other in the sense that major collisions endangering human lives, structures and environment must have low probability of occurrence while minor impacts occurring frequently must have small consequences. The probability as well as the consequences of collisions are affected by several factors such as traffic monitoring, navigational aids, operational limits, size of vessels and platform design and fendering. Consequently, a design procedure including a full evaluation of probability and consequences would be complex and not very feasible for practical use. Instead, socalled design accidents are evaluated based on judgement of probability of occurrence and consequences.

2. PRESENT DESIGN METHODS

The most frequent impacts against offshore platforms come from authorized vessels operating close to the platform. The consequencies of such impacts are normally small like local deformation of tube wall in bracing elements. However, with increasing size of supply vessels collision from such ships evidently defines a design limit state for the platform. The DnV rules for mobile offshore units [2] specify a ship of 5000 tons displacement with impact speed 2 ^{m}/sec as a design limit state.

A new design philosophy is related to impact analysis in the sense that structural capacity is given as energy absorbing capability rather than as ultimate load. The DnV rules [2] specify 14 MJ (Mega Joule) as impact energy for sideway collision (40 percent added mass included) and 11 MJ for bow or stern collision (10 percent added mass included).

The present methods for design of offshore platforms against collision are conservative in the sense that the striking ship is normally considered as undeformable so that the platform is designed to absorb all impact energy.

In order to get a representative model of a ship/platform collision, deformation and energy absorbing characteristics of the two colliding bodies must be known. Pioneering work on the energy absorbing capability of ships has been carried out by Minorsky [3] relating the amount of energy absorbed to the volume of damaged material. Most of the research on ships has been directed towards the protection of the reactor in nuclear powered ships [4] and few attempts have been made to develop general analytical models for the deformation process.

3. IMPACT MECHANICS

The derivation of a mathematical model of ship/platform impact is based upon two criteria:

a. Conservation of momentum
b. Conservation of energy

Assuming that the impact duration is short compared with the natural periods of motion for platform and ship the subsequent energy expression emerges

$$E_s + E_p = \frac{1}{2} m_1 v_1^2 \frac{(1 - v_2/v_1)^2}{1 + \frac{m_1}{m_2}} \qquad (1)$$

where

m_1 = mass of striking ship including added mass (40 percent of vessel displacement for sideway collision and 10 percent for bow or stern collision [2])
m_2 = mass of semisubmersible platform including added mass
v_1 = velocity of striking ship immediately before collision
v_2 = velocity of semisubmersible platform immediately before collision
E_s = energy absorbed by ship
E_p = energy absorbed by platform

From Eq. (1) it is seen that in case ship and platform have opposite directions of velocity prior to impact the amount of plastic energy to absorb may exceed the kinetic energy of the ship.

For collision against a fixed jacket type of structure the corresponding energy expressions are obtained by introducing $m_2 = \infty$, $v_2 = 0$ in Eq. (1).

In the lack of reliable data for energy absorption in ships E_s is usually neglected, leading to a conservative design of the platform structure.

4. LOAD-DEFORMATION CHARACTERISTICS OF PLATFORM BRACING

For moderate impacts the energy absorption associated with global deformation of the platform is of minor importance and is usually neglected. The main contribution comes from deformation of the stroken bracing element either in the form of local deformation of tube wall for high D/t ratios, beam deformation or a combination of both modes.

4.1 Theoretical Models

4.1.1 Local Deformation of Tube Wall

It is not possible to present one single analytical model for local energy absorption. Several types of models must be considered related to various impact situations. A head-on collision gives a more concentrated force than a sideway impact (Fig. 1) and results in a larger amount of local energy absorption.

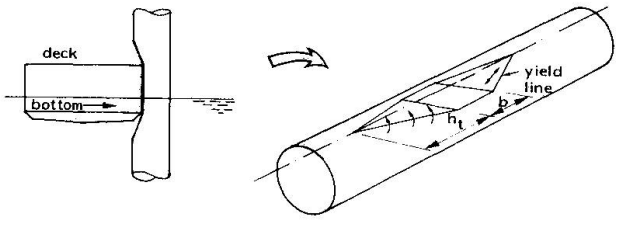

Fig. 1 Plastic mechanism for sideway impact by supply vessel

A simple yield line model for the case of sideway impact has been presented by Furnes and Amdahl [5]. The theoretical model gives good agreement with test results for moderate indentations.

4.1.2 Analytical Model for Beam Deformation

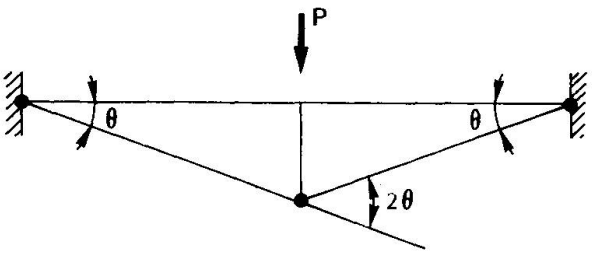

Fig. 2 Collapse mechanism for bracing element

Fig. 2 shows a collapse model of a bracing element where the ends are assumed restrained against axial movement and rotation. In this case the load carrying capacity increases considerable as the beam undergoes finite deflections due to the development of membrane tension forces. For a centrally loaded tubular beam the load-deflection expression reads [6]

$$\frac{P}{P_0} = \sqrt{1 - \left(\frac{w}{D}\right)^2} + \frac{w}{D} \arcsin \frac{w}{D} \; ; \; \frac{w}{D} \leq 1 \qquad (2)$$

$$\frac{P}{P_0} = \frac{\pi}{2} \frac{w}{D} \; ; \; \frac{w}{D} > 1 \qquad (3)$$

where w is the central deflection at the point of impact and D is the tube diameter. P_0 is the plastic collapse load of a circular tube in pure bending:

$$P_0 = \frac{8M_p}{\ell} = \frac{8\sigma_y D^2 t}{\ell} \qquad (4)$$

In a real frame structure the bracing elements sustain a certain degree of elastic support from the joints. Such elastic restrictions can be included in the above model [6], the major problem being to obtain realistic estimates on tubular joint flexibility.

Restrictions must be set on the maximum D/t-ratio for which this rigid-plastic theory can be used so that the full plastic capacity is retained during deformation. Sherman [7] predicts from tests $D/t < 35$ while the API rules [8] prescribe $D/t < 9000/\sigma_y$ (σ_y is yield stress in N/mm^2).

4.1.3 Tubular Joint Capacity

A major requirement for the yield hinge model in Fig. 2 to be valid is that the tubular joints can sustain bending moment and membrane force at the beam ends. Thus, failure criteria for tubular joints must be checked against plastic capacities of the bracing elements in order to ensure full energy absorption capability. Valuable information on capacity of unstiffened tubular joints has been presented by Yura et al. [9] and in design codes [8,10].

4.2 Tests on Bracing Elements

For jackets and semisubmersible platforms characteristic dimensions of bracing elements in water plane are:

$1.0 < D < 2.0$ m
$20 < D/t < 100$
$10 < L/D < 30$

A series of model tests on energy absorption in bracing elements has been performed with the following range of variation:

$63 < D < 125$ mm
$22 < D/t < 61$
$10 < L/D < 20$
$204 < \sigma_y < 328$ N/mm^2

The effect of membrane forces on the energy absorption capability of bracing elements is illustrated by Fig. 3 in which load-displacement curves are shown for static testing of two similar models with different end conditions. The lower curve relates to horizontally free end conditions and the upper curve relates to horizontally fixed ends. In both cases the ends are clamped against rotation.

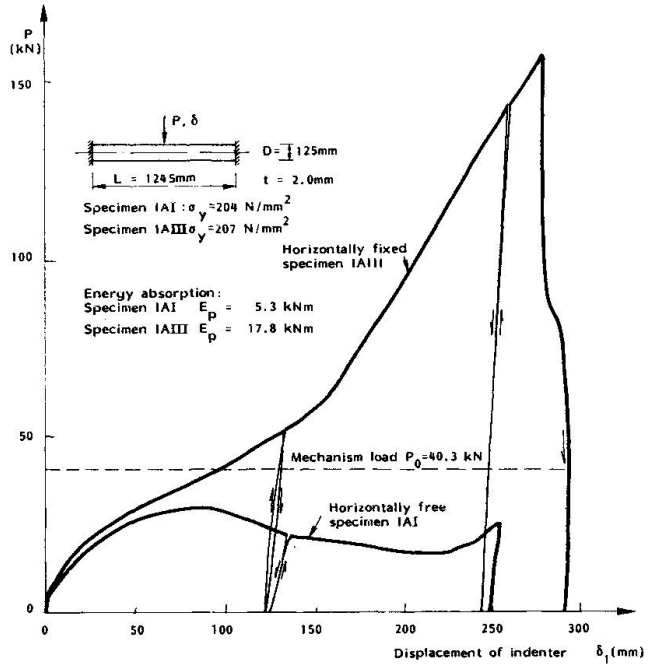

Fig. 3 Load-displacement curves for indenter.
Horizontally free and horizontally fixed ends

The energy absorbed is 5.3 kNm and 17.8 kNm, respectively. The two models showed two different collapse modes. For the horizontally free case local wall crippling occurred on the compression side of the end, while the membrane tension caused a rupture type of failure for the horizontally fixed specimen.

The effect of dynamic loading on the load-displacement curve is demonstrated by Fig. 4. Solid line represents static load and dotted line dynamic load corresponding to a real velocity of 2.0 m per second. It is seen that the energy absorption capability is raised by approximately 10 percent. Inertia forces are negligible for the actual range of velocity and the main increase in stiffness comes from the strain-rate effects.

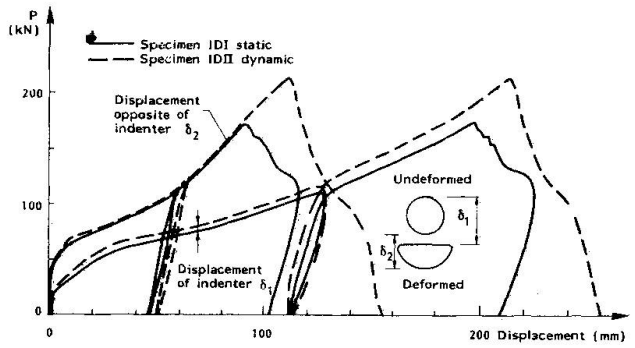

Fig. 4 Static and dynamic load-displacement curves

5. ENERGY ABSORPTION IN BULBOUS BOWS

The structural configuration of a ship bow is complex, being comprised of an outer shell stiffened by a grid of frames and stringers. This complexity makes it difficult to apply conventional collapse models for panels for estimating energy absorption capability.

5.1 Plastic Collapse Models for Bulbous Bows

Bulbous bows bear some resemblance to cylindrical shells. The simplest configuration as far as structural modelling concerns is a bulb in the form of a ringstiffened circular cylinder. Plastic collapse models for this case have been derived by Alexander [11] and by Johnson et al. [12].

After initial buckling [13] the ringstiffened cylinder continues to deform into the plastic region. Depending on the shell geometry the post-buckling behaviour may take on two forms, either with the shell in axisymmetric convolutions or with asymmetric folds.

For axisymmetric collapse the average load during plastic deformation is found to be [11]

$$P_{av} = \frac{\pi \sigma_y t^2}{\sqrt{3}} \left(\frac{\pi}{2}\frac{D}{h} + 1 + \sqrt{3}\frac{h}{t}\right) \qquad (5)$$

where

σ_y = yield stress
t = shell thickness
D = shell diameter
h = stiffener spacing

Static considerations of impact may underestimate the energy absorption capability. A simple method of including strain rate effects, has been suggested by Cowper and Symonds [14]

$$\frac{\sigma_y'}{\sigma_y} = 1 + \left(\frac{\dot{\varepsilon}}{\dot{\varepsilon}_0}\right)^{\frac{1}{m}} \qquad (6)$$

where ε_0 and m are material constants determined from experiments. Recommended values for steel are m = 5, $\dot{\varepsilon}_0 = 40$ sec^{-1}.

The average strain rate in the cylinder wall may be approximated by [15, 16]

$$\dot{\varepsilon} = \frac{\dot{u}}{4h} \tag{7}$$

5.2 Tests on Bulbous Bows

A series of collision tests on bulbous bow models has been carried out. The first ten models comprised ringstiffened cylindrical shells. All models have diameter 400 mm and shell thickness and stiffener spacing are given in Table 1. The specimens MA1-MA4 are machined cylinders that are almost ideal in the sense that residual stresses and shape imperfections are small. FA1-FA6 are fabricated models rolled from 2 mm plate, and then closed by a longitudinal butt weld.

Table 1 gives comparison between average loads from experiments and according to the above mechanism models. The rate of displacement is $\dot{u} = 0.125$ mm/sec. for all models and the theoretical solutions are based upon the dynamic yield stress according to Eqs. (6-7).

Test specimen	Wall thickness mm	Stiffener spacing mm	Static yield stress MPa	$P_{av,e}$ Exper. MN	$P_{av,th}$ Theory MN	$\frac{P_{av,th}}{P_{av,e}}$
MA1	0.97	23.0	267	68.1	63.6	0.93
MA2	1.22	37.0	267	103.2	75.3	0.73
MA3	0.99	33.5	267	80.5	55.5	0.69
MA4	0.98	33.5	267	62.5	55.6	0.89
FA1	2.03	47.0	236	158.2	126.6	0.80
FA2	2.06	57.0	236	147.8	122.7	0.83
FA3	2.06	67.0	236	143.6	120.6	0.84
FA4	2.04	97.0	228	139.9	125.9	0.90
FA5	2.05	117.0	228	147.4	141.5	0.96
FA6	2.05	-	228	101.4	82.1	0.81

Table 1 Experimental and theoretical average loads for bulb models

Table 1 indicates some discrepancy between analytic predictions and test results. For all models the mechanism calculations underestimate the average load. Several factors can explain this discrepancy. The most important effects are:

a. Inaccurate representation of deformation mode in mechanism models
b. Movable plastic hinges are not included in theoretical models
c. Inaccurate representation of material data

The load-displacement curve for specimen MA4 is shown in Fig. 5. The post-buckling behaviour is explained by the successive formation of plastic mechanisms between ring stiffeners.

The above ringstiffened cylindrical shells represent idealized models of bulbous bows. In addition to transverse stiffening the bulbs normally also contain longitudinal stiffening system consisting of stringers and centerline bulkhead. Further, the cross sections of bulbs are more elliptic in shape.

Test on a more realistic model is illustrated in Figs. 6-8.

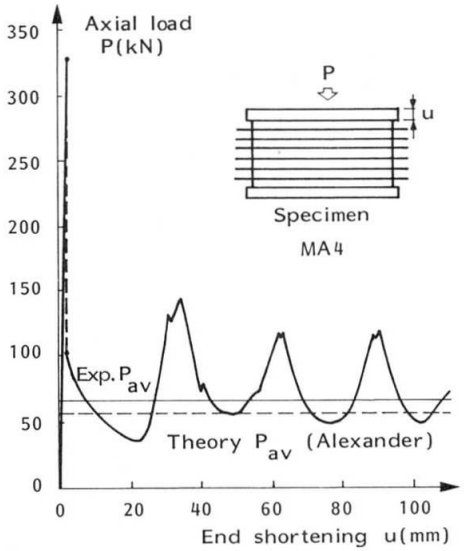

Fig. 5 Load-displacement curve for ringstiffened cylinder MA4

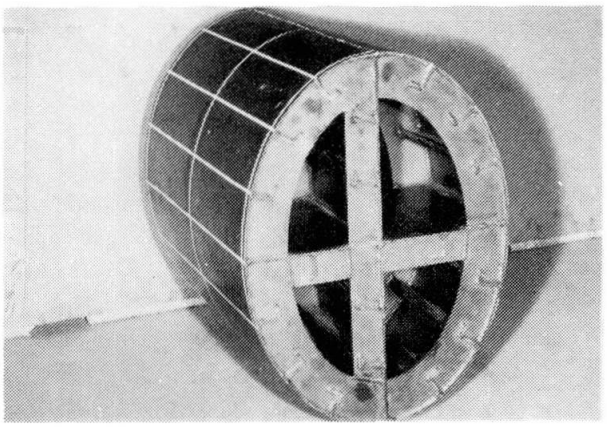

Fig. 6 Bulb model with combined stiffening

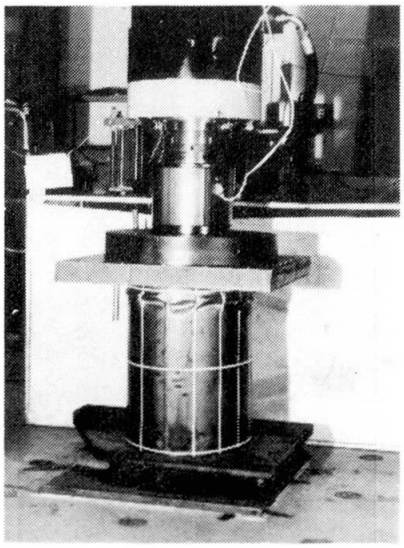

Fig. 7 Initial buckling of model in Fig. 6

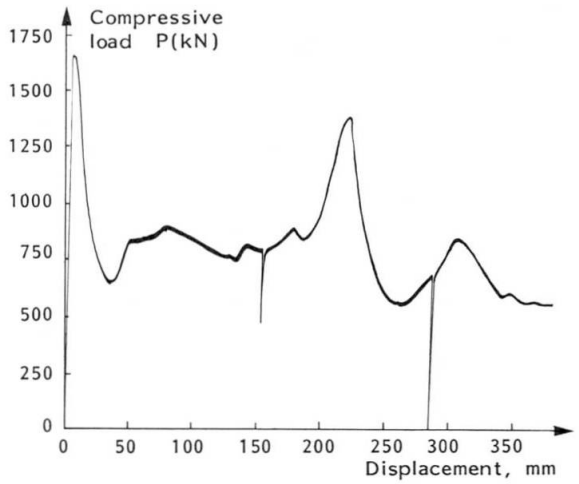

Fig. 8 Load-displacement curve for model in Fig. 6

6. CONCLUSIONS

The present work clearly demonstrates the difficulties in developing theoretical models for estimating energy absorption in ship/platform collisions. For representing collapse behaviour of platform bracing a simple beam mechanism model can be applied, combined with a yield line model for local wall indentation. However, the variation in structural configuration of ship bows makes it difficult to come up with a general design formula for energy absorption. The paper proves the need for combined experimental and theoretical work within this field.

REFERENCES

1. MOAN, T. and HOLAND L., Risk Assessment of Offshore Structures. Experience and Principles. Structural Safety and Reliability (ed. Moan and Shinozuka), Proceedings of ICOSSAR '81, Elsevier Scientific Publishing Company, 1981.

2. DET NORSKE VERITAS, Rules for Classification of Mobile Offshore Units, 1981.

3. MINORSKY, V.V., An Analysis of Ship Collisions with Reference to Nuclear Power Plants. Journal of Ship Research, Vol. 3, 1959, pp. 1-4.

4. WOISIN, G., Die Kollisionsversuche der GKSS. Jahrbuch der Schiffbautechnischen Gesellshaft, 70.8, Hamburg 1976.

5. FURNES, O. and AMDAHL, J., Ship Collisions with Offshore Platforms. Intermaritec, Hamburg, 1980.

6. SØREIDE, T.H., Ultimate Load Analysis of Marine Structures. Tapir publishing company, Trondheim, Norway, 1981.

7. SHERMAN, D.R., Tests of Circular Steel Tubes in Bending. ASCE J. Struct. Div., Vol. 102, No. ST11, 1976, pp. 2187-2195.

8. AMERICAN PETROLEUM INSTITUTE, Recommended Practice for Planning, Designing and Constructing Fixed Offshore Platforms. API RP ZA, 1979.

9. YURA, J.A., ZETTLEMOYER, N. and EDWARDS, I.F., Ultimate Capacity Equations for Tubular Joints. OTC 3690, 1980.

10. DET NORSKE VERITAS, Rules for the Design, Construction and Inspection of Offshore Structures, 1977.

11. ALEXANDER, J.M., An Approximate Analysis of the Collapse of Thin Cylindrical Shells under Axial Loading. Quart. Journal of Mech. Appl. Math., Vol. XIII, Pt 1, 1960.

12. JOHNSON, W., SODEN, P.D., AL-HASSANI, S.T.S., Inextensional Collapse of Thin-Walled Tubes under Axial Compression. Journal of Strain Analysis, Vol. 12, No. 4, 1977.

13. ODLAND, J., On the Strength of Welded Ring Stiffened Cylindrical Shells Primarily Subjected to Axial Compression. Dr.ing. Report, Division of Marine Structures, The Norwegian Institute of Technology, Trondheim, 1981.

14. COWPER, G.R. and SYMONDS, P.S., Strain Hardening and Strain Rate Effects in the Impact Loading of Cantilever Beams. Brown Univ. Techn. Report No. 28, 1957.

15. WIERZBICKI, T. and ABRAMOWICZ, W., Crushing of Thin-Walled Strain Rate Sensitive Structures. Euromech Colloquium No. 121, August 1979.

16. AMDAHL, J. and SØREIDE, T.H., Energy Absorption in Axially Compressed Cylindrical Shells with Special Refernce to Bulbous Bows in Collision. Norwegian Maritime Research, Vol. 9, No. 4, 1981.

Leere Seite
Blank page
Page vide

Dynamical Determination of the Collision's Transient Load

Détermination dynamique de la charge transitoire, lors d'une collision

Bestimmung der dynamischen Belastung beim Schiffsanprall

Leonel F. REQUENA
Ingénieur ENSAE
CONSULAR
Buenos Aires, Argentine

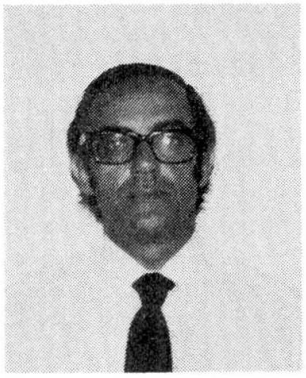

Leonel F. Requena, né en 1933, ingénieur diplômé à l'ENSAE, France, a travaillé dans plusieurs domaines d'application de la mécanique des milieux continus. Depuis cinq ans a conduit à Consular plusieurs études et projets de systèmes de protection de ponts contre les chocs de bateaux.

SUMMARY
The ship collision against a bridge pile is a transient phenomenon where, although the mechanical properties of the ship and the structure are known, the applied load as a function of time is not fully understood. This load is nevertheless necessary for the application of computer programs to the dynamical analysis of strains of several degrees of freedom structures. An evaluation method of the transient load by means of simplified models and results obtained while studying two existing bridges Argentine and Uruguay, is presented.

RÉSUMÉ
Le choc d'un bateau sur une pile de pont est un phénomène transitoire pour lequel, même en connaissant les propriétés mécaniques du bateau et de la structure, on ne connaît pas directement la charge appliquée en fonction du temps. La connaissance de cette charge est pourtant nécassaire pour l'application des programmes de calcul dynamique des efforts aux structures à plusieurs degrés de liberté. On présente une méthode de calcul au moyen de modèles simplifiés et des résultats obtenus pendant l'étude de deux ponts existants entre l'Argentine et l'Uruguay.

ZUSAMMENFASSUNG
Der Anprall eines Schiffes gegen einen Brückenpfeilerkopf ist ein vorübergehendes Phänomen: Obwohl die mechanischen Eigenschaften des Schiffes und des Tragwerks bekannt sind, ist die dynamische Last im Verlauf der Zeit ungenau bekannt. Die Kenntnis dieser Last ist jedoch notwendig für die Verwendung von EDV-Programmen zur dynamischen Berechnung des Tragwerks mit mehreren Freiheitsgraden. Es werden eine Berechnungsmethode mit vereinfachten Modellen vorgeführt und die erhaltenen Ergebnisse bei der Analyse zweier Brücken zwischen Argentina und Uruguay dargestellt.

1. PRESENTATION

C'est pour le compte de la C.A.R.U. (Comisión Administradora del Río Uruguay) que le consortium formé par Consular, d'Argentine, et Inasur de l'Uruguay, a entrepris, en 1981, l'étude de faisabilité des protections contre les chocs de bateaux des deux ponts existants sur le fleuve Uruguay entre l'Argentine et l'Uruguay. Parmi les problèmes posés par l'étude de la vulnerabilité des ponts et des viaducs d'accès aux chocs de bateaux était celui de définir la charge dynamique avec laquelle devait etre vérifiée chaque pile, ainsi comme la masse du bateau qui détruit la pile pour une vitesse d'approche donnée. On a était bien obligé d'imaginer une méthode. On a pris connaissance, à posteriori, que M. Fauchart, en France, (2), en avait imaginé une semblable. Il est, malgré tout, intéressant de montrer que le modèle de M. Fauchart (Modèle dynamique C) peut etre verifié et ajusté au moyen d'un modèle complet de la structure (Modèle dynamique A), a plusieurs dégrés de liberté, donnant et les déplacements et les efforts. Il a paru intéressant aussi de montrer quelle proportion de l'énergie du bateau était absorbée par la structure dans chaque cas analysé, montrant que l'hypothèse, parfois admise, du 50 %, est, en général, trop grossière.

Les ponts, construits en béton précontraint, possèdent les caractéristiques suivantes:

Pont Libertador General San Martín, entre les localités de Fray Bentos (U) et Puerto Unzué (A), comprend:
- un ouvrage principal, pont continu à trois travées (145 m, 220 m, 145 m).
- deux viaducs d'accès de portée courante de l'ordre de 70 m.

Pont General Artigas, entre les localités de Paysandú (U) et Colón (A), comprend:
- un ouvrage principal, à trois travées (97 m, 140 m, 97 m).
- deux viaducs d'accès de portée courante de l'ordre de 46 m.

2. PILE RIGIDE

On suppose que la charge F_1, pour une pile infiniment rigide et infiniment résistante est une fonction du temps $F_1(t)$ du type de la Figure 2.1. où Fmáx est la charge de plastification de la coque du bateau, d'apres G.Woisin & Gerlach (1). Pour définir la montée élastique de la function $F_1(t)$ on fait des hypothèses sur le comportement de la coque; on suppose que la déformation s_1, au temps t_1, de la demi-longuer L/2 de la coque est obtenue à partir d'une répartition linéaire de la tension de compression σ tout le long de la coque, du type:

$$\sigma = \sigma máx(1 - \frac{x}{L}) \qquad (2.1.)$$

où $\sigma máx$ est la tension de plastification. En intégrant la déformation

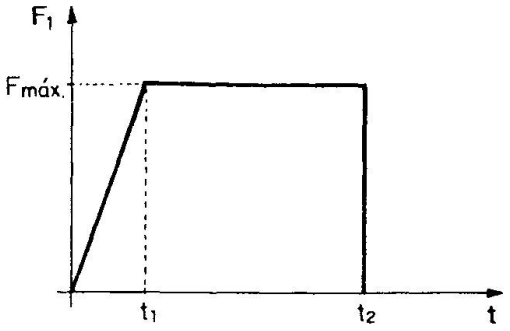

Figure 2.1

élastique sur la demi-longueur on obtient:

$$s_1 = \frac{3 \cdot \sigma máx \cdot L}{8 \cdot E} \qquad (2.2.)$$

où E est le module d'élasticité de l'acier.

La coque est remplacée par un ressort de rigidité:

$$k_2 = \frac{Fmáx}{s_1} \qquad (2.3.)$$

interposé entre le centre de gravité du bateau (supposé situé à L/2) et le point de contact avec la pile.

Pendant le processus élastique le centre de gravité du bateau avance comme la masse m_2 d'un systeme dynamique à un dégré de liberté de rigidité k2 et vitesse initiale Vo, dont la pulsation propre est:

$$\omega_2 = \sqrt{\frac{k2}{m2}} \qquad (2.4.)$$

Le temps t_1 est:

$$t_1 = \frac{1}{\omega 2} \cdot \text{arc sin} \frac{\omega 2 \cdot s1}{Vo} \qquad (2.5.)$$

La vitesse V_1, au temps t_1, est:

$$V_1 = V_o \cdot \cos \omega_2 \cdot t_1 \qquad (2.6.)$$

La quantité de mouvement du bateau s'annule au temps t_2, d'où:

$$t2 = t1 + \frac{m2\ V1}{Fmáx} \qquad (2.7.)$$

3. PILE SOUPLE

L'élasticité de la pile modifie, en géneral, l'évolution de la force $F_1(t)$. Nous appellerons "modèle dynamique A" à un modèle approprié de la structure du pont et introduit dans un programme de calcul dynamique des déplacements et des efforts (STRUDL, par exemple), pour lequel la charge F1(t) doit être une donnée. Si l'on applique la charge F1(t) obtenue pour la pile rigide a ce modèle on obtient en général une déformation de la structure en fonction du temps. Le calcul de la charge F1(t) doit donc être repris pour tenir compte de la rigidité réelle de la pile. Pour cela on propose de représenter le phenomène au moyen d'un modèle simplifié que nous appellerons "modèle dynamique B", où la structure est réprésentée par sa masse effective m_1 au point d'application de la charge et sa rigidité effective au même point. (Figure 3.1.)

B

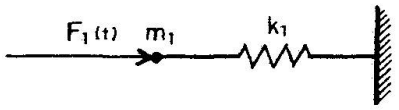

Figure 3.1

C

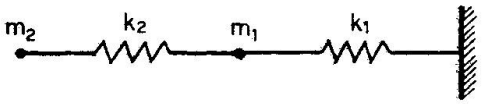

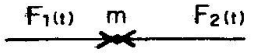

Figure 3.2

Pour ce modèle les inconnues son m_1, k_1. Il s'agit de trouver une paire de valeurs m_1, k_1 tels que la réponse du modèle dynamique B sous la charge F1(t) soit égale a la réponse du modele A sous la même charge. On procède par tatônnements à partir des valeurs estimées de m_1, k_1. Ceci fait on calcule F1(t) en utilisant le "modele dynamique C", Figure 3.2., à deux degrés de liberté, où les conditions initiales sont $y_1 = y_2 = y_1 = 0$; $\dot{y}_2 = V_o$. La force F2 est la réaction élastique de la structure à chaque instant.

Les différentes phases du phenomène transitoire sont:

a) Phase élastique

$$F1 = k2\ (y2 - y1) \qquad (3.1.)$$
$$F2 = k1\ y1 \qquad (3.2.)$$

Equations du mouvement:

$$m1\ \ddot{y}1 + F2 - F1 = 0 \qquad (3.3.)$$
$$m2\ \ddot{y}2 - F1 = 0 \qquad (3.4.)$$

La phase se termine quand F1(t) = Fmáx, et commence la phase plastique.

b) Phase plastique

Dans les équations (3.3.) et (3.4.), F1(t) = Fmáx, les équations son indépendantes. Dans un intervale de temps dt la déformation plastique dsp de la coque est égale a la différence des déplacements:

$$dsp = dy2 - dy1$$

Le processus termine quand dsp = 0, soit quand dy2 = dy1, ou (en divisant par dt) quand $\dot{y}2 = \dot{y}1$, c'est à dire quand les vitesses des deux masses son égales.

On reprend une phase élastique en repositionnant la masse m2 d'après la formule:

$$y2 = y1 + s1$$

de façon de commencer la phase élastique descendante avec la valeur F1 = Fmáx (Formules 3.1. et 2.3.).

c) "Vol libre" de m2

La masse m2 est répoussée transitoirement ou définitivement (la force F1(t) = 0 pour tout y1 ≥ y2) les équations (3.3.) et (3.4.) sont indépendantes. On recommence una phase élastique s'il existe un temps t pour lequel on retrouvre y1 = y2.

La charge obtenue par cette méthode est appliquée au modèle dynamique A. On vérifie que la réponse de ce modèle est semblable à celle du modèle C sous la meme charge F1(t) (en particulier le maximum positif du déplacement du point d'impact). En général cette première approximation est suffisante.

4. APPLICATION

Le bateau a una longueur L = 180 m; une masse m2 = 17.000 t; une vitesse initiale Vo = 1,81 m/seg.

On prend σmáx = 1.400 kgf/cm2; E = 2,1 x 10^6 kgf/cm2; Fmáx = 13.000 tf.

On obtient:

s1	= 0,045 m	t1	= 0,025 s
k2	= 289.000 tf/m	V1	= 1,714 ms^{-1}
ω2	= 12,9 s^{-1}	t2	= 0,254 s

l'énergie cinétique Ec = 2.839 tf.m

Dans la Figure 4.1. on présente la réponse du modèle dynamique A (programme STRUDL) et celle du modèle dynamique B, celle-ci obtenue avec la paire de valeurs:

$$m1 = 3.433 \text{ t}$$
$$k1 = 23.500 \text{ tf/m}$$

Dans la Figure 4.2. on présente la charge obtenue avec le modèle dynamique C, dans la Figure 4.3. le déplacement du point d'impact obtenu avec les modèles dynamiques A et C.

La rigidité statique de la pile au point d'impact obtenue du modèle dynamique A était:

$$k1' = 19.800 \text{ t/m}$$

et la masse de la pile plus la partie majorante du tablier était:

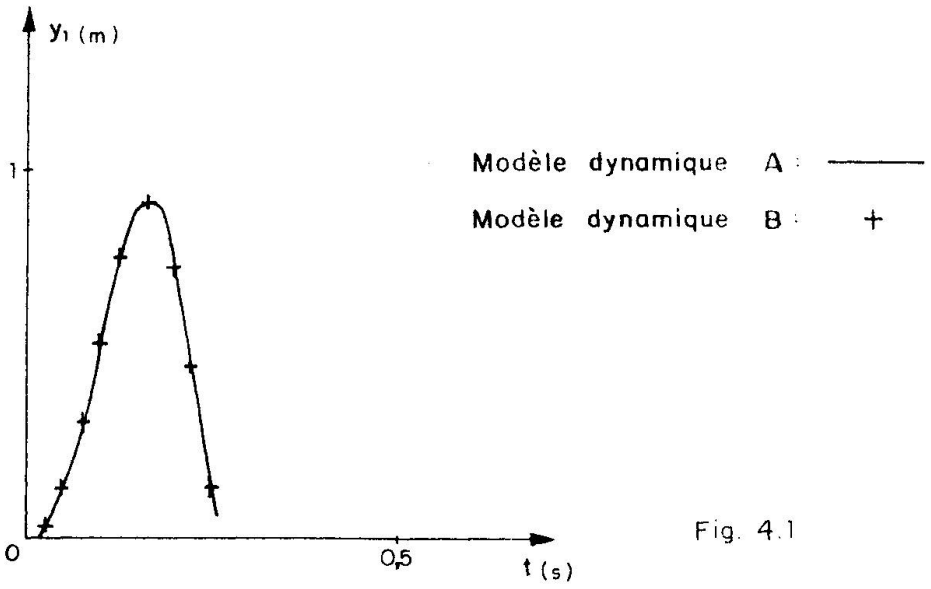

Fig. 4.1

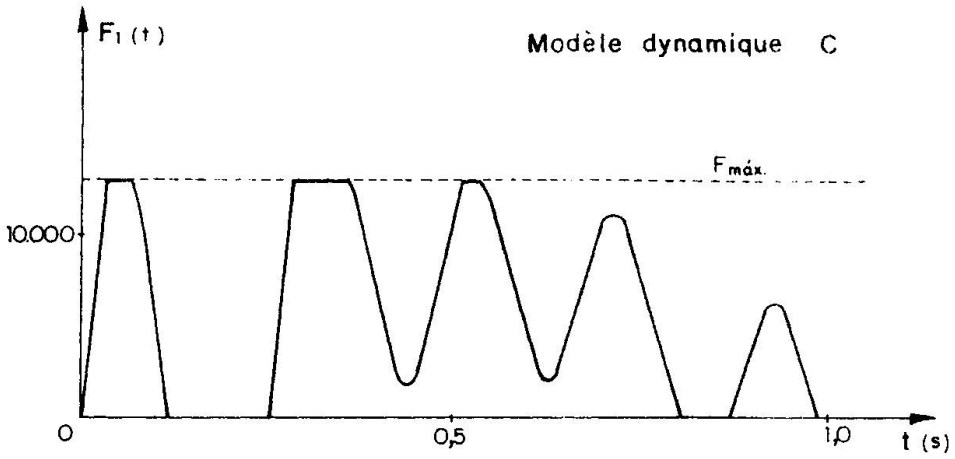

Fig. 4.2

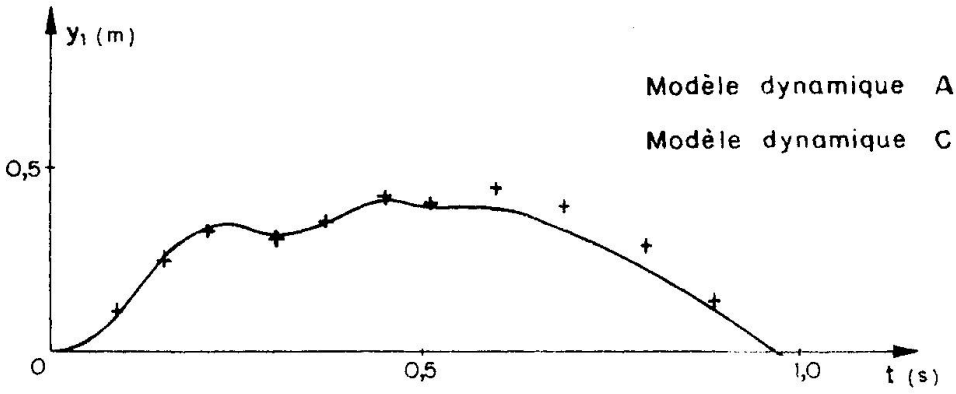

Fig. 4.3

$$m1' = 6.450 \text{ t}$$

Il fallait donc ajuster le modèle dynamique B a la réponse du modele A, qui est le résultat de la superposition de plusieurs modes de vibration, pour représenter convenablemente les caractéristiques dynamiques de la pile.

Pour des valeurs 10 k2 et k2/10 les résultats sont semblables, la rigidité de la coque n'etant donc pas relevante. Une valeur quelque peu supérieure de Fmáx ne change pas non plus les résultats.

5. DETERMINATION DE LA MASSE DU BATEAU QUI DETRUIT LA PILE

On a trouvé dans tous les cas que les charges dynamiques appliquées aux piles dépassaient largement leur résistance. Il se posait donc la question de définir la masse du bateau qui détruit chaque pile, afin de connaître la probabilité de qu'un bateau donné, dont la fréquence relative de passage est connue, détruise la pile, étant donnée une vitesse d'approche Vd.

Pour ce faire on s'est appuyé sur le modele dynamique C. Les efforts étant proportionnels au déplacements on a cherché la valeur de m2 (associée a une valeur correspondante de Fmáx) qui réduit le déplacement maximum y1máx a la valeur:

$$y1'máx = \nu \cdot y1máx \qquad (5.1.)$$

où ν est le coefficient de sécurité à la rupture trouvé pour le cas analysé ($\nu < 1$, modèle dynamique A).

La masse du bateau qui rempli cette condition pouvait être définie a partir de l'énergie cinétique donnée par:

$$E'c = \alpha \cdot \nu \cdot Ec \qquad (5.2.)$$

ou α était proche de l'unité.

On obtient:

$$m2' = \frac{2\ Ec'}{Vd^2} \qquad (5.3.)$$

On pense que la valeur de α dépend de la structure considerée et des valeurs Vo, Vd.

6. ENERGIE ABSORBEE PAR LA STRUCTURE

L'énergie absorbée par la structure dans chaque cas analysé peut être stimée a partir de la rigidité k1:

$$Ec = \frac{1}{2} k1 \cdot y_1^{2}\ máx \qquad (6.1.)$$

On a trouvé que cette valeur était placée entre le 2 % de l'énergie cinétique du bateau pour les piles les plus rigides jusqu'au 86 % pour les plus souples.

REFERENCES

1 - G. Woisin & Gerlach.

"On the Estimation of Forces Developed in Collisions between Ships and Offshore Lighthouses".

IALA Conference, Stockholm, 1970

2 - J. Fauchart.

"Choc de bateau sur un obstacle déformable. Essai d'analyse pour l'étude de faisabilité du pont du Verdon, sur la Gironde".

Travaux. N° 562. Janvier 1982.

Indentation Tests on Simplified Models of Ship Structures

Essais de déformation sur des modèles de navires

Verformungstest an vereinfachten Modellen von Schiffstragwerken

H. Y. LOW
Eng.
Det norske Veritas
Oslo, Norway

C. T. MORLEY
Lecturer
University of Cambridge
Cambridge, England

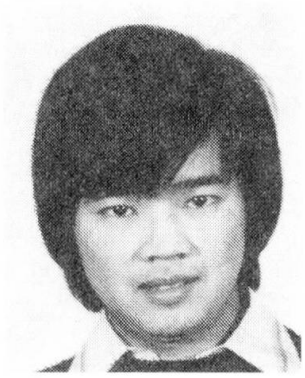

SUMMARY
The paper describes loading tests on scale models of ships' sides, indented by a stiff circular indenter representing the shaft of an offshore concrete platform. Simplified theoretical analyses based on large-deflection plastic theory are described and compared with the experimental results. Design forces for typical supply boats are derived.

RÉSUMÉ
La présente étude décrit des essais en charge effectués sur des modèles de flancs de navires gardant l'empreinte d'un objet rigide et circulaire, représentant le puits d'une plate-forme pétrolière en béton. Des analyses théoriques simplifiées, fondées sur la théorie plastique des grandes flèches, sont décrites et comparées aux résultats d'expériences. Il en est déduit les forces pour la conception des bateaux.

ZUSAMMENFASSUNG
Der Artikel beschreibt Lastversuche an Modellen von Schiffsseiten, die durch einen starren kreisförmigen Stempel verbeult werden, der einen Pfeiler einer küstenfernen Betonplattform darstellt. Vereinfachte theoretische Analysen im plastischen Zustand mit starker Durchbiegung werden beschrieben und mit den experimentellen Ergebnissen verglichen. Entwurfsregelungen für typische Schiffe werden abgeleitet.

INTRODUCTION

In recent years designers of offshore concrete platforms have become increasingly aware of the need to design for accidental loads arising from ship impact. Ship-offshore concrete platform collisions generally come into the category of "soft impact" problems and the deformation properties of the ship are then of crucial importance. In order to throw light on the deformation properties of the various components in the side structure of a ship as it is indented, a series of model tests has been carried out. A further objective of the tests was to help develop and verify simple methods of analysis to predict the force-indentation and hence energy absorption characteristics of the various structural components of a ship. There seems to be little published experimental work, with the notable exception of [1], on the deformation properties of ship structures indented by a body with a substantial radius of curvature. The test models used in [1] appear to have rather thicker plating than is of relevance to the problem of collisions between supply vessels and offshore concrete platforms.

2. TEST MODELS AND ARRANGEMENT

The test models were intended to reproduce, at a scale of approximately 1:10, the main structural features of supply vessels in the 1275 dwt category. Cold rolled mild steel sheets of thickness 1 mm were spot welded together to form simplified scale models of one or two bays of the side structure, each bay having a width of 360 mm. Fig. 1 shows the loading scheme used while Fig.2 and Table 1 give details of the test models. Both transversely and longitudinally stiffened models were tested. An attempt was made to simulate the support conditions for the indented part of the side structure thought to be afforded by the rest of the ship. Mild steel plates 3mm thick were spot welded to the edges of each test model to enable it to be bolted to a test rig constructed from standard laboratory channel sections. The models were loaded by means of a pair of screw jacks through a solid concrete indenter of part circular section and radius 720 mm so that first contact occurred either at a main transverse frame or between main transverse frames. The loading sequence was deflection controlled and the

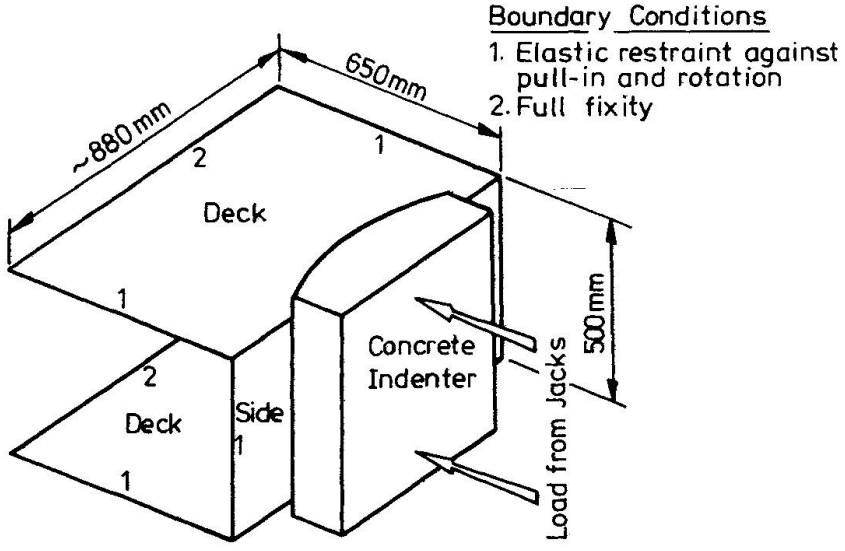

Fig.1 Overall dimensions of Typical Test Model and Loading Scheme

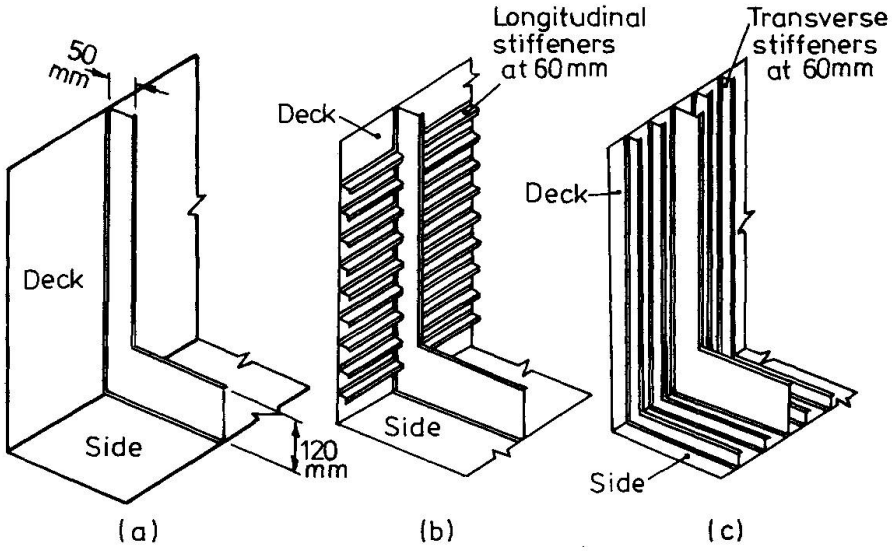

Fig. 2. Stiffener Arrangements used in Test Models

Test Model	Stiffener Arrangement (ref. Fig.2)	Position of First Contact	Average Yield Stress σ_o N/mm^2
TV/2/M	(a)	m	205
TV/3/M	(a)	m	200
LT/4/M	(b)	m	229
LT/8/M	(b)	m	271
TV/5/B	(a)	b	216
LT/6/B	(b)	b	265
TV/7/M	(c)	m	268

m = midspan between main transverse frames.
b = at a main transverse frame

Table 1 Details of Test Models

stiff loading system enabled the falling parts of the load - indentation curves to be recorded. The maximum indentation in each test was of the order of 50 mm applied in discrete increments over a period of approximately 5 hours.

3. TEST INSTRUMENTATION

Instrumentation consisted of two compression load cells, strain gauges, dial gauges and a shadow moiré grid. The strain gauges were used to monitor the development of any membrane tension in the side plating. The indentation and deformed profile of one of the deck plates were determined by means of dial gauges. The profile of the second deck plate was determined by a shadow moiré technique, utilizing a coarse grid and point light source producing a fringe pattern giving contours of out-of-plane displacement over a large area.

4. ANALYSIS OF TEST RESULTS

The main test results in the form of force - indentation curves are given in Fig.3 (a)-(e). The basic approach adopted in a simplified theore-

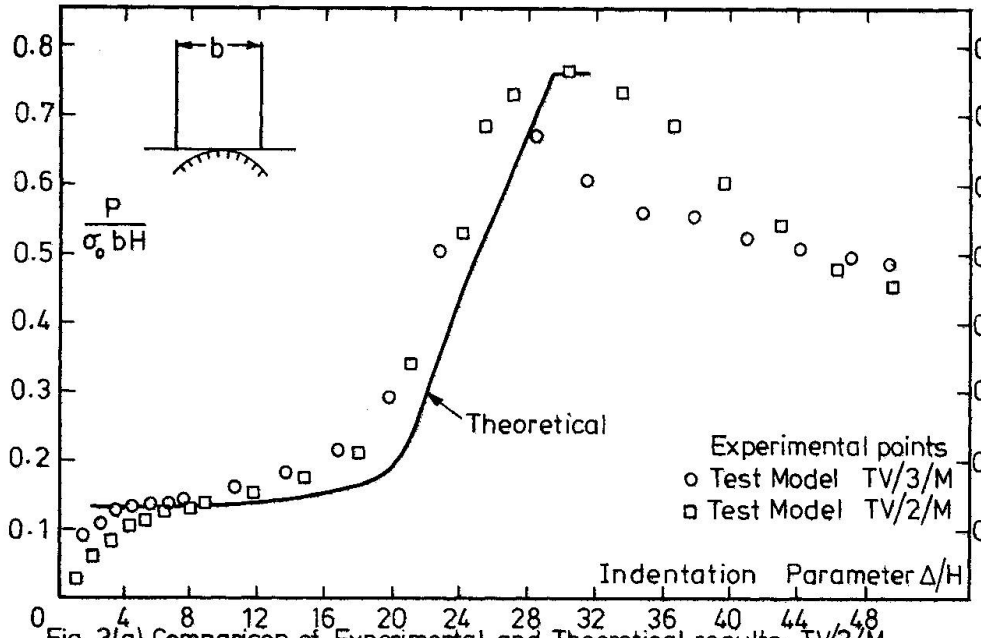

Fig. 3(a) Comparison of Experimental and Theoretical results: TV/3/M

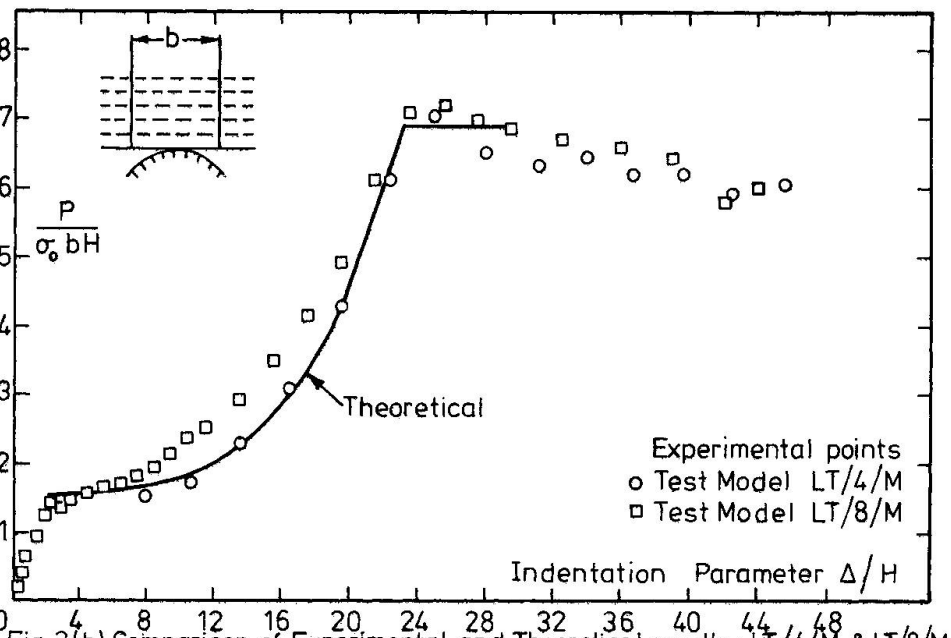

Fig. 3(b) Comparison of Experimental and Theoretical results: LT/4/M & LT/8/M

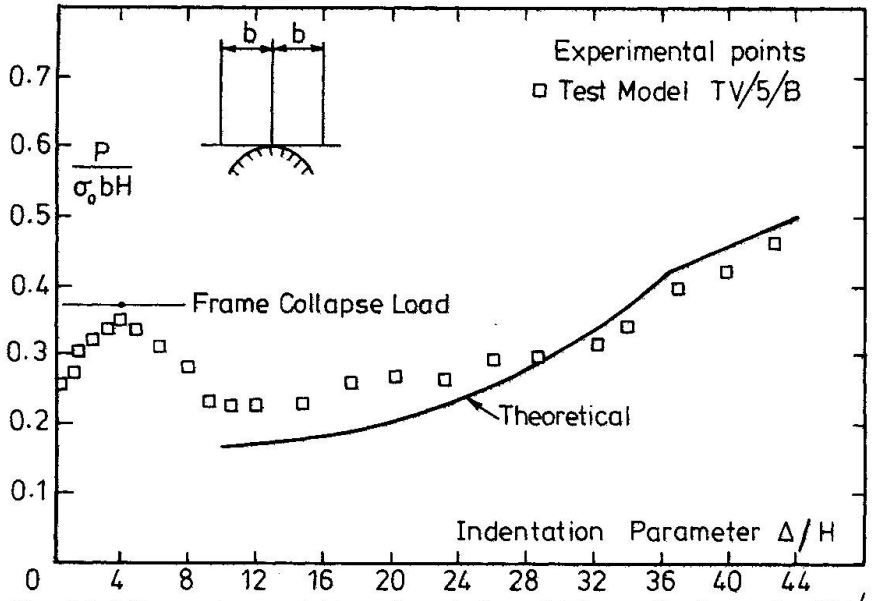

Fig. 3(c) Comparison of Experimental and Theoretical results: TV/5/B

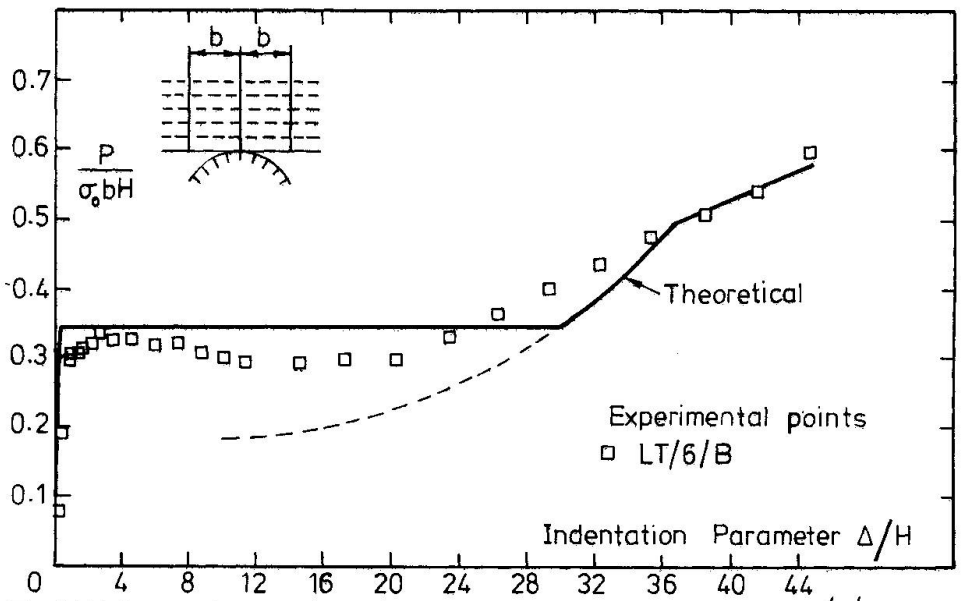

Fig 3(d) Comparison of Experimental and Theoretical results: LT/6/B

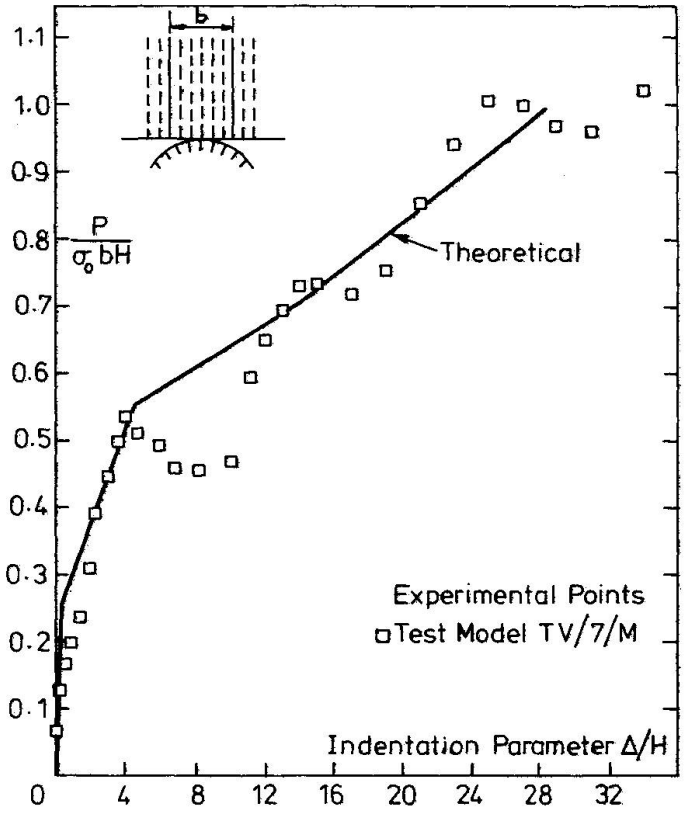

Fig.3 (e) Comparison of Experimental and Theoretical Results : TV/7/M

tical analysis of the models was to divide each model into simpler elements, to treat each element by an appropriate form of plastic theory allowing for large deformations, and to sum the force contributions of these elements at a given indentation.

4.1 Side Plating

The side plating was analysed as a beam spanning between the main transverse frames and subject to a transverse spreading load applied through a rigid circular indenter (Fig.4). The analysis for such a loading case has been presented in [2]. The degree of restraint against pull-in at the beam supports was determined empirically and reflected the flexibility of the test rig as well as the model itself.

4.2 Main Transverse Frame

The post-buckling strength of the frame corners was assessed by means of an upper bound plastic analysis involving tension field theory (following [3]). The mechanism considered is shown in Fig.5. The total strength of a main transverse frame is then given by the sum of the frame corner load and the axial load in an effective width of associated deck plating. Dwight's [4] effective width formula has been used here but there is no objection to the use of other well-founded formulae.

4.3 Unstiffened Deck Plating (apart from main frames)

The strength of the unstiffened deck plating bounded by a pair of main transverse frames was determined by an ultimate load method proposed by Roberts and Rockey [5]. A portion ($\frac{1}{t}$) of the side plating has been assumed to act as a flange to each deck plate, and the flange plastic moment has

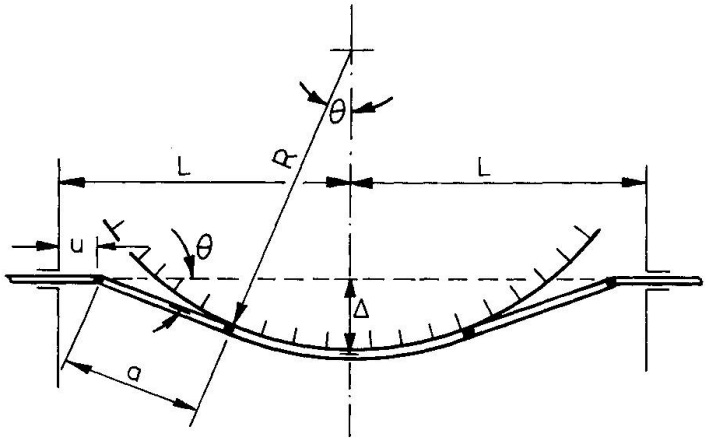

Fig. 4 Beam Loaded through a Circular Indenter

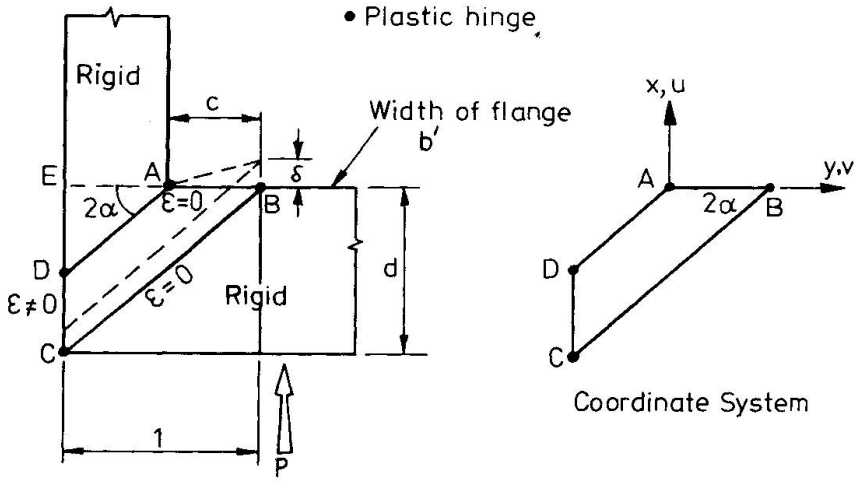

Fig. 5 Assumed Shear Collapse Mechanism

been reduced by an amount commensurate with the magnitude of axial force in the side plating.

4.4 Longitudinally Stiffened Deck Plating

A fresh approach to analysing the behaviour of a longitudinally stiffened deck at finite out-of-plane deflection was made. This involves dividing the region in contact with the indenter into strips with the adjacent material in the panel on the point of buckling. An upper bound plastic analysis for the load-end shortening relationship of an axially loaded strip (Fig.6), which retains the geometrical effects of large rotations and allows for the interaction of bending moment and axial force, has been developed [6].

4.5 Transversely Stiffened Deck Plating

The load sustained by the transverse stiffeners in the deck plating was determined by an effective width approach and corner shear calculation, as described above for the main transverse frames. For the small transverse stiffeners, the value of c in Fig.5 is chosen equal to the distance AE. Both the main transverse frames and small transverse stiffeners were taken to have a residual strength of 25% of their ultimate strengths after

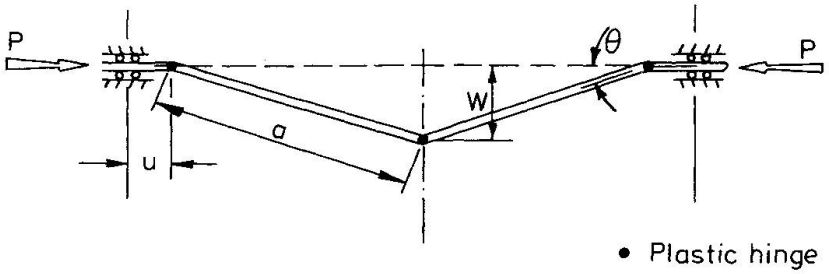

Fig.6 In-Plane Loaded Strip

collapse. This is an empirical figure which was found to work well and may be explained rationally by reference to the strip analysis outlined in 4.4.

5. COMPARISON OF EXPERIMENTAL AND THEORETICAL RESULTS

The theoretical predictions have been plotted on Fig.3 (a)-(e) for comparison with the test results. On the whole the agreement between the theoretical and experimental results is encouragingly good and reasonably consistent. In the theoretical predictions, no account has been taken of strain-hardening. At large out-of-plane deflections, structural elements which are loaded in compression in their initial planes would have lost a large proportion of their strength so that strain-hardening is unimportant to the theoretical predictions. Even in the case of plating with adequate restraint against pull-in at the unloaded edges, some out-of-plane buckling effects would counter any strain-hardening. For the side plating, the large radius of the indenter relevant to ship-offshore concrete platform collisions alleviates the effects of large concentrated strains so that strain-hardening may be ignored with no major loss in accuracy.

6. APPLICATION TO FULL SCALE SUPPLY VESSELS

The test results presented above refer to the static deformation properties of ship structures, and since this is purely a problem of structural plasticity non-geometrical scaling parameters need not be considered and the results should be applicable to full scale ships conforming with the idealizations underlying the tests. The understanding thus gained from the testing and analysis of the models has been applied to the analysis of two actual offshore supply vessels. Four cases of sideways and two cases of stern-on quasi-static collisions with a 10 m diameter concrete shaft have been studied. Design forces based on these studies, which considered wholly static deformation properties of the vessels, are proposed in Table 2 for

STERN COLLISION AT 0.5 m s^{-1}		
Maximum Force (MN)	Elliptical Contact area — Semi-axis dimensions	
8.80	133 x 48 (mm x mm)	
SIDEWAYS COLLISION AT 2 m s^{-1}		
Maximum Force (MN)	Cylindrical Contact area	
	Contact Arc(m)	Vertical Side(m)
14.81	0.013	6.75
26.94	1.633	"
33.80	3.259	"

Table 2. Design Forces : Collision with 10m dia. Column

both sideways and stern collisions, the former for design against local bending failure and the latter for local punching shear failure. The forces determined for the stern collisions suggest that local punching failure of existing concrete shafts of typical platforms with multiple supports could occur.

7. CONCLUSIONS

The results of a series of tests on simplified ship structural models have been presented. The behaviour of these models may be predicted fairly well by analysis based on the theory of large plastic deformations.

ACKNOWLEDGEMENTS

The authors are grateful to T.X. Yu who helped to carry out the tests. The generosity of St. John's College, Cambridge, England in awarding the first author a research studentship is also gratefully acknowledged.

REFERENCES

1. NAGASAWA H. et al, A Study On The Collapse Of Ship Structures In Collision With Bridge Piers. Trans. Soc. Nav. Arch. Japan, Vol. 142, 1977, 345-354.
2. LOW H.Y., Behaviour of A Rigid-Plastic Beam Loaded To Finite Deflections By A Rigid Circular Indenter. Int. J. Mech. Sci., Vol. 23, 1981, 387-393.
3. CALLADINE C.R., A Plastic Theory For Collapse Of Plate Girders Under Combined Shearing Force And Bending Moment. Struct. Engr., Vol. 51, 1973, 147-154.
4. DWIGHT J.B., Structural Steel Lecture Notes - Engineering Tripos Part II, University of Cambridge, 1980.
5. ROBERTS T.M. and ROCKEY K.C., A Mechanism Solution For Predicting The Collapse Loads Of Slender Plate Girders When Subjected To In-Plane Patch Loading. Proc. Instn. Civil Engrs., Vol. 67 Pt. 2, 1979, 155-175.
6. LOW H.Y., Some Structural Aspects Of Collisions Between Ships And Offshore Concrete Platforms. PhD Dissertation, Univ. of Cambridge, 1982, 230 pp.

Punching of Concrete Shells under Ship Collision

Poinçonnement de coques en béton lors des collisions de navires

Durchstanzen von Betonschalen bei Schiffskollisionen

M. KAVYRCHINE
Head of Struct. Dep.
C.E.B.T.P.
Paris, France

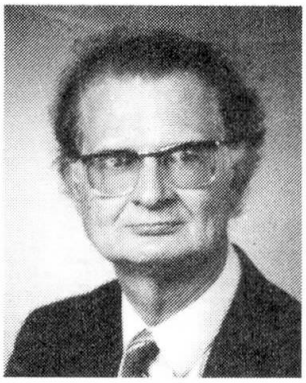

Engineer for French Administration of Highways for a short time, then Director of works and chief design engineer for French contractors. Since 1972 Head of C.E.B.T.P. Structural Studies Department Field of Activity Civil Engineering Buildings, Tall Buildings, Bridges, Prestressed and Reinforced Concrete, Structural Steel.

N. ASHTARI
Doctor Engineer
CETEN-APAVE
Paris, France

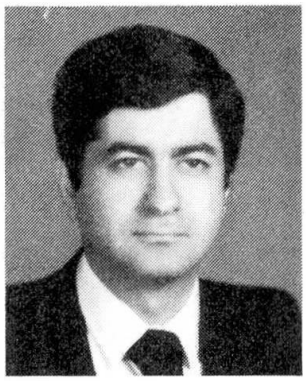

Nader Ashtari, born 1945, got his Civil engineering degree at Lausanne Institute of Technology, Switzerland and his Ph. D. from Paris University. For nine years he was involved in teaching and researches. He was for many years a consulting engineer. Nader Ashtari, now in an inspection office, is expert in structure analysis.

SUMMARY

In connection with the problems of ship collision with supporting systems of concrete gravity structures, many concrete cylinder specimens were subjected to impact load with a speed of about 1.5 m/s. The local effects of the tests are compared with the effects of concentrated load on concrete cylinders. In the tests the size and shape of the load application area, the rate of reinforcements and the level of prestressing were varied in order to investigate the effect of this upon the failure load. A design method for punching shear of concrete cylinder is presented.

RÉSUMÉ

Pour étudier le comportement des piliers des structures offshore en béton sous l'effet de la collision de bateaux, plusieurs coques cylindriques en béton ont été soumises à l'impact d'un projectile avec une vitesse de 1,5 m/s. L'effet local d'impact a été comparé avec l'effet de la charge concentrée sur des cylindres en béton. Les dimensions et la forme de la zone d'application de la charge ont été modifiées ainsi que le pourcentage d'armature, afin de voir leur influence sur la charge de rupture. Une méthode de calcul de la résistance au poinçonnement des coques cylindriques est présentée.

ZUSAMMENFASSUNG

Um das Verhalten der Betonpfeiler von Offshore-Bauten unter dem Zusammenstoß von Schiffen zu studieren, sind mehrere zylindrische Betonschalen an einem Geschoßeinschlag von 1,5 m/sek Geschwindigkeit unterworfen. Die lokale Stoßwirkung wurde mit einer Einzelkraftswirkung auf einer Betonschale verglichen. Die Größe und die Form der Stoßzone wurden verändert, ebenfalls der Bewährungsprozent, um den Einfluß auf der Bruchlast zu bestimmen. Eine Durchstanzwiderstandrechnungsmethode wurde für zylindrische Schalen vorgestellt.

1. INTRODUCTION

To study the local effect of ship collision on offshore gravity structures, C.E.B.T.P.* has undertaken a research program since 1979. At first the aim was to determine the nature of impact and see the difference between its local effect and punching shear failure.

An attempt is made to find the influence of reinforcement and longitudinal prestressing. In this field many tests have been performed on cylindrical concrete shells. These tests allowed us to propose a design method for punching shear. We wish to mention that this research program was financialy supported by ARBEM (French Association for concrete at Sea) and French Ministry of Transport.

2. DESCRIPTION OF TESTS

2.1 Models and test equipments

The tower of structure receiving the collision was modelized by a cylindrical concrete shell showing an approximate ratio of 1/10 between thickness and diameter. We consider only the accidental collision (see definition - Ref [1]) of the supply boat with a collision speed about 1.5 m/s. In this case the duration of impact is longer than the shaft's own period and the problem of dynamic amplification, due to structure vibration, is not encountered. Therefore in our test we have not studied the effect of vibration. To reduce the flexural effects we maintened our concrete cylinder in a special steel device (fig. 1). Mortar was injected between the steel cylinder and concrete shell.

A 30 x 60 cm opening is left at the top of the device to allow load application.

2.2 Orientation tests

The aim of these tests was to compare the local effect of impact of a rigid body at a low speed (about 1.5 m/s) with punching shear failure (load applied by a hydraulic jack).

In both cases, the load was applied by a circular, 120 mm diameter, steel puncheon.

The impact tests were carried out by fall of a steel ram. The ram was made of 300 mm diameter steel discs, assembled around a steel rod (see fig. 2). The mass may be modified according to the needs of the test. The ram falls from heights of 115 mm (v = 1.5 m/s). The deformations and local deflections in several points of the cylinder and also the impact force were recorded.

It emerged from the tests that at failure, the impact loads are nearly the same as punching shear loads.

In both cases, at failure, a concrete plug is punched out in the direction of the load, the rest of the cylinder remaining intact. The upper part of the plug keeps the shape of the puncheon. The dimensions and shape of failure surface are very similar (see fig. 3).

After this phase we continued our tests with static concentrated load. Many tests were performed with different shape (circular and elliptic) and different size of puncheon.

In some cases to achieve a good contact between concrete and puncheon we used a concave puncheon with a interposed rubber sheet. In these particular cases we observed an increase of failure load about 18 %.

* C.E.B.T.P. : Centre Expérimental de Recherches et d'Etudes du Bâtiment et des Travaux Publics.

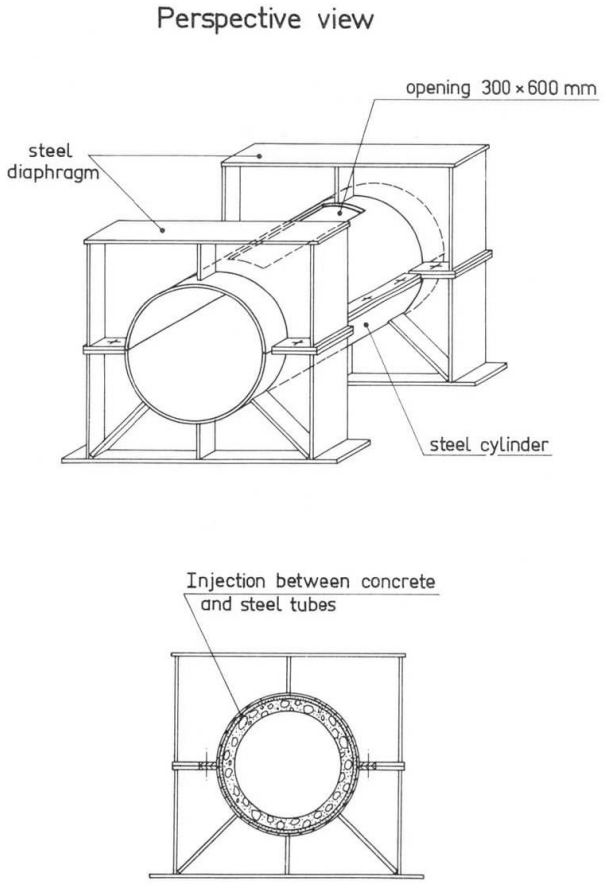

Fig. 1 Testing equipment

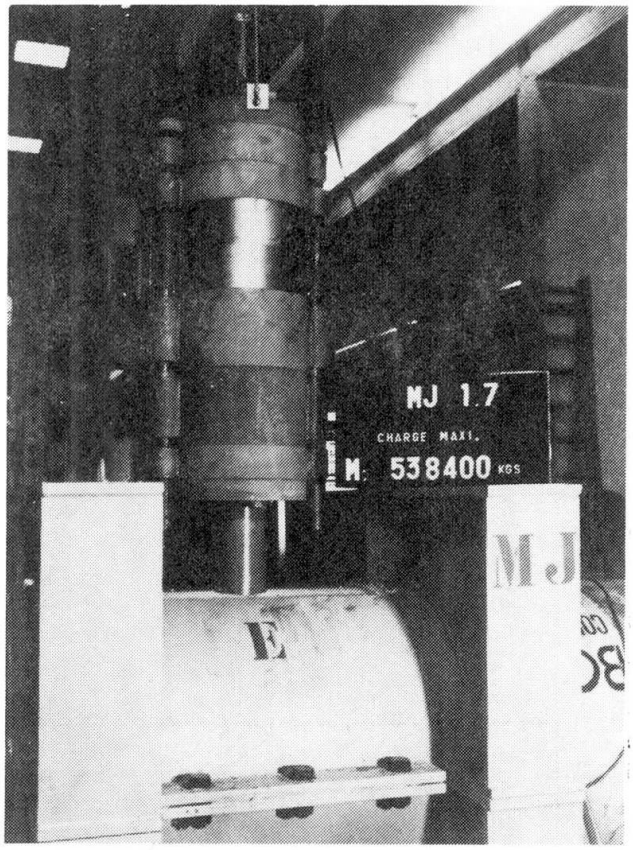

Fig. 2 Steel ram

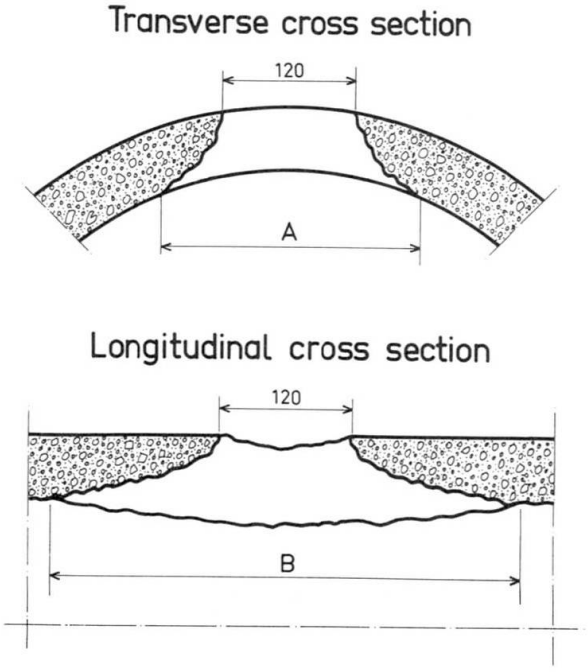

Fig. 3 Failure surface

	Essai	Amm	Bmm
Static Test	MJ1.1	270	440
	MJ2.1	290	400
Dynamic Test	MJ1.7	260	430
	MJ1.9	230	420
	MJ1.13	260	460
	MJ2.5	290	440

Reference of test	Form of Steel nose	Failure load (KN)	Ratio $\frac{\text{Test failure}}{\text{Theoretical failure}}$	Ratio $\frac{\text{Experimental B}}{\text{Theoretical B}}$	Ratio $\frac{\text{Experimental A}}{\text{Theoretical A}}$
1.1	circular 120 mm	233,7	0,98	0,99	1,14
2.1	circular 120 mm	254,8	0,95	0,90	1,22
3.2	circular 100 mm	225,4	0,99	1,08	1,07
3.3	elliptic 150 x 100 mm	254,8	0,98	0,93	1,11
3.4	circular 140 mm	401,8	1,1	1,04	1,22
3.5	circular 50 mm	170,5	1,23	1,1	1,26
4.1	elliptic 150 x 100 mm	235,2	0,91	1,00	1,11
4.2	elliptic 150 x 100 mm with neoprene	331,1	1,09	0,97	1,16
4.3	elliptic 150 x 100 mm curved with neoprene	313,6	1,03	1,00	1,16
5.1	"	224,4	0,94	0,91	0,99
5.2	"	234,6	0,99	0,98	1,18
5.3	"	234,6	0,96	1,00	1,04
5.4	"	244,8	0,99	0,95	1,18
5.5	"	265,2	1,06	0,98	1,13
5.6	"	244,8	0,96	0,95	1,18
5.7	"	153,0	0,87	0,80	1,08
5.8	"	145,9	0,83	0,87	1,13
5.9	"	153,0	0,81	0,87	1,04
5.10	"	163,2	0,85	0,78	1,18

TABLE 1

The observation of failure surface confirmed the previous results. All these tests were carried out on the standard ducts produced by BONNA (716 mm external diameter and 58 mm thickness). The rate of reinforcement was not very high.

2.3 Tests with prestressed concrete

In order to investigate, the influence of concrete strength, reinforcements and prestressing, we used five specially made concrete cylinders. Two types of reinforcement (Ø 6 mm spaced 5 cm in two directions and Ø 6 mm spaced 8 cm in two directions) are considered. The reinforcement was in the mid thickness of cylinder. The ultimate strength of concrete varied between 28 to 58 MPa. The prestressing force varied from 0 to 500 KN.

The effect of reinforcement and longitudinal prestressing upon the failure load turns to be slight, on the other hand a higher rate of reinforcement leads to higher ductility of failure.

3. DESIGN METHOD

Our tests have shown that local effect of ship collision with offshore plateforms is similar to punching shear failure. To estimate the punching shear strength of cylindrical concrete shells an analytical solution is developped. The method is a generalization of the method presented by BRAESTRUP [2] for punching shear in concrete slabs.

A plastic limit analysis based upon the failure mechanism is used to calculate the punching load, we equate the external work produced by the punching force with the internal work dissipated in the failure surface. To satisfy the requirements of limit analysis, we assumed that concrete is a rigid, perfectly plastic material with the modified coulomb failure criterion as yield condition and the deformations governed by the associated flow rule (normality condition).

The load found by equating the rate of external and internal work is an upper bound solution for the punching load. By minizing this load, we approach the real punching load. For more details see réf [3].

This solution does not give only the punching load but it also determines the failure surface and takes in account the exact shape of puncheon. A comparison between calculated and experimental failure load and failure surface is given in table 1. To compare the experimental and calculated failure surface, we have chosen the length of the two perpendicular axes at the base of plug, as comparison criterion. See fig. 3.

REFERENCES

1. Bo CARLIN, Chris MORLAY, Industrial and Offshore Division - Det Norske Veritas, Technical Report, November 1977

2. BRAESTRUP M.W., Punching shear in concrete slabs. IABSE Colloquium on Plasticity in Reinforced Concrete, Introductory Report p ; 115-136, Copenhagen 1979

3. ASHTARI N., Poinçonnement des coques en béton armé, calcul et justification expérimentale, Annales de l'I.T.B.T.P. n° 411, Janvier 1983

4. KAVYRCHINE M., ASHTARI N., Choc de bateaux sur les structures offshore en béton, étude du poinçonnement, 2nd international Symposium on Behaviour of Offshore Concrete Structures, Paris, Octobre 1982

Leere Seite
Blank page
Page vide

Ultimate Strength of Bow Construction

Résistance structurale limite de la proue d'un navire

Bruchfestigkeit des Buges

Tokio OHNISHI
Naval Architect
Kawasaki Heavy
Industries Ltd.
Akashi, Japan

Hajime KAWAKAMI
Naval Architect
Kawasaki Heavy
Industries Ltd.
Akashi, Japan

Wataru YASUKAWA
Naval Architect
Kawasaki Heavy
Industries Ltd.
Akashi, Japan

Hitoshi NAGASAWA
Naval Architect
Ministry of Transport
Tokyo, Japan

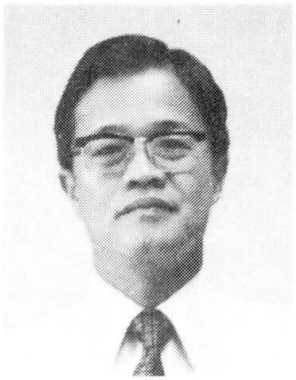

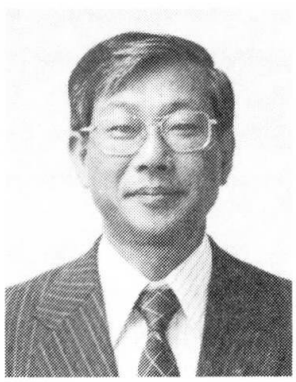

Tokio Ohnishi, born 1948, received his Masters Degree in engineering from Osaka University, Osaka, Japan. For ten years, he was involved in dynamic problem and nonlinear problem in structural analysis region, and he is now a research engineer at the Structure Analysis Section of Strength Laboratory in the Technical Institute.

Hajime Kawakami, born 1940, obtained a degree in Naval Architecture from Osaka University, Osaka, Japan. He is a specialist in ship hull vibration and now manager at the Structure Analysis Section of Strength Laboratory in the Technical Institute.

Wataru Yasukawa, born 1933, received his doctor of engineering degree from Osaka University, Osaka, Japan. His major fields of research activities include strength of ship structures, plastic analysis buckling and ultimate strength of structures, and he is now a senior manager of Strength Laboratory in the Technical Institute.

Hitoshi Nagasawa, born 1925, got his doctor of engineering degree at the University of Tokyo, Tokyo, Japan. For about 30 years he studied the strength of ship structure in the Ship Research Institute, Ministry of Transport, and now he is the director general of the Institute.

SUMMARY

A study of the ultimate strength of the bow construction of two ships which have suffered a collision, has been made by means of a theoretical calculation by the FEM and experiments on static collapse by using 1/10 scale bow models have been conducted. It has been possible to estimate the load acting on the side structure of the struck ship and the bow deformation of the striking ship.

RÉSUMÉ

La résistance structurale limite de la proue de deux navires qui sont entrés en collision, a été déterminée par un calcul théorique au moyen la méthode des éléments finis et aussi par des expériences sur leur rupture statique au moyen des modèles réduits au 1/10e des proues précitées. Il a été possible d'évaluer la charge exercée sur la structure latérale du navire endommagé et la déformation de la proue du navire opposé.

ZUSAMMENFASSUNG

Die Bruchfestigkeit des Buges zwei zusammenstossenden Schiffen - wurde anhand einer Berechnung mit finiten Elementen sowie einem Modell untersucht. Die Last auf der seitlichen Struktur des beschädigten Schiffes und die Umformung des Buges des gegnerischen Schiffes konnten geschätzt werden.

1. INTRODUCTION

So far the capacity of the collision-resisting structure of a nuclear-powered ship designed to protect its reactor from a collision has been evaluated in that it absorbs the kinetic energy of the striking ship through its own structural destruction. But it is reported that recent researches have developed collision -resisting structure of a resisting type intended to minimize the demage of one's own ship and mainly to destroy the bow of the striking ship in collision [1] [2] [3].

In order to design such a barrier of a resisting type it is necessary to precisely estimate the load acting on the side structure of the nuclear-powered ship. In the case of the side structure of a resisting type this load is found by the following procedure.

(1) To find the relation between the load and the deformation at the moment of collapse of the bows of the ships in collision.

(2) To find the bow deformation by carrying out a collision simulation analysis by means of the above-mentioned relation.

(3) To estimate the load corresponding to the bow deformation by using the load -deformation curve.

In order to find the collapse load it is necessary to analyze the ultimate strength of the bow construction but so far this analysis has scarcely been carried out [4] - [7], nor does any established method of its calculation seem to exist.

In this study, for the purpose of establishing the method of analyzing the ultimate strength of the bow construction and finding the load acting on the side structure, first, we have made a theoretical calculation by the FEM by means of an ideal mathematical model of the frame of bow construction. Next, in order to clarify the behavior of the bow collapse and verify the method of calculation, we have carried out static collapse experiments by using 1/10 scale models of the bows of a tanker and a container carrier and compared the results of the experiments with those of the theoretical calculation, thereby a reasonable agreement between the two has been confirmed. And further, we have estimated the collapse loads of bow construction of actual ships (tanker, container carrier and ice-strengthened ship) and obtained the load-deformation curves.

By using these load-deformation curves of bow construction we can estimate the load acting on other types of structure such as bridges, offshore structures when ships strike against them.

2. THEORETICAL ANALYSIS

When calculating the ultimate strength of bow construction, it is considered necessary, strictly speaking, to deal with bow construction as a plate structure. But then it will entail a complicated process and will take a much time for computation. Therefore, in order to obtain the load-deformation curves, we regard the bow construction as an ideal frame structure with effective plate width and analyze the ultimate strength by FEM, which utilizes the plastic hinge method.

We regard the side structure of a nuclear-powered ship as rigid and we consider such a case as the bow collapsing one-sidedly in collision. According to the results of the experiment, the sub-structure between the transverse frames collapses as a unit

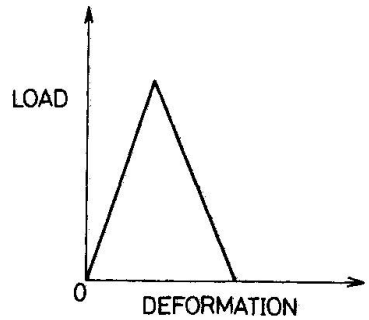

Fig.1 Load-deformation curve of longitudinal member

structure, and the weaker sub-structure collapses first. In calculation, we assume that the sub-structure collapses first at stem and down to stern. The load is applied to the frame section by forced displacement, and the loading point is shifted to the next frame after each sub-structure has collapsed.

As the side shell plate, the web plate of girders, etc. are considered to have already buckled under the maximum load, we have used the effective width of the buckled plate for an ideal mathematical model of the frame of the longitudinal member. The above-mentioned effective width is given in the following formula [8]

$$b_e = b \qquad \text{for} \quad \frac{b}{t} \leq \sqrt{E/S_y}$$

$$b_e = t\sqrt{E/S_y}\left(2 - \frac{t}{b}\sqrt{E/S_y}\right) \qquad \text{for} \quad \frac{b}{t} \geq \sqrt{E/S_y} \tag{1}$$

where b is the plate width, b_e is the effective width of the plate, t is the plate thickness, E is the young's modulus and S_y is the material yield stress. The results of the box column experiment carried out by the authors [9] are in good agreement with the results of the calculation made with the above formula. According to the above mentioned experiment, the load decreases rapidly after it has reached the maximum. Therefore in this calculation, the load-deformation curve of longitudinal member is assumed as shown in Fig. 1.

3. STATIC COLLAPSE EXPERIMENTS ON BOW CONSTRUCTION

Static collapse experiments have been carried out by using 1/10 scale bow models of a container carrier and a tanker (Fig.2, Fig.3). The test apparatus is shown in Fig. 4. The load acting on the bow model and the deformation and strain of the bow models were measured, and load-deformation curves and the mode of collapse were obtained.

Fig. 5 and Fig. 6 show the load-deformation curves of the models of a container carrier and a tanker. In these figures, peak load and the corresponding collapse mode are shown. The shaded portion collapsed under peak load and the blackened portion had collapsed before. The solid black circles in Fig. 5 and Fig. 6 show the results of the calculation by FEM, which are in good agreement with the results of the experiments.

The sub-structures between the frames are numbered ①, ②, ----- in order fore and aft, as shown in Fig. 5 and Fig. 6. Regarding the container carrier, we considered that theoretical collapse occurs in the order of ① ③ ④ ⑤ ②, which, however, changed to ① ⑤ ④ ③ ② in experiment. This disagreement is considered to be due to the following reason. The difference in strength between ③ and ⑤ is so small that the strength of ⑤ decreased in experiment because of end effect. As for the tanker, the analytical and experimental orders of collapse agree with each other.

In the case of the model of the container carrier, the load decreases rapidly after peak load is reached, and the entire load-deformation curve is saw-toothed. In theoretical calculation, we can obtain only the peak load, and in order to obtain the entire load-deformation curve we must study further in the future. With the tanker model, the load does not decrease so rapidly after peak load is reached.

With the tanker model, a big discrepancy is noticed between calculation and experimentation when deformation exceeds 1200 mm. This is probably because experimentally the upper deck buckled totally at the moment of such deformation, and afterwards the loading capacity of the upper deck decreased remarkably. The total buckling of the upper deck is not treated in this calculation. For

reference, we calculated the maximum load, supposing that the loading capacity of the upper deck is entirely lost after buckling. The results of calculation marked ◉, as shown in Fig. 6 approach the value obtained through experiments.

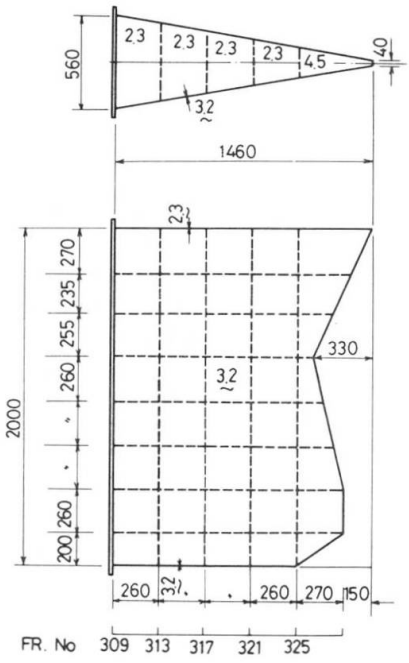

Fig.2 Bow model of container carrier

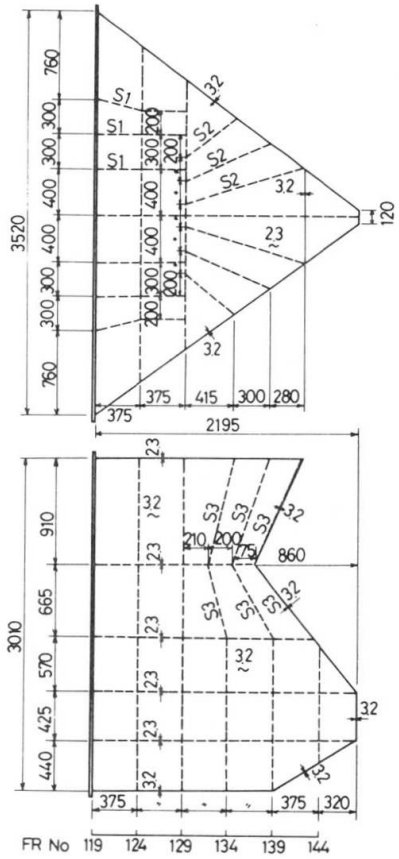

Fig.3 Bow model of tanker

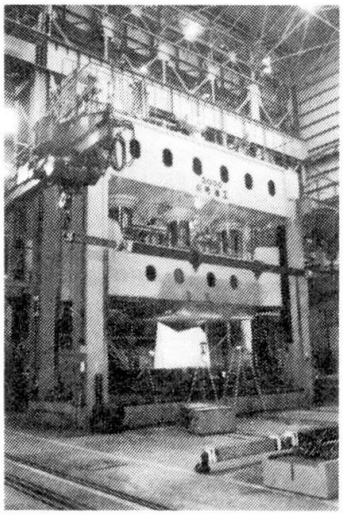

Fig.4 Test of Bow model

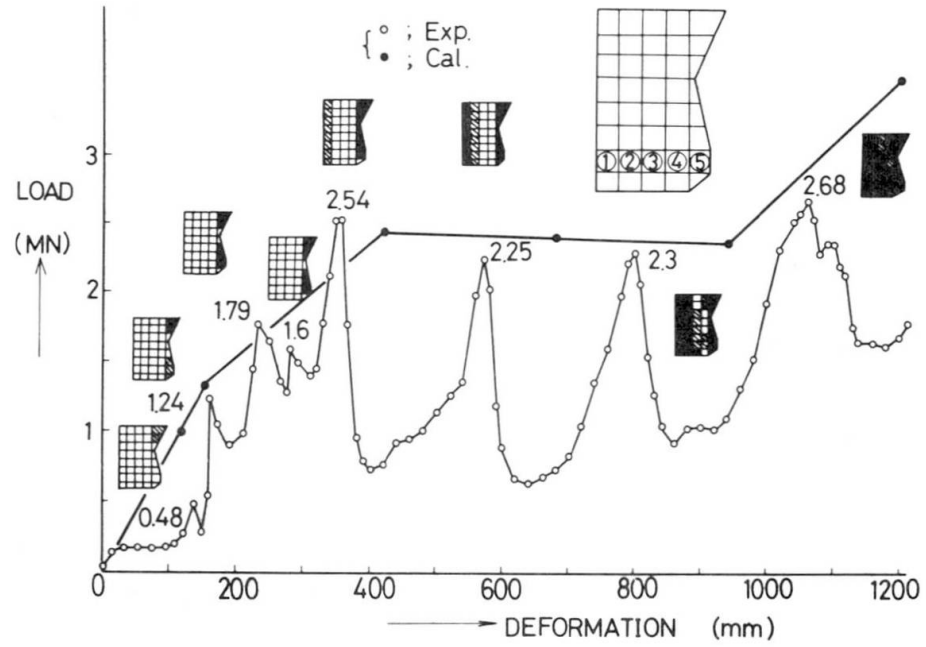

Fig.5 Load-deformation curve of container carrier model

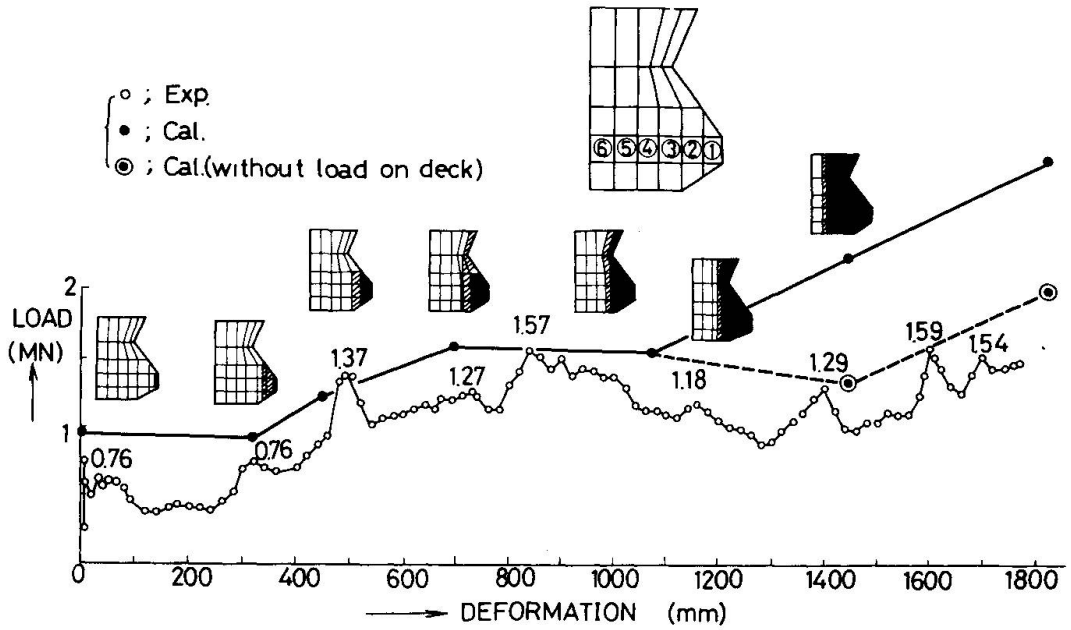

Fig.6 Load-deformation curve of tanker model

4. ULTIMATE STRENGTH OF BOW OF ACTUAL SHIP

As typical ships, we chose a container carrier, a tanker and an ice-strengthened ship. Their principal dimensions are shown in Table 1. The ultimate strength of the bow structure of these ships is calculated, based on the method mentioned in Chapter 2. In consideration of symmetry, we have modeled a counterpart of the bow construction for calculation. The ideal mathematical model of the frame is shown in Fig. 7 ∿ 9. The model is fixed at the collision bulkhead and the load is applied to the frame section by forced displacement. In the calculation, 242 MPa was used for yield stress. Fig. 10 ∿ 12 show the results of calculation. "Full yield" mentioned therein means the load caused when the longitudinal member yielded entirely by axial load. The load resulting from "full yield" becomes larger than that obtained through FEM. Fig. 7 ∿ 9 show with a mark ○ where the plastic hinge is produced when the maximum load is reached.

We compare the collapse loads of the bows of these three ships. As the collapse loads vary with sectional position we have taken up the collapse load arising midway between the forepeak and the collision bulkhead. These collapse loads are shown in Table 2. Generally the collapse load of the tanker is the largest, but when calculated per unit area, the load of the container carrier turns out largest. When we design the side structure of the struck ship, we must take into account not only the magnitude of the load but also the load per unit area.

5. SOME CONSIDERATIONS ON COLLISION ANALYSIS

When the side structure of the struck ships is rigid, the deformation of the bow and the load acting on the side structure are calculated by collision analysis by means of the load-deformation curves of the bow as mentioned in Fig. 10 ∿ 12. When the load-deformation curve is sawtoothed, the energy absorbing capacity of the bow is reduced, and the collapse deformation is intensified. Accordingly the load acting on the side structure becomes larger. But if the increase of load corresponding to the increase of deformation is not remarkable, the difference between the two is considered to be small.

Next, we consider the case where not only the bow construction but also the side structure of the struck ship collapses. Suppose the load-deformation curve of the side structure or other damaged structure is already obtained and is denoted by S_1 in Fig. 13. The load-deformation curve of the bow construction is

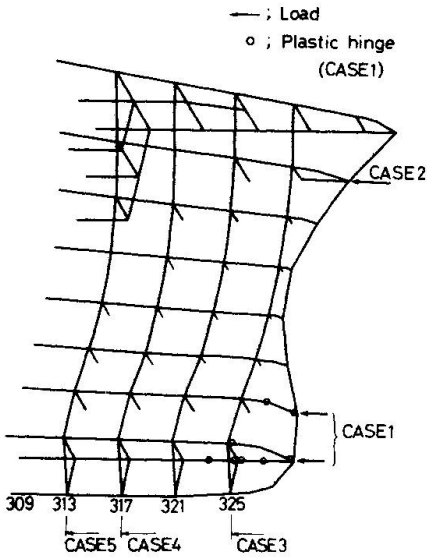

Fig.7 Idealized model of container carrier

Table 1 Principal dimensions

Item	Container carrier	Tanker	Ice strengthend ship
Lpp(m)	248.0	360.0	134.5
B (m)	32.2	69.0	32.2
D (m)	19.9	28.7	20.3
d (m)	12.0	22.75	7.8
DWT (ton)	35,000	409,000	11,200

Table 2 Comparison of bow strength

	P (MN)	A(m^2)	P/A(MN/m^2)
Container carrier	88	74	1.19
Tanker	245	602	0.41
Ice strengthend ship	98	108	0.91

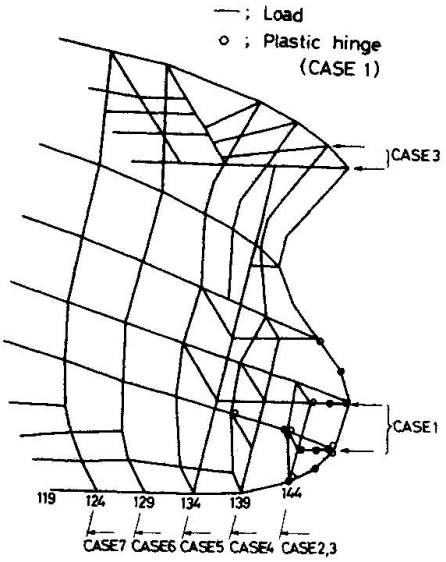

Fig.8 Idealized model of tanker

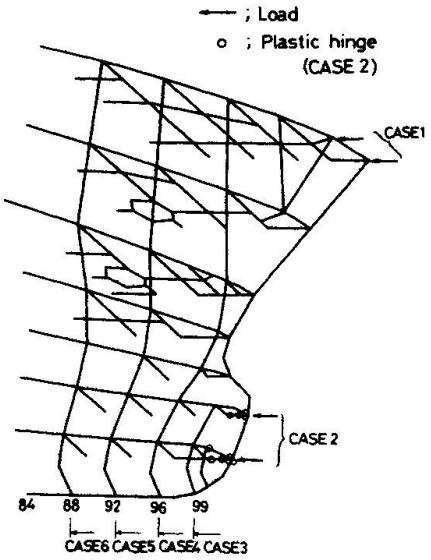

Fig.9 Idealized model of ice strengthend ship

denoted by S_2 therein. The collapse deformations corresponding to the load P_A are d_1 for the side structure and d_2 for the bow construction. The total deformation is $d_1 + d_2$, and the load-deformation curve is denoted by S_3. Through the collision analysis using S_3, we can obtain the deformation of the side structure and bow construction. If the load-deformation curve of the bow construction is sawtoothed, the treatment becomes slightly complex, but it is made possible to analyze in the same way.

6. CONCLUSION

In order to estimate the load acting on the side structure of the struck ship, we carried out experiments by using 1/10 scale bow models and studied the method of calculating the ultimate strength of the bow construction.

The theoretical calculation shows results in good agreement with those of the experiments and it is made possible to calculate the ultimate strength of the

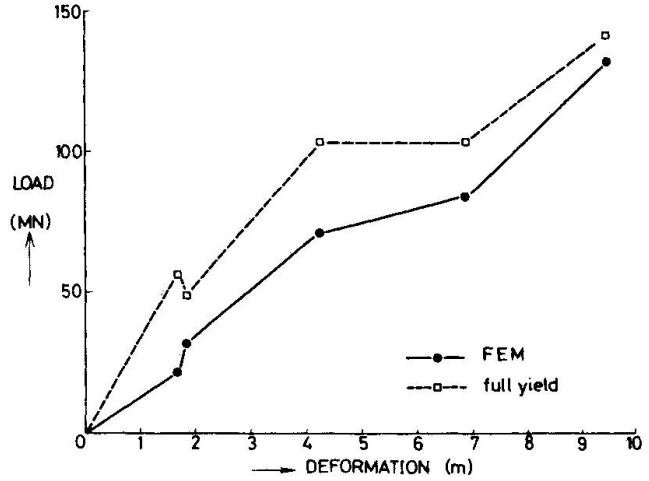

Fig.10 Load-deformation curve of container carrier by FEM

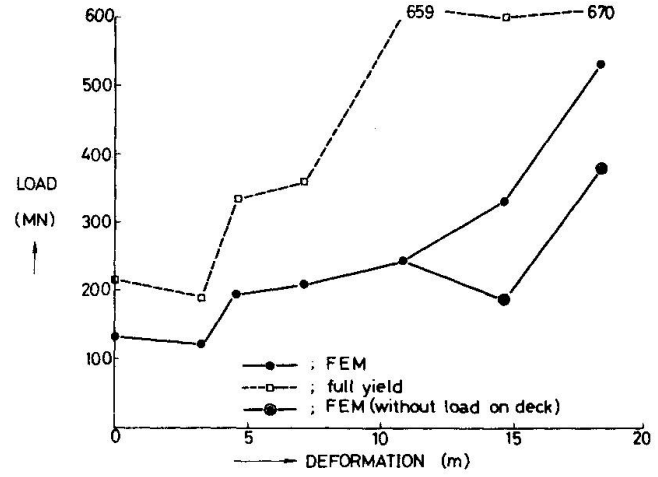

Fig.11 Load-deformation curve of tanker by FEM

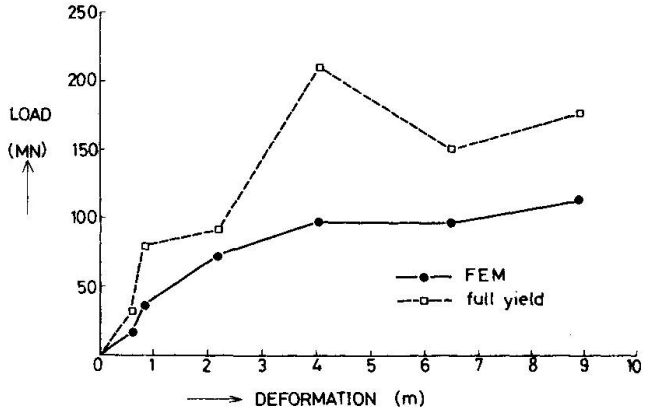

Fig.12 Load-deformation curve of ice strengthend ship

bow construction by FEM by using an ideal mathematical model of the frame.

Among the three ships treated in this paper, the collapse load of the bow of the tanker is the largest. But the load per unit area of the bow of the container carrier is also large. When we design the side structure of the struck ship, we must take into account not only the magnitude of the load but also the load per unit area.

Finally, the items to be pursued further are :

(a) To develope the method of obtaining entire load-deformation curves, and
(b) To establish the method of analyzing collision problems more precisely when not only the bow construction but also the side structure collapses.

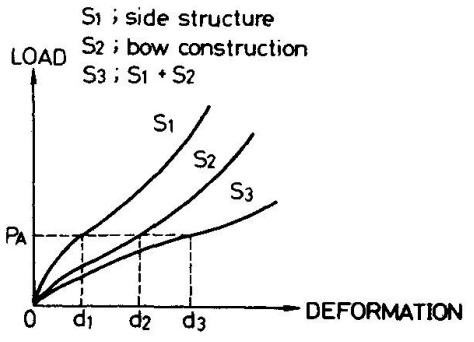

Fig.13 Load-deformation curve of bow and side structure

REFERENCES

1. WOISIN, G., Bericht über Kollisionsshutzersuche, GKSS, 1976.

2. WOISIN, G., Conclusion from Collision Examinations for Nuclear Merchant Ships in the FRG, Proc. of Symp. on N.S. Humb., 1977.

3. RECKLING, K.A., On the Collision Protection of Ships, PRADS Sympo. Tokyo, 1977.

4. MINORSKY, V., Bow Loading Values (Bulbous bow) Task II, U.S. Maritime Adm., 1977.

5. MINORSKY, V., Development of Ship Loading Values (Bow in Collision) Task VIII, U.S. Maritime Adm., 1978.

6. RECKLING, K.A., Beitrag der Elasto und Plasto mechanik zur Untersuchung von Shiffscollision, Jahrbuch STG, 1976.

7. NAGASAWA, H., ARITA, K., TANI, M., OKA, S., A study on the Collapse of Ship Structure in Collision with Bridge Piers, Jr. Soc. of Nav. Arch. of Japan, Vol 142, December 1977.

8. FAULKNER, D., A review of Effective Plating for Use in the Analysis of Stiffened Plating in Bending and Compression, Jr. of Ship Research, Vol 19 No.1, 1975.

9. OHNISHI, T., KAWAKAMI, H., YASUKAWA, W., and NAGASAWA, H., On the Ultimate Strength of Bow Construction, Jr. Soc. of Nav. Arch. of Japan, Vol 151, June 1982.

Ship Impact on a Shaft of a Concrete Gravity Platform

Collision d'un bateau avec une plate-forme en béton

Schiffsstoß gegen eine »Offshore« - Konstruktion aus Beton

Bernt JAKOBSEN
Dr. Eng.
Norwegian Contractors
Oslo, Norway

Tor Ole OLSEN
Dr. techn.
Olav Olsen
Lysaker, Norway

Bjørn RØLAND
Principal Surveyor
Det norske Veritas
Høvik, Norway

Einar SKÅRE
Project Engineer
Statoil
Asker, Norway

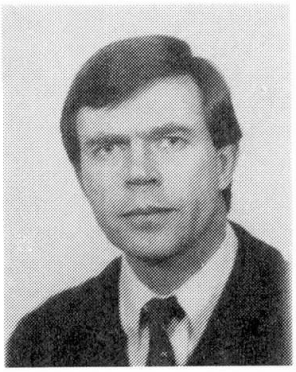

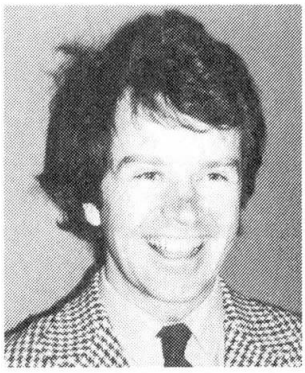

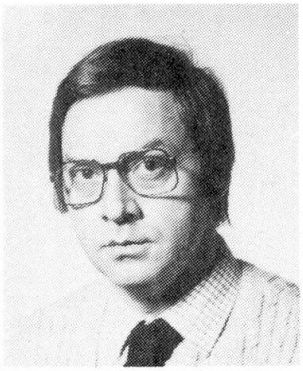

After graduation in 1968, Bernt Jakobsen born 1944, had 5 years of consulting practice before receiving his Dr. ing-degree in 1980, also at the Norwegian Institute of Technology. He is at present working with Norwegian Contractors in Oslo.

Since graduation from University of Toronto, Tor Ole Olsen, born 1950, has been engaged in design of concrete gravity platforms for the North Sea.

Bjørn Røland, B.Sc. in Civil Engineering from University of Strathclyde, Glasgow, 1969. Head of department for marine civil engineering. Worked during the past eight years with several aspects of offshore concrete structures, such as design criteria, control of structural design, construction and behaviour of structures in service.

Einar Skåre, born 1943, graduated with a degree in structural engineering from University of Minnesota. For seven years involved in engineering and construction of concrete gravity platforms for the North Sea. At present project engineer and responsible for engineering of steel jackets riser platforms for Statoil.

SUMMARY
An impact between a 150 000 dtw tanker and the shaft of a concrete gravity platform is investigated. Although several uncertainties are present, the main conclusion is that the platform may be designed to resist such impacts.

RÉSUMÉ
L'impact d'un pétrolier de 150 000 tdw contre la colonne d'une plate-forme de production type gravitaire en béton est étudié. Malgré certaines incertitudes, il est possible de conclure que la plate-forme peut être conçu de façon à résister des impacts de cette envergure.

ZUSAMMENFASSUNG
Stoßbeanspruchung zwischen einem 150 000 tdw Tankschiff und dem Turm einer »Offshore« - Konstruktion wurde untersucht. Trotz gewisser Unsicherheiten ist es möglich zu schließen, daß die Konstruktion so entworfen und gebaut werden kann, daß sie solchen Zusammenstößen widerstehen kann.

1. INTRODUCTION

Experience has shown that ship collisions with offshore platforms do occur and must be considered in design.

Previously it has been shown, ref. (1), that concrete platforms have, or may be designed to have, sufficient strength to sustain the loads resulting from present day ship collision criteria without damage.

With offshore loading of oiltankers being more and more common, the impact behaviour between a 150 000 tdw tanker and a concrete shaft is of increasing interest. Detailed static and dynamic analyses have been performed to investigate this question. The impact velocity chosen is 2 m/s; for a tanker this is extreme and should not be considered as an ordinary design situation.

The intention of this paper is to show that the concrete platforms may also be designed to have sufficient strength to sustain the loads resulting from a tanker collision without unacceptable damage.

2. DESIGN FOR SHIP IMPACT

Design criteria for offshore structures are given in (2) and (3). Design practice for collision as accidental loads is summerized by S.Fjeld (4) and in (1). DnV's Technical Note TNA 202 (5) "Impact loads from boats" specifies load-indentation characteristics for a 5000 t supply ship, and forms a useful design aid.

Essential for concrete design is the impact load area. This is derived from simple geometry, such as height of ship, radius of shaft and ship indentation.

To summarize briefly:

$$E_S = 1/2\ (m + \Delta m)\ v^2$$

where E_S is kinetic energy of the ship

m is mass of ship

Δm is added hydrodynamic mass

v is velocity of ship

The absorbed energy of concrete gravity platforms is negligible compared to the energy absorbed by the ship.

For the supply ship considered in TNA 202 (5) the following characteristics are used:

$$m = 5000 \text{ t}$$

$$\Delta m = \begin{cases} 0{,}1 \text{ m for bow and stern impacts} \\ 0{,}4 \text{ m for sideway impact} \end{cases}$$

v = impact velocity to be taken as the drifting velocity in the out-of-control condition. $v = 0{,}5H_S \geqslant 2$ m/s, where H_S is the maximum significant wave height for operation of ship near the platform.

Knowing the load-indentation relationship the impact load P is found by equating the kinetic energy and the energy absorbed by the ship.

To account for local and uneven distribution of the contact stresses TNA 202 (5) suggests a reduction factor (= 0,4 for sideway, = 0,7 for bow and stern) on the contact area.

Applying this procedure for the 5000 t supply ship on a typical offshore platform showed that, regardless of ship impact velocity, the shaft would not be destroyed. The main findings from (1) are included here, as local flexural strength (fig.1) and punching strength (table 1), both related to applied loads. Note that the entire load-indentation curve is included to velocities many times the corresponding accidental design condition. The design values of strength are used.

TYPE	P	Q	Q_d	Q_d/Q
	7.5	.66	1.54	2.36
	7.91	.64	1.56	2.44
BROAD	8.31	.65	1.57	2.41
SIDE	9.51	.70	1.60	2.28
	11.5	.80	1.65	2.07
	6.	.71	1.55	2.18
	6.68	.66	1.57	2.40
STERN	7.69	.69	1.61	2.34
	9.34	.76	1.66	2.19
	2.8	1.08	1.48	1.37
BOW	4.8	.41	1.55	3.77
	8.2	.51	1.65	3.23
	13.7	.69	1.78	2.59

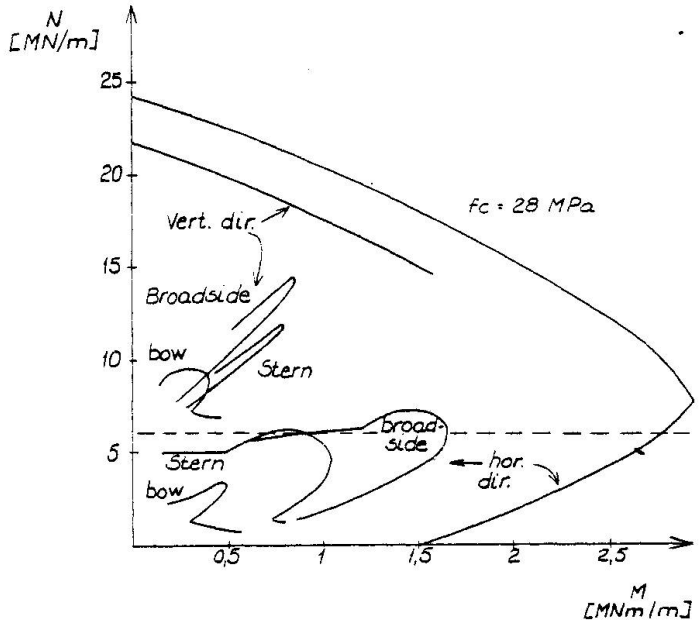

Table 1 Shear Strength Fig. 1 Flexural response and strength

The load-indentation relationship is in reality a description of the strength of the ship. If the strength had been expressed in terms of load per unit area it would not have varied much from ship to ship and from shaftdiametre to shaftdiamtre. This is not surprising, since most ships are designed for similar loadings.

3. IMPACT RESPONSE

It is convenient to distinguish between global and local response.

3.1 Global response

The dynamic ship impact is carried out using the structural model shown in Fig.2.

The 150 000 tdw tanker colliding broadside with the platform is represented by two stiff beam elements, as seen in Fig. 2. The distribution of mass at the three nodes of the "ship" is chosen to represent the translation as well as the rotational inertia of the ship. Included in these mass quantities is a hydrodynamic mass corresponding to an added mass coefficient of 0.4 as expressed in section 2.

A ship velocity of 2.0 m/s is chosen for the case presented. This has been evaluated to represent a reasonable upper limit corresponding to an accidental impact case.

Only one impact direction has been considered, see Fig. 2. The eccentricity of the tanker relative to the shaft has been varied to examine the effect of eccentric impact.

The deformations in the tanker during the impact is represented by a non-linear spring having the load-indentation characteristics as shown in Fig.3. This curve is obtained as described in (1). The curve is only applicable in the compression stage before the tanker starts to move away from the platform. However, the maximum platform response for the cases presented is reached during or immediately after the compression stage. The corresponding inaccuracies in the results are thus expected to be of minor importance.

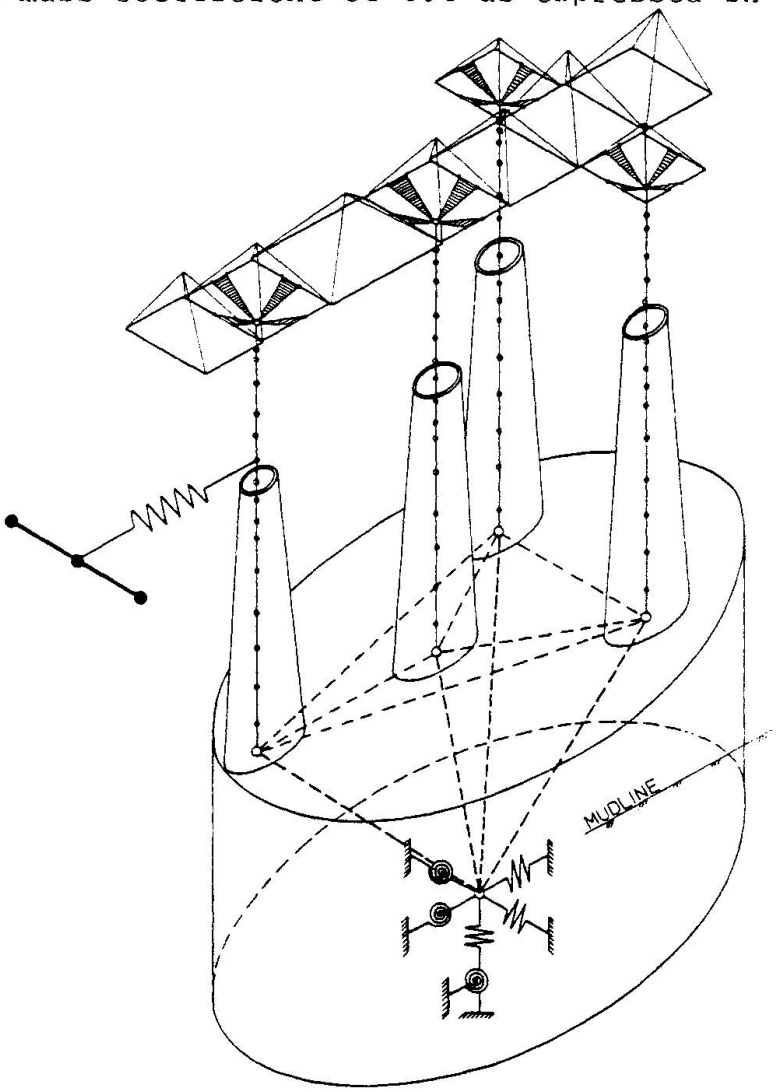

Fig. 2 Space frame model

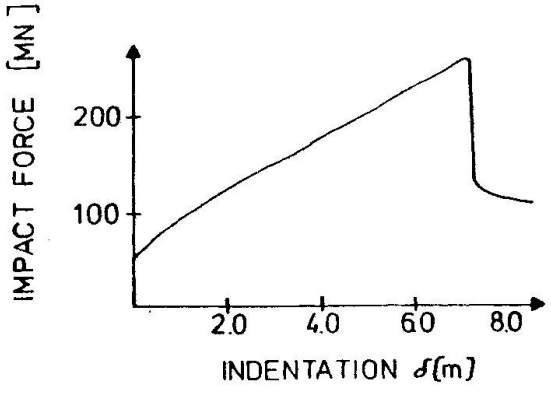

Fig. 3 Load-indentation relationship for tanker in broad side impact.

The dynamic analysis is carried out by direct time-integration using the constant acceleration method of the Newmark family. The tanker-platform system is allowed to perform free vibrations with initial conditions corresponding to the tanker velocity of 2.0 m/s.

Table 2 presents some typical response quantities for the central impact together with the time for occurence of the maximum response.

In Fig.4 the maximum impact force, shear force in shaft below the impact point, bending moments at the load and at the shaft base are given as function of the eccentricity. The curves should be interpreted as indicative only since the maximum response in several cases occurs after the maximum impact has been reached. Further, influence of nonlinear platform response is not considered.

LOCATION	RESPONSE QUANTITY							
	M (MNm)	t (s)	Q (MN)	t (s)	N (MN)	t (s)	δ (m)	t (s)
Base of shaft	7274	3.09	131.6	3.12	22.5	0.76	0.021	3.51
At/under point of impact	2153	3.09	127.0	2.97	20.3	0.33	0.169	3.09
At intersection with deck	528	3.00	77.4	2.07	19.9	0.33	0.159	3.03
Mudline	30238	3.09	225.6	3.12	18.5	0.81	-	-
Impact load/ tanker	-	-	-	-	153.9	2.70	3.17	2.76

Nomenclature: M : Bending moment
Q : Shear force
N : Axial force
δ : Displacement in impact direction
t : Time for occurrence of maximum response

Table 2 Maximum response quantities, central impact.

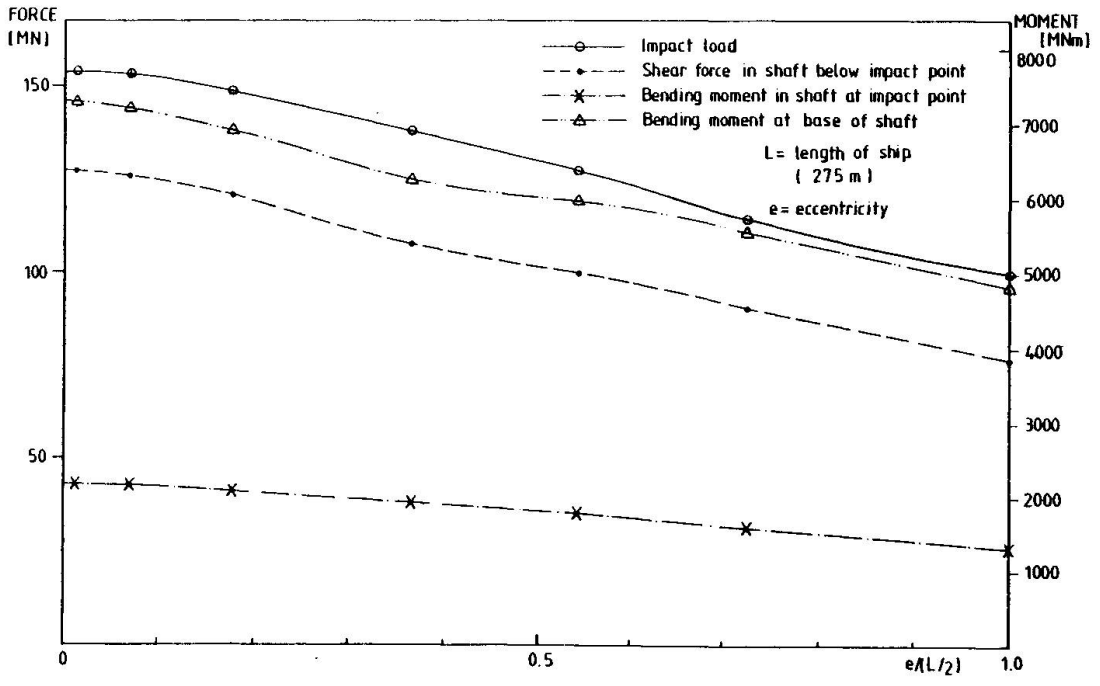

Fig. 4 Impact load and typical response quantities as function of eccentricity.

3.2 Local response

A linearly elastic analysis, as described in (1), is adopted to calculate the stress resultants in the vicinity of the load. The geometry of the shell investigated is shown in fig.5. The length of the cylindre is determined from the global moment, a length of 75m was chosen, corresponding to the maximum moment.

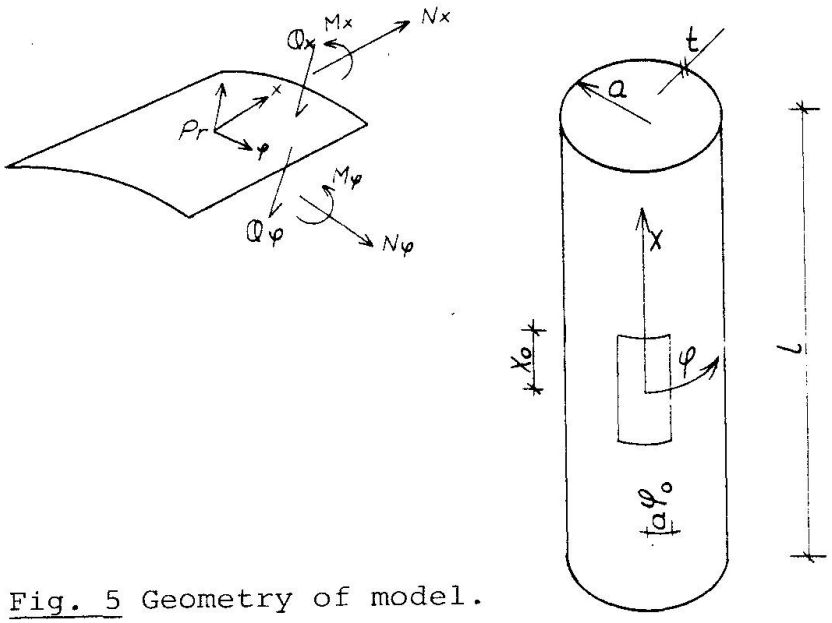

Fig. 5 Geometry of model.

To account for the possible uneveness the 0.4 reduction factor on contact area is used, as suggested for the supply ship. How appropriate this is for tanker is not known. Most likely it will be smaller in the early phase. However, then the width is very small, since $P \neq 0$ when $\delta = 0$.

Unfortunately load-deformation characteristics are not available for corner impact. This is of particular interest when the shaft is conical, which is sometimes the case. Most likely this geometric aspect should be considered during design.

There are indications, however, that the strength of the corner, in terms of load per unit area, is not so different from broadside strength at bulkhead.

4. IMPACT STRENGTH

4.1 Material properties

When investigating the extreme accidental tanker impact realistic values of strength should be used:

Concrete:

The compressive strength according to DnV Rules (3) with material factor of 1.0 is thus chosen:

$$f_c = 0,85 \times f_{cyl} = 0,85 \times 0,80 \times f_{cube}$$

A 20% increase due to aging is assumed. Thus, for C60

$$f_c = 0,85 \times 0,80 \times 1,2 \times 60 = 49 \text{ MPa}$$

Shear strength is assumed $0,33 \sqrt{f_{cyl}} = 2,5$ MPa

Core tests have shown the structural strength to be $0,9 \times f_{cube}$ at an average for slipformed parts of a platform. Also the relatively high rate of loading will tend to increase the strength, such that the adopted values should be conservative.

Reinforcement:

longitudinal bars: KS50 $f_s = 480$ MPa
stirrups : KS40S $f_s = 400$ MPa

Cables : $f_{ps} = 1575$ MPa
$T_s = 4,29$ MN
At stressing $T = 2,9$ MN

4.2 Global strength

At the mudline the loading due to tanker impact is smaller than due to environmental loads, thus evaluation of global strengths may be limited to the shaft.

At the top of the shaft the load effects are very small, and need not be considered.

At the base of the shaft the load effects are considerably larger than those caused by environmental loads. However, the design criteria are very different, as membrane tension should be avoided for the latter loads.

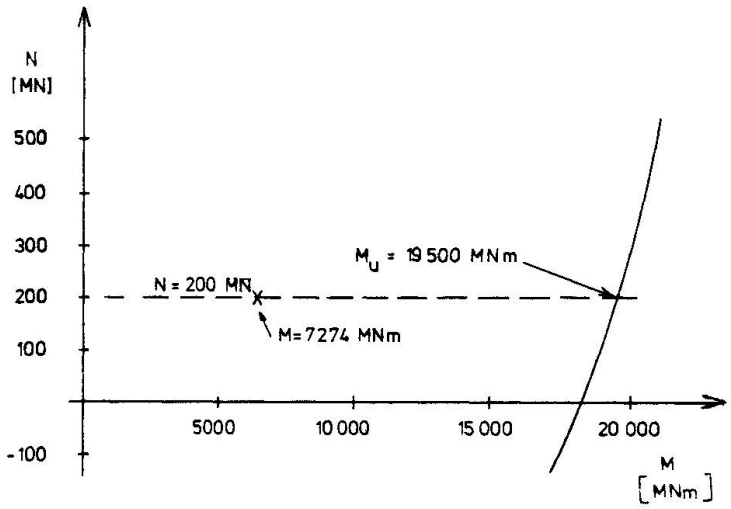

Fig. 6 Response and strength of shaft base.

The flexural strength of the shaft base is shown in fig.6. The vertical compression due to deck weight is approx.200 MN.

It is seen that the applied load is far below the capacity. In fact the strength is so high that the failure load of the tanker (=265 MN) is not likely to damage the shaft base.

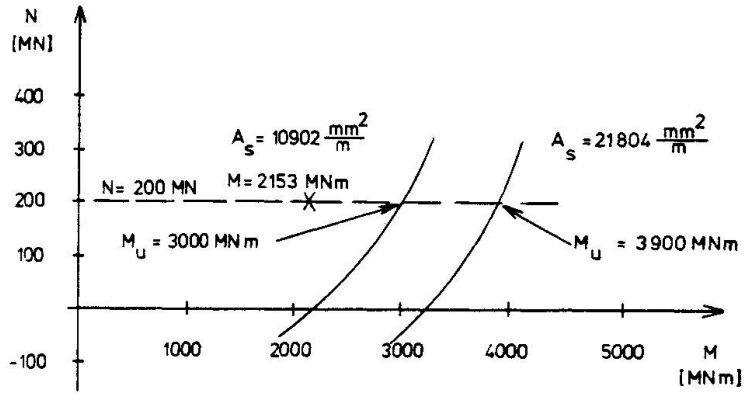

Fig. 7 Strength of shaft at waterlevel.

Also the section at the level of impact has sufficient capacity (fig. 7) to resist accidental impact without any damage. The reserves are, however, smaller than for the section at base of shaft.

4.3 Local strength

The flexural strength of shaft wall at the level of impact is shown in fig. 8.
The shear strength is expressed

$$Q_u = .33\sqrt{f_{cyl}} \times d + A_{sv} \times f_s \times h' + N/6$$

For $A_{sv} = 3095\ mm^2/m^2$

$d = .65 - .0625 = .5875\ m$

$h' = .65 - .125 = .525\ m$

$f_s = 400\ MPa$

$$Q_u = 2.5 \times .5875 + 3095 \times 10^{-6} \times 400 \times .525 + N/6$$

$$= 1.47 + .65 + N/6 = 2.12 + N/6$$

The local response is plotted on fig. 8. The applied shear and shear strength are shown in table 3. Thus, both flexural and shear strength compare favourably with the applied load, also for velocities in excess of 2m/s.

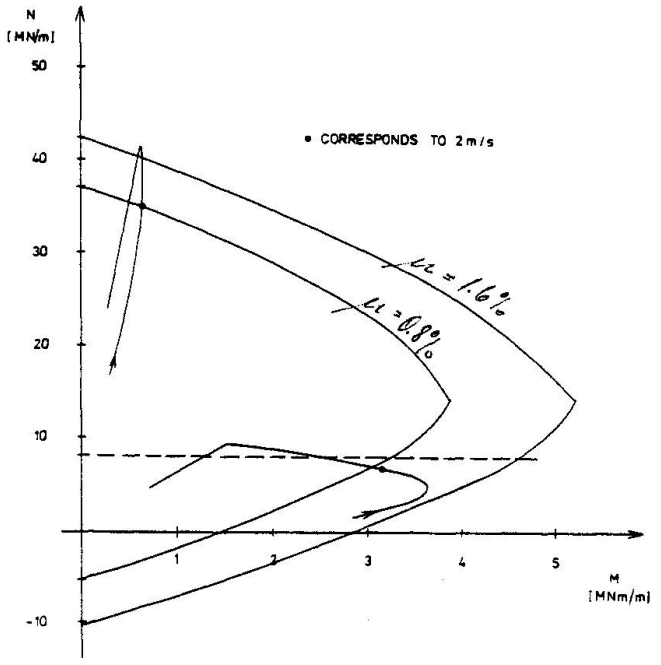

Fig. 8 Strength of shaftwall at waterlevel.

Q	N	Q_u	Qu/Q
1.42	1.72	2.41	1.69
1.46	2.32	2.51	1.71
1.49	2.60	2.55	1.71
1.51	2.79	2.59	1.72
1.50	2.92	2.61	1.74
1.49	3.26	2.66	1.79
1.51	3.55	2.71	1.79
1.49	3.93	2.77	1.87
1.46	4.70	2.82	1.93
1.42	4.50	2.87	2.03
1.31	5.02	2.96	2.26
1.23	4.60	2.89	2.35
1.21	4.67	2.90	2.40
1.19	4.70	2.90	2.43
1.02	5.63	3.06	3.00
.90	4.88	2.93	3.24
.71	6.14	3.14	4.44
.55	6.29	3.17	5.81

Table 3
Shear strength.

5. CONCLUSIONS

It has previously been demonstrated, ref.(1), that supply ships up to 5000 t do not have sufficient strength to overstress the concrete shaft, regardless of ship velocity.

The present investigation of the impact behaviour between a 150 000 tdw tanker and the concrete shaft can be summarized as follows, bearing in mind the uncertainties in the various assumptions:

At the mudline, the loading due to tanker impact is smaller than those caused by environmental loads.

At the base of shaft, the loading due to tanker impact exceeds those due to environmental actions. However, design criteria are widely different, thus strength is adequate for the 2 m/s velocity. Most likely the rupture load of the tanker may also be resisted by adequate design.

At the top of the shaft the loading due to tanker impact is very small.

The highest strained area seems to be at the level of the impact. Nevertheless, it is possible to design this area such that failure of the shaft is avoided, even for the extreme accidental case of a 2 m/s impact from a 150 000 tdw tanker.

6. REFERENCES

1. RØLAND, SKÅRE AND OLSEN, Ship Impact on Concrete Shafts. Nordisk Betong 2-4, 1982.

2. NPD., Regulations for the Structural Design of Fixed Structure on the Norwegian Continental Shelf, 1977.

3. VERITAS., Rules for the Design Construction and Inspection of Offshore Structures, 1977.

4. SVEIN FJELD, Design Assumptions and Influence on Design of Offshore Structures, IABSE Report Volume 41, 1983

5. VERITAS., Impact Loads from Boats TNA 202, 1982.

Leere Seite
Blank page
Page vide

Ship Impact in Ferry Berths

Choc de navire dans les bassins de mouillage

Schiffsstoß in Fährbetten

Jesper LARSEN
Civil Engineer
Danish State Railways (DSB)
Copenhagen, Denmark

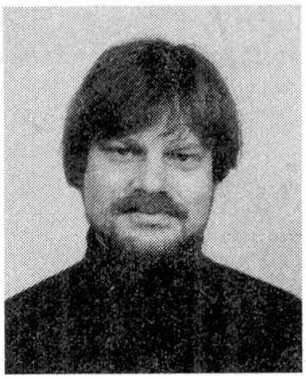

Jesper Larsen, born 1950, holds M. Sc. and Ph. Degrees from the Technical University of Denmark. For six years he has been a consultant in applied mathematical modelling. For DSB he has been involved in the design of ferry berths.

SUMMARY
The paper reports on the computation of reaction forces from ship impact in ferry berths. Actual berthing records and computed results are presented.

RÉSUMÉ
L'article présente le calcul de force de réaction dans les bassins de mouillage par suite de choc de navire. Les forces réelles lors d'accostage et les résultats de calcul sont présentés.

ZUSAMMENFASSUNG
Der Artikel behandelt die Berechnung von Reaktionslasten nach einem Schiffsstoß in Fährbetten. Theoretische und tatsächliche Lasten beim Anlegen werden angegeben.

1. INTRODUCTION

Since the time required for the berthing of a ferry often is a substantial part of the total operational time of the ferry, considerable gains can be obtained by reducing this time as far as possible. For that purpose many ferry berths consist of two lead-in jetties which guide the ferry to its final position in the berth. The lead jetties are constructed of a rigid, movable part which is separated from a fixed quay wall by elastic elements. The fender construction is made of panels linked by loose joints in order to limit the bending moments in the construction and to activate only a rather limited number of elastic elements and accordingly limit the stiffness of the total system and hence the resulting force. To assure sufficient mobility of the system the joints are constructed with play.

In the present paper we analyse the problem of designing these constructions. From the horizontal motion of the ship we estimate the impact energy which is stored in the elastic elements at maximum compression. The ship - structure interaction is sufficiently complex to warrant the development of a computer program for the evaluation of the forces and the deformations involved in the impact. The computer program is based on conservation equations for energy, forces and moments on the structure at maximum compression.

In the next section we analyse ship manoeuvres in ferry berths from simulated data and actual measurements. The impact energy is considered next. In the the last two sections the computer program is described and an example of a computation is presented.

2. FERRY MANOEUVRES

In order to possibly improve the navigation in the danish ferry harbours Nyborg and Korsør a series of manoeuvring simulations has been carried out by the Danish Ship Research Laboratory. The simulations are carried out with a navigation program simulating in real time the combined effect of propeller, rudder, wind and current forces on the ship. The navigator controls the propellers and the rudder. Due to the large surface area of the ferry, which are exposed to the wind, a considerable drift can be observed in storms.

In parallel with the simulations a series of actual measurements of ferry arrivals and departures was conducted. With two optical laser instruments the horizontal angle and the distance to two prisms, attached to the ferry some distance apart, are recorded every two seconds. From the data the ferry position and horizontal velocity components can be tracked throughout the berthing procedure. Two trackings are shown in Fig. 1. In Fig. 1a the ferry enters the berth with a fairly high velocity (5 knots) but is slowed down to 3.3 knots at the time of impact. The ship has no sway and only little yaw motion. In Fig. 1b the ferry enters the berth with a slower speed, but now it has considerable sway and yaw motions. The positions are shown every 10 seconds.

3. IMPACT ENERGY

A definition sketch of the impact situation is shown in Fig. 2. We consider only the horizontal degrees of freedom, i.e. the surge,

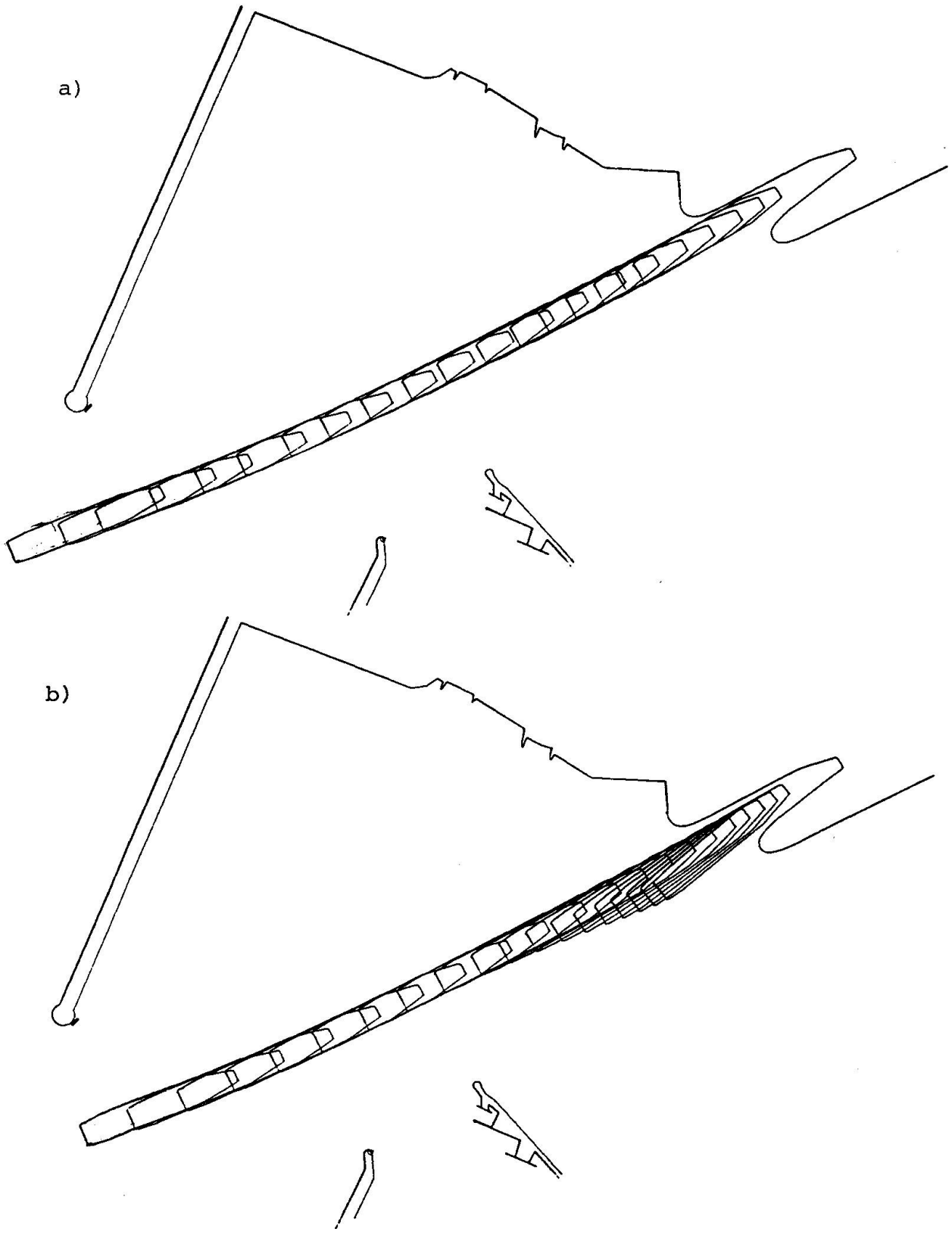

Fig.1 Actual ship manoeuvres in Korsør ferry harbour. 1a) normal berthing. 1b) berthing with considerable sway and yaw motion.

sway and yaw motions and we denote the corresponding velocities u, v and ω, respectively. The distance between the center of gravity and the point of impact is a. We include here a derivation of an expression for the impact energy, since existing formulas [1] and [2] are either too simple or inadequate.

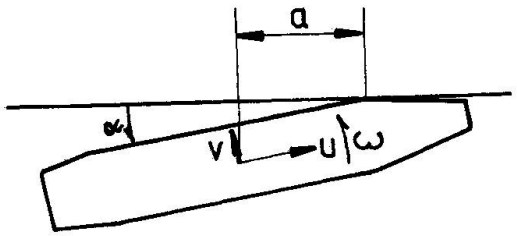

Fig.2 Definition sketch.

The impact energy is estimated as

$$\Delta E = \tfrac{1}{2}M(w^2-w_m^2) + \tfrac{1}{2}I(\omega^2-\omega_m^2). \quad (1)$$

Here

$$w = u\cdot\sin\alpha + v\cdot\cos\alpha \quad (2)$$

is the velocity of the ferry perpendicular to the fender construction at the time of impact. The subscript m refers to the corresponding quantities at maximal compression of the fender construction. The mass M and the moment of inertia I include the induced hydrodynamic inertia. The friction of the fender construction is neglected, hence the contributions from the velocity along the quay cancel. At maximal compression the velocity perpendicular to the fender construction at the point of impact is zero. Thus

$$w_m = -a\cdot\omega_m. \quad (3)$$

From conservation of angular momentum about a vertical axis through the point of impact we find

$$I(\omega-\omega_m) = aM(w_m-w). \quad (4)$$

Elimination of ω_m and w_m between (1), (3) and (4) yields

$$\Delta E = \tfrac{1}{2}M(w+a\omega)^2/(1+a^2/k^2), \quad (5)$$

where $k = (I/M)^{\frac{1}{2}}$ is the radius of gyration. The energy estimate in (5) is conservative since friction losses are neglected. A considerable uncertainty in the estimate is the determination of the added mass coefficient (c.f. [3]). The ferry shown in Fig. 1 has a displacement of about 12,000 m^3. With an added mass coefficient of 1.5 and $a \approx k \approx 40$m we find ΔE = 0.4 MJ and ΔE = 1.3 MJ for the situations shown in Fig. 1a and 1b, respectively. But considerably higher energies have been recorded.

4. COMPUTATION OF REACTION FORCES

The fender constructions are shown in Fig. 3. Rigid steel panels are separated from the quay wall by elastic rubber cylinders. The panels are connected by loose joints. The play in each joint is 3 cm. Each panel has three degrees of freedom, a translation perpendicular to the quay wall and rotations about a vertical axis and a horizontal axis parallel to the quay wall. When the displacements are given the compression of each cylinder can be found and correspondingly the reaction forces and the energy stored in each

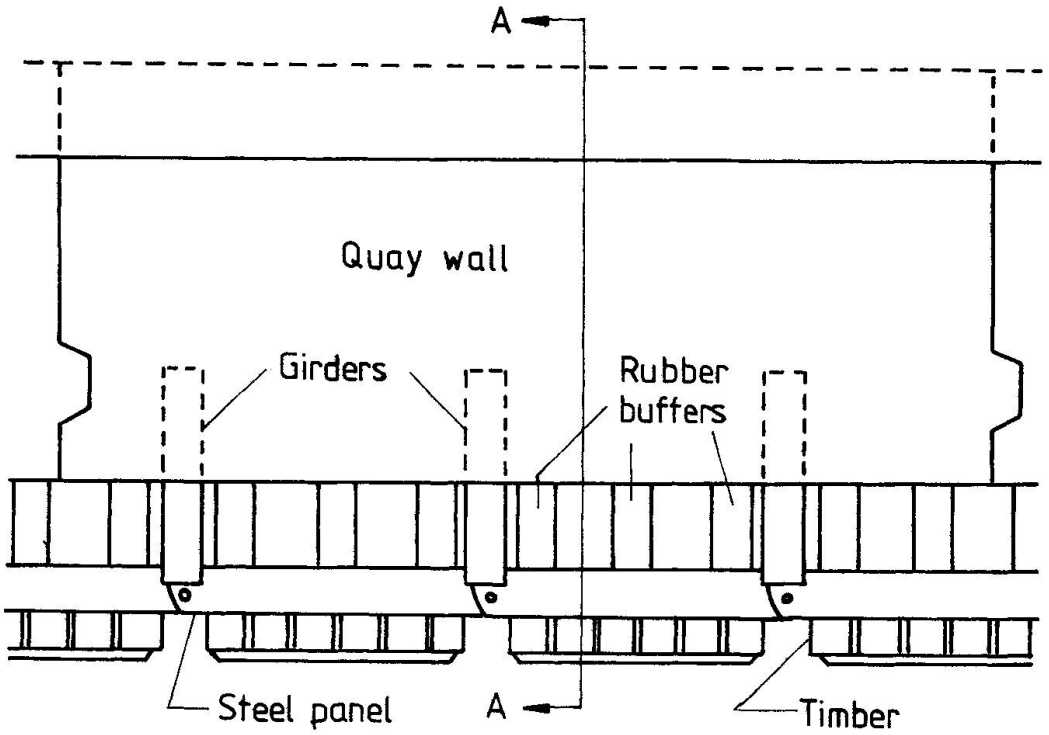

A - A

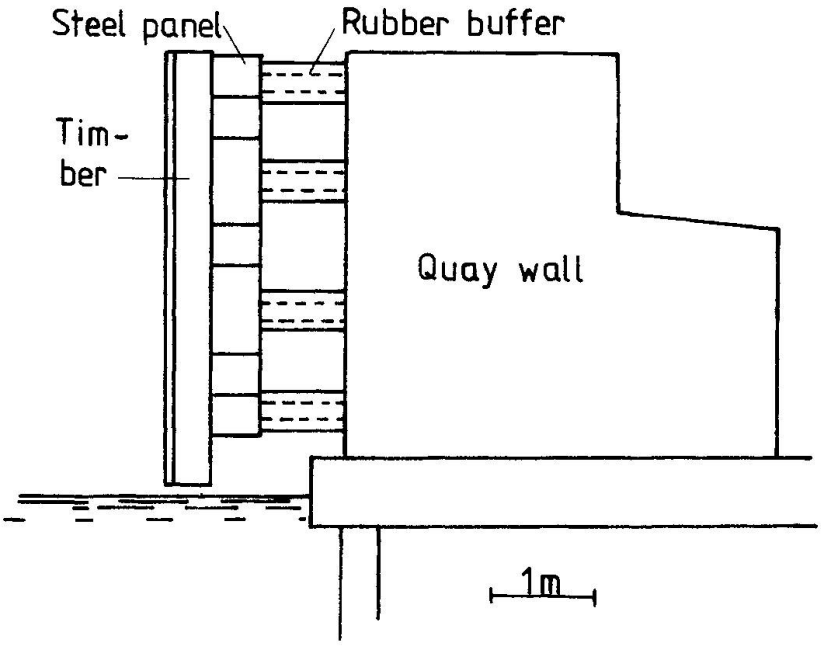

Fig.3 Fender constructions in Korsør ferry harbour.

cylinder can be computed. The panels are suspended in vertical chains and their horizontal motions are limited by horizontal chains. For a section of N panels we have 3N+1 unknowns, viz. the three degrees of freedom per panel and the total impact force. For the determination of these unknowns we have 2(N-1) geometrical constraints at the joints, N moment balance equations about vertical axes through the joints, a moment balance equation about a horizontal axis, a horizontal force balance and an energy balance, in all 3N+1 equations. These non-linear equations are solved by an iterative technique based on a combination of the steepest descent method and Newton's method [4] . In Fig. 4a we have shown a load-deflection curve for the rubber cylinders. This curve is represented by a third-order spline [5] in the program. In Fig 4b we have sketched the force-deformation curve for the horizontal chains which also must be treated as elastic elements, although of very high stiffness, in order to close the system of equations. The energy stored in the rubber cylinders is calculated

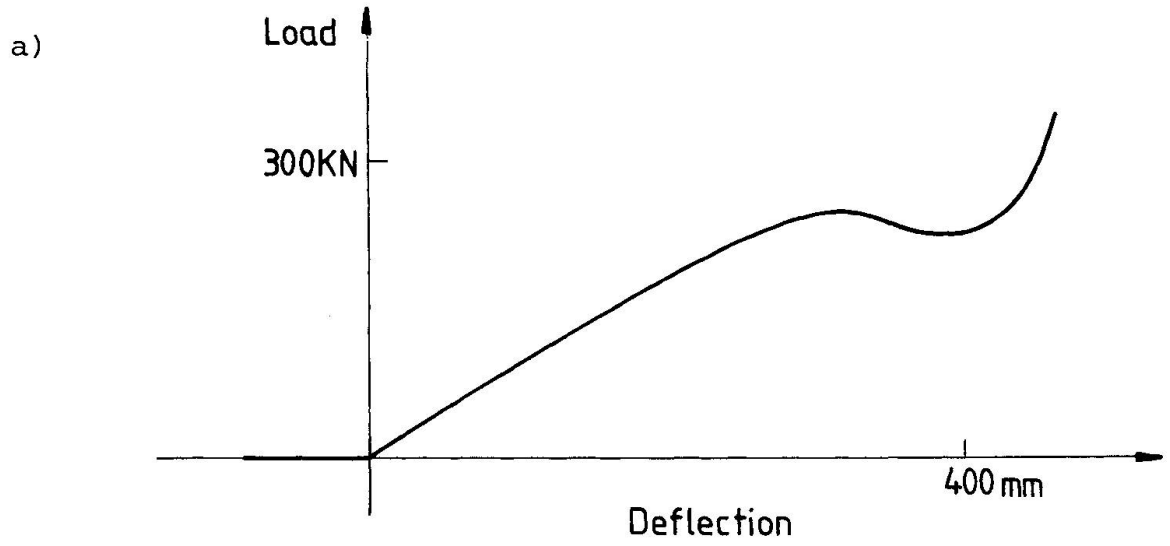

from the load-deflection curve as

$$E(\delta) = \int_0^{\delta} K(x)\,dx, \qquad (6)$$

where E is the energy stored, δ is the deflection and K is the reaction force as a function of the deflection.

If a certain impact force F is exceeded, the quay wall will slide on the lower part. A special mechanism, which gives a well defined friction force and which allows for an easy re-establishment of the pertinent quay wall section, has been developed. If the quay wall slides a distance s, an additional energy of F•s is absorbed.

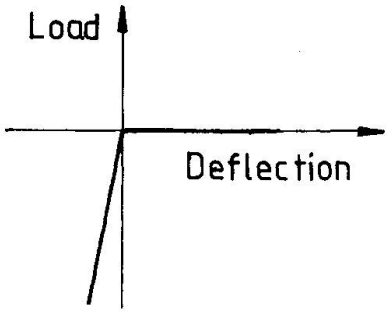

Fig.4 Load-deflection diagrams for rubber cylinders a) and chains b).

5. EXAMPLE

The input to the program comprises the number of panels, the placements of the joints, the specification of the placement and the load-deflection curves of the elastic elements, the point of impact and the energy to be absorbed. The output comprises the total impact force and force in each elastic element. In Fig. 5 the resulting forces on a section of nine panels are shown. The impact energy is 0.9 MJ. Only the results in the three panels closest to the point of impact are shown. We see that although the right hand panel has a smaller displacement than the one in the middle, it is supported by the buffer with the highest reaction force. Thus the nonlinear character of the problem is clearly demonstrated.

ACKNOWLEDGEMENTS

The author wish to thank Ellen Hess Thaysen for her interest in and support of this work, Jørgen B. Jørgensen for the testing of the program and Bjarne Pankchik for the navigation data.

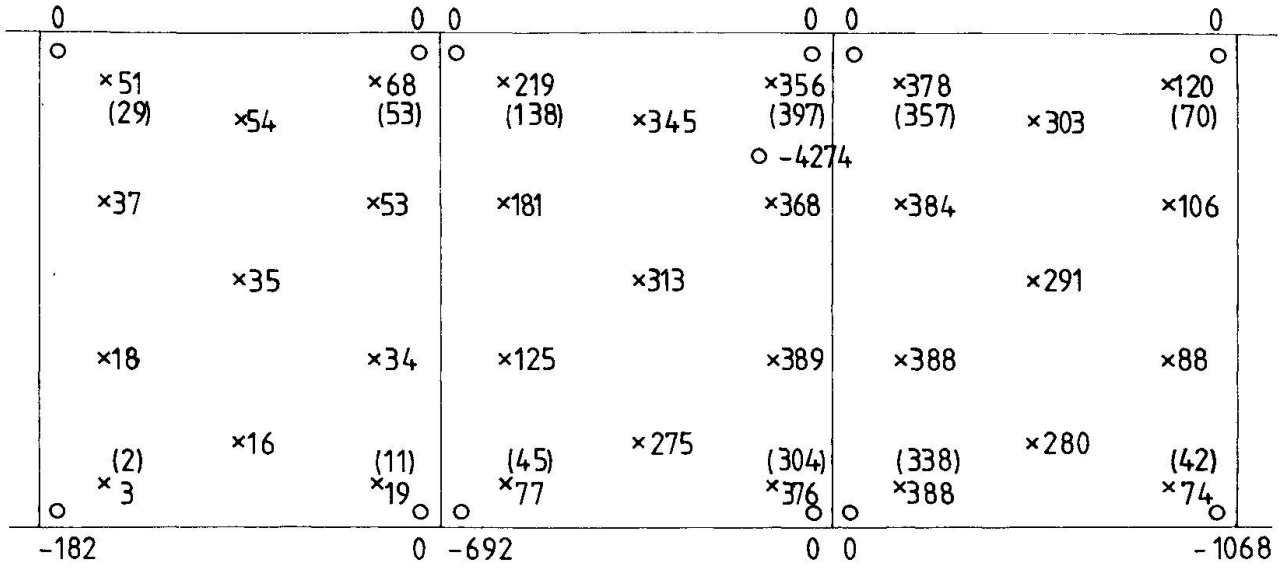

Fig. 5 Resulting forces and deformations of a fender construction shown on a sketch of the construction. Forces are in KN and deformations (shown in parentheses) are in mm. Crosses mark the rubber cylinders and circles mark the chains and the point of impact.

REFERENCES

1. PORT Planning Design and Construction. The American Association of Port Authorities. 1973, pp. 423-426.

2. VASCO COSTA, F., Berthing Maneuvres of Large Ships. In Per Bruun Port Engineering. Gulf Publishing Comp. 1973, pp. 401-417.

3. BALL, D.J. and Markham, A., Maximum added mass for a berthing tanker in very shallow water. The Dock & Harbour Authority LXIII No. 743, 1982, pp. 209-210.

4. BLUE, J.L, Robust Methods for Solving Systems of Nonlinear Equations. SIAM J. Sci. Stat. Comp. 1, 1980, pp. 22-33.

5. DAVIS, P.J. and Rabinowitz, P., Methods of numerical integration. Academic Press. 1975, p. 367.

Leere Seite
Blank page
Page vide

Damage on Offshore Tubular Bracing Members

Endommagements de renforcements tubulaires

Schaden an Rohrelementen von »Offshore« - Bauten

Charles P. ELLINAS
Senior Engineer
J. P. Kenny & Partners Ltd
London, England

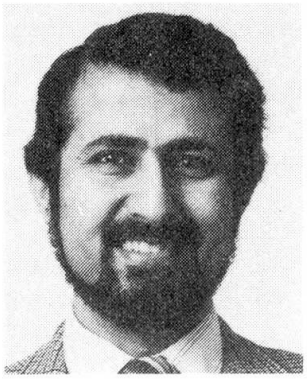

Charles Ellinas, born 1949, received his B.Sc. and Ph.D. degree at University College London, where, for eight years, he was involved in research on the buckling behaviour of structures. He is now responsible for the preparation of guidance notes on the buckling design of offshore structures, for the UK Department of Energy.

Alastair C. WALKER
Assoc. Techn. Director
J. P. Kenny & Partners Ltd
London, England

Alastair Walker, born 1937, received his B.Sc. at Royal College of Science & Technology, Glasgow, and his Ph.D. degree at the University of Glasgow. In addition to being Associate Technical Director of J P KENNY, he holds the Chair of Professor of Experimental Mechanics at the University of Surrey.

SUMMARY
This paper deals with the analysis of collision and impact effects on circular tubular beam-columns and offshore bracing members. Methods for estimating the possible extent of damage and its effect on member strength are developed and compared to available theoretical and experimental results. Finally, it is recommended that the simplicity and explicitness of the developed analytical expressions make them ideal for use in design.

RÉSUMÉ
Cet article traite de l'analyse des effets résultant de la collision et des impacts sur une colonne circulaire rigide et les membrures de renforcement d'une structure marine. Les méthodes d'estimation de l'extension possible des dommages et leurs effets sur l'intégrité des membrures, sont developpées et comparées avec les résultats expérimentaux et théoriques. La simplicité des expressions analytiques developpées rendent celles-ci idéales pour le calcul et le projet.

ZUSAMMENFASSUNG
Die Einwirkungen von Kollisionen und Anstößen an Rohrelementen und deren Verstärkungen für »Offshore«-Bauten werden untersucht. Methoden zur Abschätzung möglicher Schäden und der resultierende statische Verlust wurden entwickelt und mit experimentalen Resultaten verglichen. Die Einfachheit der vorgeschlagenen Berechnung spricht für deren Anwendung im Entwurf.

1. INTRODUCTION

The capability of assessing the effects of an impact between a moving object and a structural component of an offshore installation is of considerable interest to design engineers. The task is twofold; first to determine the probable extent of damage and second to evaluate the deterioration in the load-carrying capacity of the member.

So far as the first is concerned, it is a somewhat intractable problem for general design, since the extent of the damage is a function both of the kinetic energy of the impacting body and of the precise local geometry and material characteristics of the zones of impact of the moving object and the structural member. The consequences of the damage can be assessed completely only if these parameters of the damage zone can be exactly defined. A mathematical analysis of the process would require the modelling of the non-linear dynamic, geometric and material behaviours of both bodies. This is a formidable task and not one to be undertaken at the design stage, especially when the impacting objects can range from a valve body dropped from the platform deck, to a supply boat moving at an indeterminate velocity.

However, despite this analytical intractibility the offshore engineer needs to have some information on the damage tolerance of the structural members. He needs, for example, to make decisions prior to construction, regarding the need to protect the structure or to provide alternative, and possibly expensive load paths to cover the case of collision disabling a vital structural member. Guidance should be available to engineers to assess if, in the event of damage occurring, the structural strength has been seriously impaired. Such guidance appears to be lacking in presently available design codes [1,2].

Some line of approach must therefore be developed which adequately fulfills the requirement for information but which circumvents the complexity of precise mathematical formulation. The first task in such a development is to define the precision with which the information is required. In the general situation impact with an object of a certain shape and kinetic energy, for example the bow or side of a vessel, can cause either complete destruction, moderate damage or slight damage to the structural component under consideration. In the first of these categories if such an impact is likely, it will be necessary to provide protection or an alternative load path. In the second, the main concern will be to estimate the reduction in strength and to ensure that the structure can survive until the necessary repairs are effected. In the last category the question may be whether repair is really necessary, or does the damaged structure possess adequate reserve load-carrying capacity to continue being of service. Of course in jackets with a multiplicity of members, one or more of these members may be damaged in one or more of the above ways.

In this paper we restrict our attention to a discussion of the appropriate level of analysis for supplying adequate information to cope with slight to moderate damage. The particular structural component considered here is a circular tubular member, such as may be used in a braced jacket structure. It is shown that approximate and simple methods of analysis can furnish information of significance to engineers, and certainly sufficient for the evaluation of the likely safety of the structural members under consideration.

It is suggested that this level of analysis is one of the most likely to be successful in providing general information to designers. This is not to say that there is no need for more precise mathematical models. However, these may be expensive and may not provide information in an easily accessible and explicit form. Moreover, they can be developed only for special cases and research programmes [3,4,5]. As such they could provide a useful back-up and verification for simplified approaches like the one proposed in this paper.

2. EXTENT OF DAMAGE

Tubular members subjected to lateral loads as a result of impact or collision develop two main modes capable of absorbing the imparted energy. These are local denting of the tube wall and overall bending of the member as a beam. Experimental observations reported in reference [10] indicate that simply supported tubes subjected to lateral knife edge loads, initially undergo a purely local denting phase, followed by overall bending and some additional local denting deformations, until finally collapse occurs. It appears therefore to be useful from the analytical point of view to consider the two modes separately.

2.1 Local Denting Damage

The experimental results from reference [10] indicate that during the initial local denting phase there is a monotonic non-linear increase in lateral load, P, with respect to the local dent depth, d_d. In addition, the deflected profile in the longitudinal direction of the tube, shown in Figures 1 and 2, can be expressed as

$$d = d_d e^{-1.3\frac{x}{D}} \qquad (1)$$

where d is the radial deformation at a distance x from the point of application of the lateral load. As this radial deformation becomes less than 1% of the dent depth, d_d, when $x/D > 3.5$, it appears reasonable to assume that the extent of denting in the longitudinal direction, ℓ_d, is approximately equal to

$$\ell_d = 3.5\,D \qquad (2)$$

on either side of the point of application of the lateral load, as shown in Figure 1(a).

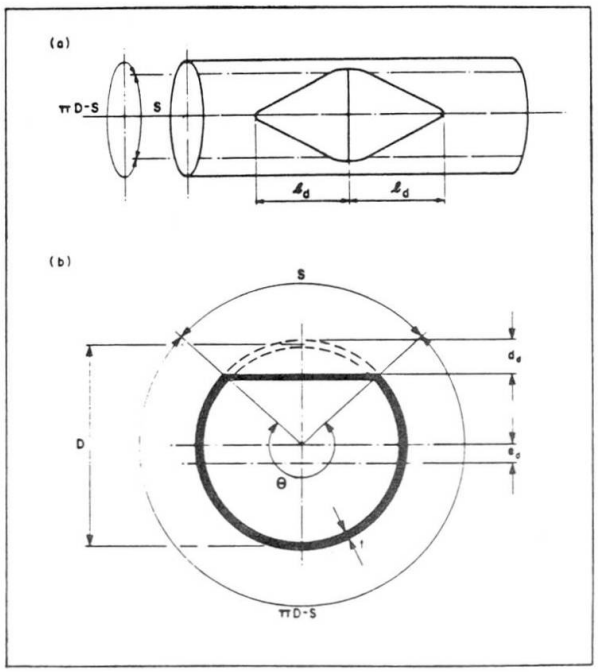

Fig.1 Dent geometry

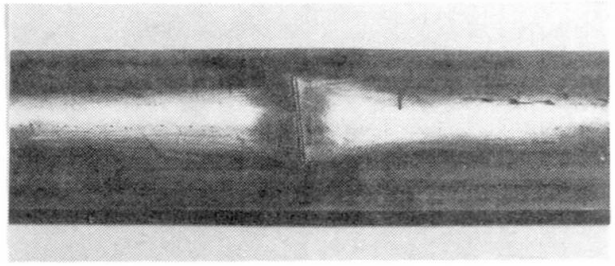

Fig.2 Typical local dent

Assuming a rigid perfectly plastic response, the relationship between this lateral load and the dent depth can be shown, through energy considerations [9], to take the form

$$P = K m_p \left(\frac{d_d}{D}\right)^{1/2} \qquad (3)$$

where K is a constant and m_p is the plastic moment resultant of the tube wall, given by

$$m_p = \frac{1}{4}\sigma_Y t^2 \qquad (4)$$

Experimental results reported in references [5,9] and plotted in Figure 3, verify the validity of eqn (3), and in addition indicate that constant K is approximately given by

$$K \approx 150 \qquad (5)$$

With the load-dent depth response and the locally deformed shape now defined it is possible to estimate the amount of energy absorbed locally. The experimental results reported in reference [10], and similar results reported in [5,9], indicate that in general the deformed shape consists of a very well defined yield line under the indenter (through which the lateral load is applied); the remainder of the deformed shape has no

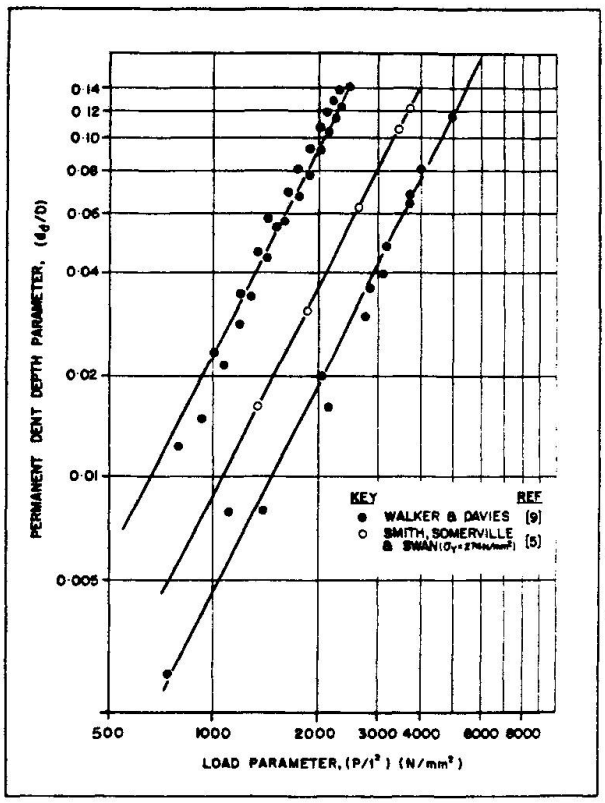

Fig.3 Dependence of dent depth on lateral load

well defined yield lines, as shown in Figure 2. Assuming that the imparted energy is dissipated locally, and that the denting process takes place at a sufficiently slow rate, to allow the replacement of the impact force by a pseudo-static load, the energy absorbed during the formation of the local dent, E_d, may be expressed as follows

$$E_d = \int P \, d(d_d) = 100 m_p (\frac{d_d^3}{D})^{\frac{1}{2}} \quad (6)$$

While the tube continues to deform into the local denting mode its stiffness against overall bending deformations decreases continually, due to the change in the tube's cross-section, as shown in Figure 1(b). At a certain critical value of the lateral load, P_o, this reduced bending stiffness will reach a certain value after which the tube will start deforming in an overall bending mode. During this second stage it is assumed that local denting ceases to increase further and that the remainder of the imparted energy is absorbed by the reduced section tube deforming plastically into this overall bending mode.

2.2 Overall Bending Damage

The extent of overall bending damage of a tubular member subjected to lateral impact loads depends strongly on the geometry of the member and its exact end support conditions. Clearly, tubes with built-in ends develop considerably smaller overall deformations than pin-ended tubes. Extensive theoretical treatment of the problem is presented in references [7,8].

However, for reasons of simplicity and as a conservative approach, it is assumed here that the tube is fully restrained flexurally at its end supports, but free to translate in the longitudinal direction. This ensures that no longitudinal tensile stresses are induced due to pull-in at the supports as a result of overall bending deformations. Under such conditions the maximum lateral load, P_o, may be obtained using classical limit plasticity theory. This shows that

$$P_o = \frac{8 M_p}{L} \quad (7)$$

where M_p is the plastic moment capacity of the tube's cross-section. For an undamaged circular tubular member

$$M_p = D^2 t \sigma_Y \quad (8)$$

For the locally dented section, shown in Figure 1, M_p becomes a function of dent depth d_d. The following approach is employed in order to obtain the required relationship between M_p and d_d. It is first assumed that a certain initial longitudinal compressive stress, σ_{pd}, needs to be applied at the damaged part of the tube's cross-section, shown as arc S in Figure 1(b), before plastification occurs and a hinge is formed. This has been shown in references [4,6] to take the form

$$\sigma_{pd} = \sigma_Y (\frac{D}{t}) [\sqrt{\frac{16}{9}(\frac{d_d}{D})^2 + (\frac{t}{D})^2} - \frac{4}{3}(\frac{d_d}{D})] \quad (9)$$

Once σ_{pd} has been exceeded in the damaged fibres, they become ineffective and any additional bending is carried by the remaining effective section, shown as arc $(\pi D-S)$ in Figure 1(b). Considering the bending equilibrium of this fully plastic effective section enables the reduced plastic moment M_{pd} to be obtained as

$$M_{pd} = M_p [\cos\beta - \beta] \quad (10)$$

where

$$\beta = (\frac{d_d}{D})^{\frac{1}{2}} [1 - \frac{\sigma_{pd}}{\sigma_Y}] \quad (11)$$

The maximum lateral load, P_{od}, that can be carried by the flexurally restrained tube that has been locally dented at the middle, can be obtained by the following modified version of eqn (7), as a function of the dent depth, d_d.

$$P_{od} = \frac{4 M_p}{L} [1 + \frac{M_{pd}}{M_p}] \quad (12)$$

In obtaining eqn (12) it has been assumed that the plastic hinges at the end supports can develop their full moment capacity, M_p, while the hinge formed at the position of the dent can only reach M_{pd}. When $d_d=0$ eqn (12) reverts to the form of eqn (7).

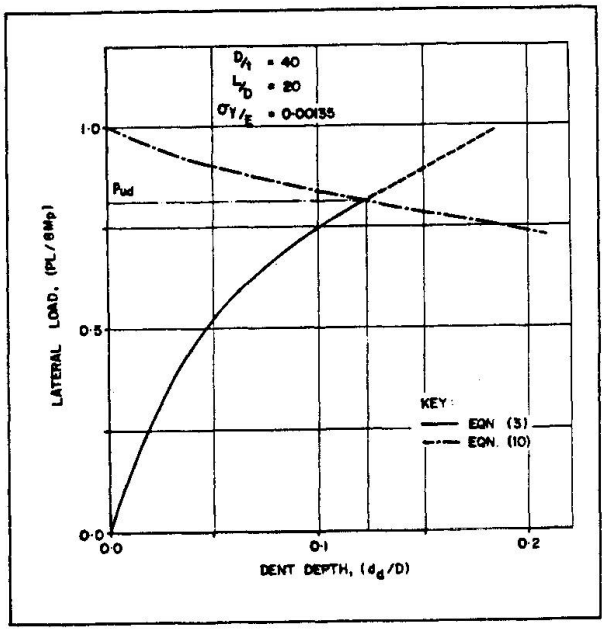

Fig.4 Estimation of ultimate lateral load, P_{ud}

The ultimate lateral load, P_{ud}, that can be sustained by the dented tube may be obtained by solving simultaneously eqns (3) and (10), as shown in Figure 4. For a bracing member with D/t=40, L/D=20 and $\sigma_Y/E=0.00135$

$$P_{ud} = \frac{6.6 M_p}{L}$$

The maximum dent depth, $\bar{d}_d$, suffered by this tube before it starts deflecting laterally is shown in Figure 4 to be

$$\frac{\bar{d}_d}{D} = 0.12$$

Although this simple approach enables the estimation of the extent of local damage and the evaluation of the ultimate lateral load carrying capacity of the damaged tube, it does not give any information on the extent of lateral deformations. The assumptions on which the present analysis is based imply that when P_{ud} has been reached the tube will cease deforming locally and will start displacing laterally at the same load. The magnitude of this lateral displacement, d_o, may be obtained by considering the energy absorption characteristics of the beam mechanism. The energy, E_o, absorbed by the flexurally restrained locally dented beam which, according to limit plasticity, collapses by the formation of a three hinge beam mechanism, is given by

$$E_o = \frac{4 M_p}{L} [1 + \frac{M_{pd}}{M_p}] d_o \quad (13)$$

The overall bending displacement, d_o, may then be obtained by assuming that the kinetic energy, E_k, released in the course of a collision or impact is absorbed by the tube developing deformations in both the local denting and overall bending modes, so that

$$E_k = E_d + E_o \quad (14)$$

substituting eqn (13) into eqn (14) allows d_o to be expressed as

$$\frac{d_o}{L} = \frac{(E_k - E_d)}{4 (M_{pd} + M_p)} \quad (15)$$

2.3 Applicability

The very simple methods developed in sections 2.1 and 2.2 allow the estimation of the extent of damage in both the local denting and overall bending modes, as well as the energy absorption characteristics of a tubular member. One of the basic assumptions used is that the tube is sufficiently compact to develop its full plastic moment capacity and therefore allow the use of plasticity methods of analysis. Guidance on geometries that can be considered compact is given in references [1,2]. However, even in cases where these geometric limitations are exceeded the present analysis may still be used in a modified form in which the material yield stress, σ_Y, is replaced by an effective limit stress equal to the local buckling stress of the section as defined in references [1,2].

In the general case a member in a braced frame is elastically restrained at its ends against both flexural rotations and longitudinal displacements. In such situations more accurate results may be obtained by using more complicated forms of analysis, in which the membrane stresses induced in the member due to the restraint against pull-in at the supports, are taken into account. This is particularly important when estimating overall bending damage. Relevant information is given in references [7,8]. However, the general approach employed in sections 2.1 and 2.2 is still applicable, and will certainly result in upper bound estimates of the extent of damage.

3. EFFECT OF DAMAGE ON MEMBER STRENGTH SUBJECT TO AXIAL COMPRESSION

The effect of local denting of the tube wall is to cause a reduction in the effective section area and modulus and an eccentricity of the neutral axis over the locally damaged region. Taken with accompanying overall bendin deformations, their combined effect can result in rapid deterioration in the load-carrying capacity of the member. Several methods have been proposed for assessing the reduced strength of damaged members, mostly dealing with the effects of local denting [4] or overall bending [3,5] in isolation. The combined effect of such damage modes on tubular member strength has been examined analytically in a recent paper [6], the important features of which are summarised here.

It is assumed that the stresses initially induced by the application of a small axial load are carried in the dented zone, shown as arc S in Figure 1(b), mainly by bending action, which rapidly leads to the formation of a hinge at the middle of the dent, as shown in Figures 1(a) and 2. These initial plastification stresses, σ_{pd}, are given by eqn (9). The consequent loss of stiffness makes this damaged zone ineffective in carrying additional axial load. Moreover, as the bending stiffness of the damaged tube is mainly controlled by that of the reduced effective section, shown as arc (πD-S) in Figure 1(b), this reduced effective stiffness may be considered to determine the loading response of the whole member. In addition, the axial load, which is still applied at the centroid of the full section, acts through an eccentricity, e_d, with respect to the neutral axis of the reduced effective section, shown in Figure 1(b).

The effects of overall bending damage are assumed to be similar to those resulting from large initial overall imperfections, and in the ensuing analysis they are treated as such.

These assumptions lead to a simplified analysis in which the damaged member is treated as a beam-column with a reduced effective stiffness. Its ultimate strength, σ_{ud}, may then be obtained by considering a first yield collapse criterion and using simple beam-column analysis, similar in form to that employed in deriving the design recommendations in reference [1]. This can be shown [6] to lead to the following quadratic expression in terms of σ_{ud}

$$\frac{1}{\sigma_e}\sigma_{ud}^2 - \left[1 + \alpha_o\lambda_d + \frac{A_d e_d}{Z_d} + \frac{f_y}{\sigma_e}\right]\sigma_{ud} + f_y + \sigma_{pd}\frac{A_d e_d}{Z_d} = 0 \qquad (16)$$

where f_y is the average squash stress of the damaged section given by

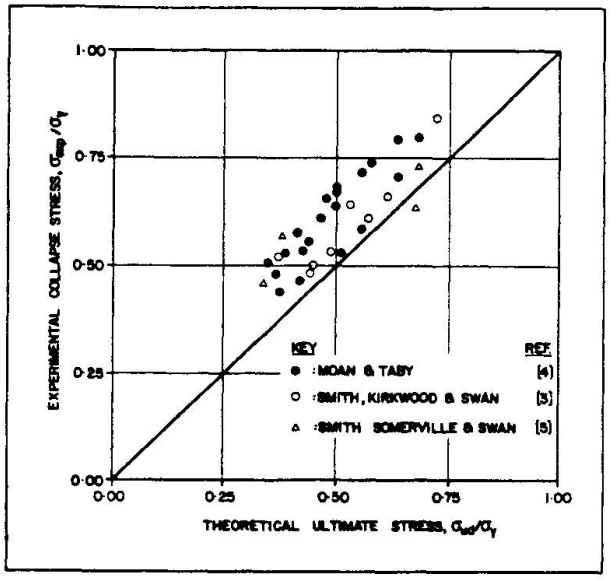

Fig.5 Theoretical and experimental comparisons for damaged tubes

$$f_y = (\sigma_y - \sigma_{pd})\frac{A_d}{A} + \sigma_{pd} \qquad (17)$$

and σ_e is the overall critical stress, which for a tubular member is given by

$$\sigma_e = \frac{\pi^2 E D^2}{8L^2} \qquad (18)$$

Parameters α_o and λ_d are respectively the overall imperfection parameter and the slenderness ratio, which for a damaged member take the form [6]

$$\alpha_o = \sqrt{2}\frac{d_o}{L} - 0.001 + 0.875\frac{\sigma_y}{E} \qquad (19)$$

and $$\lambda_d = \frac{L}{r_d} - 0.2\pi\sqrt{\frac{\sigma_y}{E}} \qquad (20)$$

The reduced effective section cross-sectional area, A_d, section modulus, Z_d, neutral axis eccentricity, e_d, and radius of gyration, r_d, may be obtained from

$$\left.\begin{aligned} A_d &= \tfrac{1}{2} D t \theta \\ Z_d &= \frac{r_d^2 t \theta}{[1 - \bar{d}_d/D + 2 e_d/D]} \\ e_d &= D\frac{\sin(\theta/2)}{\theta} \\ r_d &= \frac{D}{2}\left\{\frac{1}{2}\left[1 + \frac{\sin\theta}{\theta} - 8\frac{\sin^2(\theta/2)}{\theta^2}\right]\right\}^{1/2} \end{aligned}\right\} \qquad (21)$$

where θ is the angle subtended by arc $(\pi D - S)$ to the centre of the tube, shown in Figure 1(b), and it is given in terms of the dent depth, $\bar{d}_d$, by

$$\theta = 2\pi - 2\sin^{-1}\left[2\sqrt{\frac{\bar{d}_d}{D}\left(1 - \frac{\bar{d}_d}{D}\right)}\right] \qquad (22)$$

Thus the ultimate strength, σ_{ud}, of a damaged circular tubular member may be obtained using eqns (16) to (22).

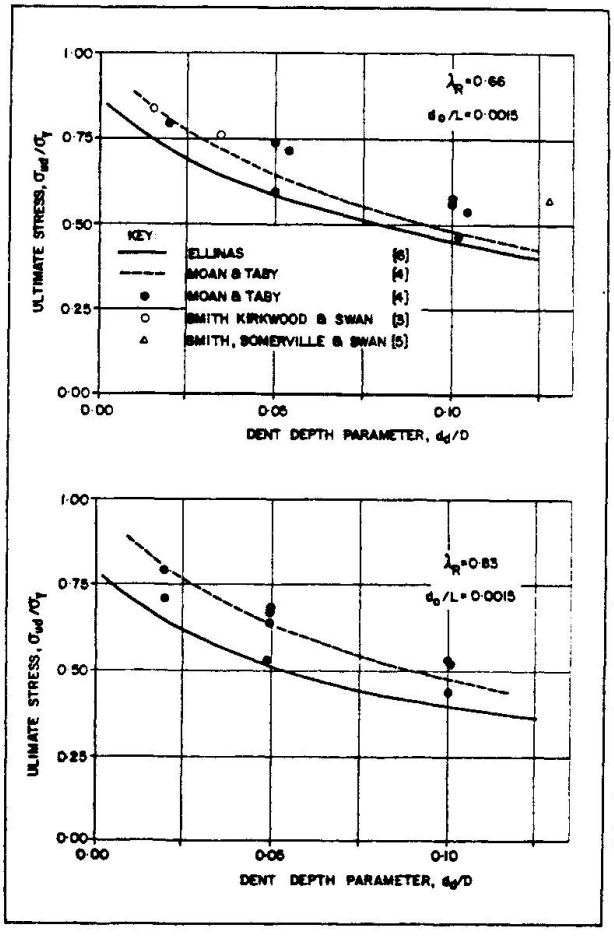

Fig.6 Comparisons for tubes with local denting damage only

4. THEORETICAL AND EXPERIMENTAL COMPARISONS

Available experimental information on the behaviour of axially loaded damged tubular columns is limited to a number of test results reported in reference [3,4,5], obtained mainly from locally dented steel specimens with geometries in the ranges $30<D/t<90$ and $0.6<\lambda_R<1.1$. For circular tubular members the reduced slenderness parameter, λ_R, is given by

$$\lambda_R = \frac{L}{D}\frac{2\sqrt{2}}{\pi}\sqrt{\frac{\sigma_y}{E}} \qquad (23)$$

Comparisons between predictions from the present theoretical method and available test results are shown in Figure 5. It is evident that a close agreement exists

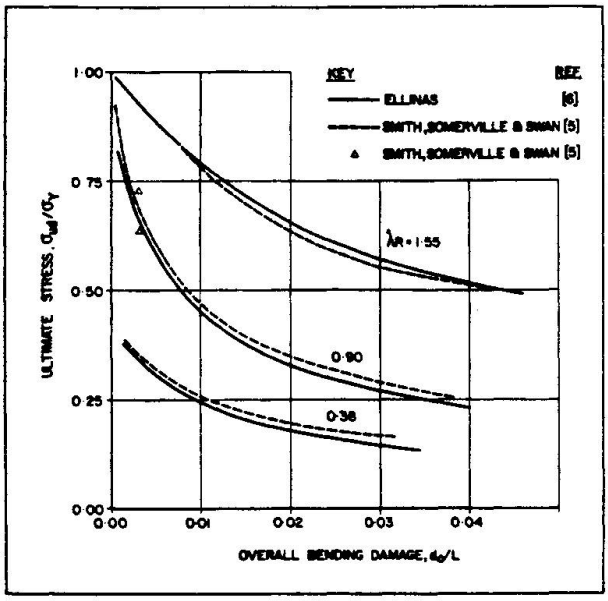

Fig.7 Comparisons for tubes with overall bending damage only

with the theory described in section 3 providing safe lower bounds to the experimental scatter. The single test result that lies below the theoretical line corresponds to a specimen reported in reference [5] to contain overall bending damage only, that might, however, have been locally dented before testing.

Further comparisons are shown in Figure 6 for tubes that contained local denting damage only. Theoretical results from reference [4] are also presented. It is again clear that the present method provides predictions in excellent agreement with those from reference [4] and with available test results.

Finally, comparisons with experimental and theoretical results from reference [5], for tubes with overall bending damage only, are shown in Figure 7. Again a close correlation appears to exist.

The theoretical and experimental comparisons of Figures 5,6, and 7 provide a convincing confirmation of the validity of the present simplified analysis in predicting the behaviour of damaged tubular member, subject to axial compression.

5. CONCLUSIONS

The methods developed in this paper for estimating the likely extent of damage in circular tubular bracing members due to accidental collision or impact, and for evaluating its effects on member strength, are based on simple physical reasoning and observed experimental behaviour. They lead to simple straightforward, analytical formulations, at a level sufficiently explicit to be of use to engineers who, faced with a damage problem, need to assess its consequences and make design or repair decisions.

The excellent agreement between predictions obtained from the present theory and available experimental and theoretical results, combined with the demonstrated lower-boundedness of the method, provide strong verification of its validity in predicting damaged member behaviour.

It is hoped that the methods presented goes some way in aurgmenting existing knowledge and in providing much needed guidance on the damage tolerance of circular tubular bracing members. Their simplicity and explicitness should make them ideal for use in design situations.

ACKNOWLEDGEMENT

The authors wish to acknowledge the help given by J P KENNY personnel in the preparation of this paper.

NOTATION

A, A_d	area of full and reduced effective section respectively
d, d_d, $\bar{d}_d$	dent depth
d_o	overall bending damage
D	tube mean diameter
e_d	eccentricity of centroid of reduced effective section from that of full section

E	modulus of elasticity
E_d	energy absorbed in local denting mode
E_k	kinetic energy released after impact
E_o	energy absorbed in overall bending mode
f_Y	average squash stress of damaged section
l_d	extent of denting in longitudinal direction
L	tubular member length
M_p	plastic moment resultant of tube wall
M_p	plastic moment capacity of full section
M_{pd}	plastic moment capacity of damaged section
P	applied lateral load
P_o	maximum lateral load sustained by undamaged beam
P_{od}	maximum lateral load sustained by local dented tubular beam
P_{ud}	ultimate lateral load sustained by locally dented tubular beam
r_d	radius of gyration of reduced effective section
t	tube wall thickness
x	longitudinal direction
Z_d	elastic section modulus of reduced effective section
α_o	imperfection parameter
β	overall bending damage parameter
θ	angle subtended by the reduced effective section to the centre of the tube
λ_d	column slenderness ratio of the reduced effective section
λ_R	reduced column slenderness parameter
σ_e	overall critical stress
σ_{pd}	dent plastification stress
σ_{ud}	ultimate axial stress carried by damaged column
σ_Y	yield stress

REFERENCES

1. DET NORSKE VERITAS (DnV), Rules for the Design, Construction and Inspection of Offshore Structures. Høvik, Norway, Reprint with Corrections, 1982.

2. AMERICAN PETROLEUM INSTITUTE (API), API Recommended Practice for Planning, Designing and Constructing Fixed Offshore Platforms. Washington D.C., U.S.A., API RP 2A, 13th Edition, January 1982.

3. SMITH C.S., KIRKWOOD W., and SWAN J.W., Buckling Strength and Post-Collapse Behaviour of Tubular Bracing Members Including Damage Effects. BOSS' 79, Imperial College, London, England, pp.303-326, 1979.

4. MOAN T., and TABY J., Theoretical and Experimental Study of the Behaviour of Damaged Tubular Members in Offshore Structures. Norwegian Maritime Research, No.2, pp.26-33, 1981.

5. SMITH C.S., SOMERVILLE W.L., and SWAN J.W., Residual Strength and Stiffness of Damaged Steel Bracing Members. 13th Annual Offshore Technology Conference, Houston, Texas, 4-7 May, 1981, Paper No. OTC 2981, pp.273-282, 1981.

6. ELLINAS C.P., Ultimate Strength of Damaged Tubular Bracing Members. Submitted to J. Structural Division, ASCE, 1983.

7. de OLIVEIRA J.G., Design of Steel Offshore Structures Against Impact Loads due to Dropped Objects, Proc. 3rd Inter. Symposium on Offshore Engineering Structures, Edited by F.L.L.B. Carneiro et al., Held at COPPE, Rio de Janeiro, Brazil, pp.466-483, 1981.

8. de OLIVEIRA J.G., The Behaviour of Steel Offshore Structures under Accidental Collisions. 13th Annual Offshore Technology Conference, Houston, Texas, 4-7 May 1981, Paper No. OTC 4136, pp.187-198, 1981.

9. WALKER A.C., and DAVIES P., Effect of Impact Loading on Denting of Tubulars. To be Published, 1983.

10. THOMAS S.G., et al., Large Deformation of Thin-Walled Circular Tubes under Transverse Loading. Int. J. Mechanical Sciences, Vol.18, pp.325-333, pp.387-397, pp.501-509, 1976.

Leere Seite
Blank page
Page vide

Rigid Bow Impacts on Ship-Hull Models

Chocs d'un arc rigide sur des modèles de coques de navires

Festbug-Aufprall gegen kleine Außenwandmodelle

Emmanuel SAMUELIDES
Research Assistant
Glasgow University
Glasgow, United Kingdom

Emmanuel Samuelides, born in Athens in 1957, degree in Naval Architecture and Marine Engineering, National Technical University of Athens in 1980, the same year he joined Glasgow University where he works as a Research Assistant on ship collisions.

Paul A. FRIEZE
Senior Lecturer
Glasgow University
Glasgow, United Kingdom

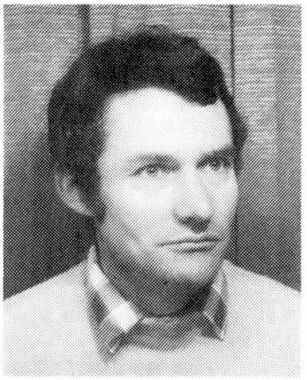

Paul A. Frieze, born 1943, degree in Civil Engineering, followed by MSc and PhD at Imperial College, London. His research was concentrated on ultimate strength studies of bridge, ship and offshore structure, using experimental and numerical methods.

SUMMARY
Results of collision tests on rigidly-supported and freely floating models are reported. The models represent the central portion of a tanker with two longitudinal bulkheads. The striker was a V-shaped rigid bow. Comparisons with a theoretical model are also presented.

RÉSUMÉ
L'étude présente les résultats d'essais de collision sur des modèles à support rigide et en flottaison libre. Ces modèles représentent la partie centrale d'un pétrolier doté de deux cloisons longitudinales. Les chocs ont été provoqués par un arc rigide en V. Des comparaisons sont faites avec un modèle théorique.

ZUSAMMENFASSUNG
Die Ergebnisse von Zusammenstoß-Tests mit starr gestützten und frei treibenden Modellen werden aufgezeigt. Die Modelle stellen den Mittelabschnitt eines Tankers mit zwei länglichen Schotten dar. Der Aufprall wurde durch einen Festbug in V-Form erzeugt. Vergleiche mit einem theoretischen Modell werden ebenfalls aufgeführt.

1. INTRODUCTION

1.1 Marine Pollution and Ship-Collision

During the last decade or so, protection of the environment against pollution whether from accidental or wilful acts has been of major concern. In the field of Naval Architecture, the emergence of nuclear-powered ships, of fleets purveying hazardous cargoes, and of the increasing number of incidents involving oil-tankers [1] which has resulted in major pollution problems have marked a turning point in the philosophy on which regulations concerning marine safety have been based. The traditional approach to safety has been to provent death, personal injury and property loss or damage [2]. The 1954 Convention on pollution by oil discharged by ships dealt only with deliberate acts, whereas the MARPOL Convention of 1973 aims not only to prevent pollution arising from accidents but also to limit the extent of any such spillage or leakage [3]. However, in the absence of adequate data concerning the resistance to penetration of ship structures from collisions and/or groundings, the cost of such regulations can be significant both at the construction stage and during operation. For example, tankers are now required to have segregated wing-tanks so that longitudinal bulkheads might act as a second line of defence. Neither the position of these bulkheads nor their design appear to have been properly justified, although their cost has had to be borne by the industry. Also the wing-tanks can only be used for ballast and must be empty when the tanker is in-cargo. This requirement not only results in a loss of cargo space but also may not provide the benefit expected since there is evidence that the presence of water in wing-tanks can probably help absorb energy as well as dilute the effect of a collision by effectively spreading it to a greater number of supporting members. On the other hand, in an attempt to reduce the risk and therefore consequences of collisions involving hazardous cargo carriers, the U.K. appears to have adopted a "restriction-on-speed" policy whenever such vessels and others in close proximity are manoeuvring in port and harbour waters. At the moment such restrictions appear to be too strict thus adding time and therefore cost to journeys.

In an effort to provide some guidance on appropriate speed restrictions, and energy-absorption capabilities of stiffening configurations and of water ballast in wing-tanks, a programme of research was initiated at Glasgow University. It was to be a combined experimental-numerical investigation into low- to medium-energy collisions, the experimental results of which were to be used to substantiate the numerical procedure. This paper reports some of these test results. In particular, tests involving stiff-bow impacts on rigidly-mounted models ('dry' tests) having wing-tanks both full and empty of water and on free-floating models ('wet' tests) are described. Comparisons with a theoretical model are also presented.

1.2 Background

Collision tests have been conducted mainly in Japan, Italy and Germany. The Japanese tests are reported in [4]. Static and dynamic tests on simple models were conducted using rigid and deformable bows. Two different fracture types were identified depending on the extent of plastic deformations. The effect of stem angle and of angle of collision were also examined. Twenty-four tests conducted in Italy between 1963 and 1971 on reasonably complex models of scale 1:15 (22 tests) and 1:10 (2 tests) are reported in [5]. An attempt was made to simulate added mass effects by immersing wings bolted to the models'sides in water. Some of the 24 tests conducted in Germany on models of scale 1:7.5 and 1:12 have been reported in [6]. The models were very detailed and both energy-absorbing and resisting type configurations were tested. The effect of water in the fore-peak tank of the striker was investigated.

Proposals have been made for full-scale tests [7]. However, the most cost-effective method of achieving the desired results is probably a combined numerical-experimental research programme using small- to medium-scale models followed by a

limited number of large-scale tests to confirm the adequacy of any allowance for scaling.

2. EXPERIMENTS

2.1 Models, Rig and Runway

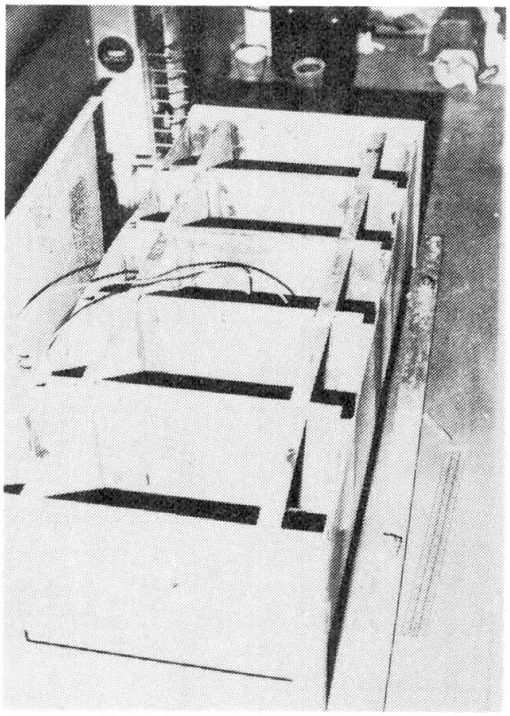

Fig. 1
Struck model

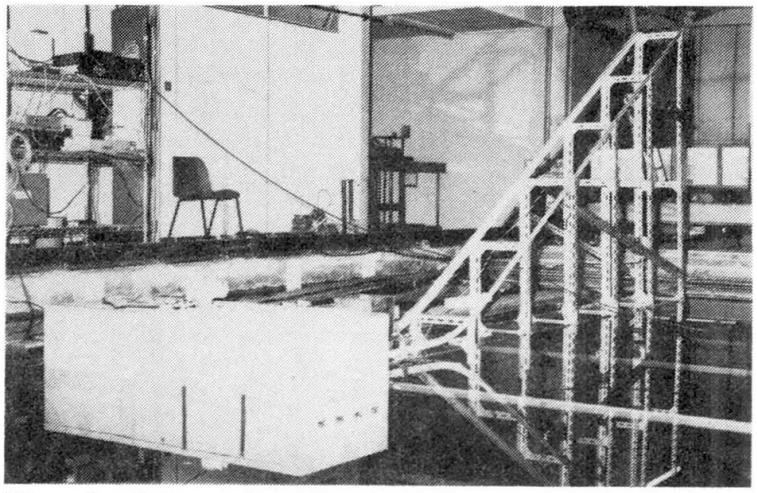

Fig. 2 Set-up for 'wet' tests

The models represent approximately 1:60 scale versions of a parallel-sided tanker with two longitudinal bulkheads and six transverse bulkheads, two of which form the ends of the model. The sides and bottom were formed from one piece of 0.79 mm thick plate to which the deck of the same thickness was rivetted. The bulkheads were made of plate 1.59 mm thick soldered to the bottom and sides of the shell and at their intersections. The models were 1.2 m long, .5 m wide and .3 m high and were fabricated from mild steel (Fig. 1). For 'dry' tests, the models were mounted between two stiff frames bolted to the laboratory floor and to the end bulkheads. For 'wet' tests, the models floated freely (Fig.2). The striker was a box mounted on four wheels to the front of which a V-shaped bow was bolted. It ran along a pair of L-shaped rails consisting of two straight sections and a curved section carefully bent according to the 1.5 power relationship. One straight section was inclined at 30° to enable the striker to gain energy, and the other was horizontal leading up to the point of impact. The mass of the striker was 10 kg which could be increased up to 60 kg by the addition of weights in the box.

2.2 'Dry' Tests

For these tests the velocities of the models just before and after impact were determined by the use of timers triggered by photo-cells activated by the passage of the striker between them. Deformations in the side-shell of the model were determined by scanning with transducers before and after the impact. Four tests have been conducted on one model, all on different tanks: details are given in Table 1. During tests 1 and 3 four tanks were filled with ballast water.

Test	B	M (Kg)	V_o (m/s)	V_a (m/s)	E_o (J)	E_a (J)	E_s (J)	E_s/E_o	S
1	0.81	28.6	3.3	-0.8	156	9	147	0.94	13.8
2	-	28.6	3.4	-0.9	165	12	154	0.93	17.0
3	0.94	39.9	3.4	-0.8	231	13	218	0.94	19.2
4	-	39.9	3.1	-0.9	192	16	176	0.92	16.7

B ratio of the volume of ballast water to the volume of the tank
M mass of the striker
V_o, V_a velocity of the striker before and after the impact
E_o, E_a kinetic energy of the striker before and after the impact
E_s energy absorbed by the struck model = $E_o - E_a$
S ratio of permanent deflection to thickness for the struck plate

Table 1 'Dry' Collision Tests Results

2.3 'Wet' Tests

Five tests were performed with the model floating freely in a towing tank except for a very small force generated by an electro-magnet used to just keep the model in position. The striker's input velocity and the side-shell permanent deflection were measured as for the 'dry' tests. The mass of the striker was kept constant at 55.4 kg and the initial velocity varied. In some instances the impact was arranged eccentrically with respect to the centre of the model. The results of the tests are given in Table 2 where e is the horizontal distance along the model's centreline between the centre of gravity and the point of impact. The mass of the model was 39.9 kg.

Test	e (m)	V_o (m/s)	E_o (J)	S
1	0	1.18	78	5.2
2	0	2.33	150	8.5
3	0.24	2.25	140	7.0
4	0.24	2.17	130	7.5
5	0.24	2.63	192	10.6

Table 2 'Wet' Collision Test Results

3. THEORY

Simulation of the tests has been affected by uncoupling the internal and external mechanics.

3.1 Internal Mechanics

The response of the side-shell has been determined using a dynamic elasto-plastic large-deflection analysis technique for a clamped-ended plate-strip. The technique is a Real-Time derivative of Dynamic Relaxation (RTDR) in which both the equations of motion and governing differential equations for equilibrium and kinematics are written in finite difference form. An elastic-perfectly plastic strain-rate sensitive material has been assumed. Yield was determined according to the von Mises criterion, and plastic flow via the Prandtl-Reuss rule. The effect of strain-rate on yield was calculated in accordance with reference[8]. A small parametric study has been performed using this technique on a plate-strip representative of the side-shell in the current models[9]. It showed that for

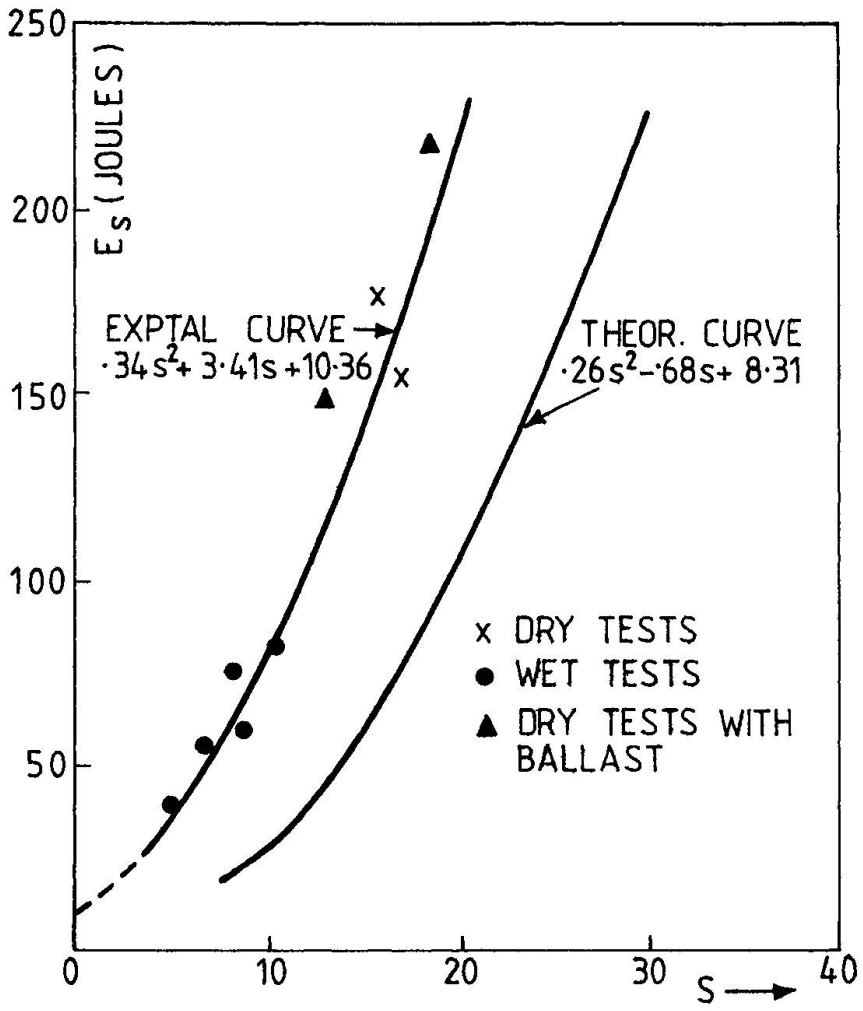

deflections greater than eight times the plate thickness, the permanent set was dictated by the energy of the striker. This led to a permanent set versus energy relationship that could be accurately represented by a parabola. The curve is shown in Fig.3 together with an expression which describes the parabola.

Fig. 3 Comparison of Experimental and Numerical Results

3.2 External Mechanics

Although the struck model after impact exhibited significant rolling, this was not felt to be an important degree of freedom as far as external mechanics were concerned. For this only sway and yaw were considered assuming a right-angled collision. On the basis of the recommendation in ref.[10] since the duration of the impact was short, the added mass for both degrees of freedom has been taken as 0.4. If the total translational and rotational energy of the striker plus the model after impact is considered, it can be shown[11] this is a minimum when the impact is purely plastic, i.e. the velocities of the striker and of the point of contact on the model are the same following impact. In this case, the minimum energy is given by

$$E_m = E_o(1 - \phi) \qquad (1)$$

where E_o is the initial kinetic energy = $\frac{1}{2}MV_o^2$, and

$$\phi = \frac{1}{1 + \mu + \mu(e/r)^2} \qquad (2)$$

μ being the ratio of striker mass to the mass of the model plus added mass, and r^2 the ratio of mass plus added mass moment of inertia to mass plus added mass of the struck model. Assuming no other losses, the energy available for

structural distortion is therefore:

$$E_s = E_o \phi \qquad (3)$$

In order to apply this derivation to the present test series, it is strictly necessary to demonstrate that the velocity of the striker after impact was indeed equal to that of the point of contact on the model. Visual observations indicated that the striker maintained forward momentum after impact but at a reduced velocity which was indeterminable with the particular testing arrangement adopted.

Using equation (3), the wet test results were plotted in Fig. 3 along with the dry test results listed in Table 1. A least squares parabola was fitted to all the tests results except those involving ballast. The close fit to particularly both sets of test data demonstrated by this curve is encouraging except there are at least two different aspects which affect the position of this curve that are compensating. Firstly, if the impact is not entirely plastic then the energy available for structural action will decrease: this will effectively lower the wet test results shown in Fig. 3. Secondly, if the added mass is greater than the value of 0.4 assumed then ϕ will increase thereby effectively raising these same points.

3.4 Comparison Between Experimental and Numerical Results

From Fig. 3 it can be seen that the system describing the numerical behaviour is less stiff than that influencing the experimental response. This stiffness can be found from the second differential of the equations describing the two parabolae. In the previous section most of the energy-absorbing mechanisms affecting the free floating tests were accounted for. The theoretical response can be altered by making allowance for the fact that the numerical model does not represent the section of plate directly above and below the line of contact which, although distorting in a different pattern, clearly absorbs some energy. No distinct pattern of hinges was observed in these regions making comparisons of plastic work done inappropriate. Some simple calculations of the ratio of energy absorbed by the entire panel compared with just that involved in the impact region indicate this may be dependent on the ratio of panel length to the length of impact. This aspect however requires further examination and plans are underway to conduct a complete panel analysis.

Another feature of the numerical modelling which also has to be improved is to extend it beyond the supports into at least a three-bay analysis so that continuity can be more effectively represented. It was reported previously[9] that for behaviour in the plastic range, the presence of rotational restraint at the supports had little effect on the final deflected shape. Of greater importance however is the inplane restraint which can only be correctly modelled by an analysis involving more than one bay. This feature is currently being incorporated into the numerical technique.

4. CONCLUSIONS

Results of both dry and wet collision tests on simple 1:60 scale models of tankers are reported: in two of the dry tests water was present in some of the ballast tanks, including the impacted ones. The striker was a V-shaped rigid bow. Parallel structural analysis studies are also reported and a scheme that allows for added mass effects on the wet models described. From these studies it has been found:

- water in impacted ballast tanks did not appear to have a significant effect on the results, although in one pair of tests where the input energy was almost the same, the permanent set in the ballasted case was 19% less than the non-ballasted results
- by assuming fully plastic impacts and added mass coefficients of 0.4 for both sway and yaw motions for the wet test results, both sets of test data could be fitted by a parabola

- the stiffness of a parabola fitted to numerically derived results for impacts on plate strips was 24% less than that fitted to the test results. No allowance, however, was made in the numerical results for energy absorbed in the sections of plating above and below the line of impact by the bow.

ACKNOLWEDGEMENT

The authors would like to thank NATO (Research Grant No. 26881) and SERC for their financial support. They also thank the technical staff of the Hydrodynamics Laboratory of Glasgow University for their help in performing the experimental part of the work.

REFERENCES

1. SNIDER, W.D.: IMCO Conference on Tanker Safety and Pollution Prevention. Marine Technology, 15, 297(1978).
2. THOMSON, E.T.: Development of a Nuclear Ship Safety Philosophy. Proceedings of Symposium on the Safety of Nuclear Ships, pp 51-60, OECD, France (1978).
3. VERDON, J.: La Convention "POLMAR" de 1973 et la Conference OMCI de Londres de Fevrier 1978. Bulletin Technique du Bureau Veritas, 7-8, 191 (July-August 1978).
4. AKITA, Y., ANDO, N., FUJITA, U. and KITAMURA, K.: Studies on Collision-Protective Structures in Nuclear Powered Ships. Nuclear Engineering and Design, 19, 365(1972), North Holland Publishing Company.
5. SPINELLI, F. and BELLI, V.: Protecteur du compartiment du reacteur nucleaire d'un navire contre les abordages. Resultats de 24 essais sur modeles", AMTA (1971).
6. WOISIN, G.: Conclusion from Collision Examination for Nuclear Merchant Ships in the F.R.G.
7. VAN MATER, P.R., GIANNOTTI, J.G., McNATT, T.R., and EDINBERG, D.C.: Vessel Collision Damage Resistance. Report CG-D-21-80 US Coast Guard.
8. JONES, N.: Response of Structures to Dynamic Loading. Int. Phys. Conf. Ser. No. 47, Chapter 3, pp 254-276 (1979).
9. SAMUELIDES, E. and FRIEZE, P.A.: Strip Model Simulation for Low Energy Impacts for Flat Plated Structures. To be presented in the Structural Crashworthiness Symposium.
10. MOTORA, S., FUJINO, M., SUGIURA, M. and SUGITA, M.: Equivalent Added Mass of Ships in Collisions. JSNA Japan, vol. 126(December 1969).
11. SAMUELIDES, E.: Ship Tanker Model Collisions. Ph.D. Thesis, Department of Naval Architecture and Ocean Engineering, University of Glasgow. (in preparation).

Leere Seite
Blank page
Page vide

Choc de bateau sur obstacle déformable

Zusammenstoß eines Schiffes mit einem verformbaren Hindernis

Impact of a Ship on a Ductile Obstacle

Jacques FAUCHART
Consulting Engineer
de. Setec/
Paris, France

Born in 1936
Engineer EP, ENCP
Lecturer at the
Ecole Nationale des Ponts et Chaussées in Paris
(Road and bridge building)

RÉSUMÉ
On étudie, dans l'hypothèse élastique, le comportement d'une structure »offshore« frappée par un bateau, avec référence aux rares résultats d'essais connus.

ZUSAMMENFASSUNG
Gegenstand der Untersuchung ist das elastische Verhalten einer Offshore-Konstruktion beim Aufprall eines Schiffes unter Verwendung der wenigen bekannten Versuchsergebnisse.

SUMMARY
The subject of this study is the elastic behaviour of offshore construction after a ship collision, with reference to the rare test results known.

0. PRESENTATION

0.1 On prévoit de franchir l'estuaire de la Gironde, à 75 Km en aval de Bordeaux (fig 1) par un pont long de 10 Km comprenant :
- 2 viaduc d'accès, à 2%, par travées de 100 m
- et au centre un pont à haubans à 3 travées de 400 m de portée centrale, libérant un chenal de 300 m de large, 55 m de haut et 12 m d'eau (fig 2) [I]

0.2 Un des problèmes majeurs de l'étude, est celui des conséquences du choc d'une de ses 2 piles principales (sous pylônes), par un bateau, dont le plus agressif a pour caractéristiques :
- déplacement (masse totale en charge) m_1 = 80 000 t
- vitesse absolue V_1 = 15 noeuds (12 propre + 3 de courant) soit 7,72 m/s
- et donc énergie cinétique : $E = \frac{1}{2}\ 80\ (7{,}72)^2 = 2\ 400$ mMN

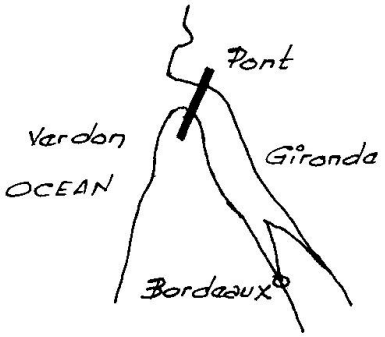

Fig. 1

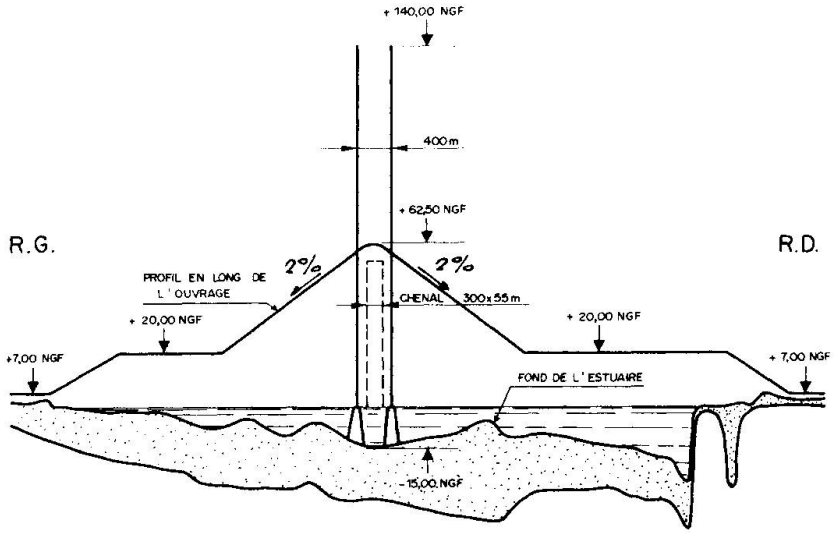

Fig. 2

Cette énergie est énorme : Pour en juger, rappelons que les "ducs d'Albe" les plus perfectionnés n'absorbent que le mMN [II et III] . La proximité du port du Verdon ne permet guère d'envisager des protections souples, par chaines flottantes, à ancrages fixes ou trainables (tels les filets d'arrêt sur porte-avions); leur efficacité exige de grands déplacements. Les employer ici reviendrait presque à barrer la Gironde dès l'entrée de son estuaire.

I. LE BATEAU-TYPE ADOPTE

En utilisant :
- d'une part la relation empirique de Minorsky, proportionnant l'effort $F_1(x)$ subi par le bateau écrasé sur la longueur x, et la variation $\frac{dA}{dx}$ à ce niveau du volume A(x) d'acier résistant du navire
- d'autre part la loi A(x) définie par les Chantiers de l'Atlantique pour un bateau de la taille à envisager (le "Cetra-Columba"), nous avons obtenu pour un choc frontal la loi $F_1(x)$ de la figure (3), schématisable par la relation plastique-pseudo élastique : $F_1(x) = F_0 + r_1 x$ où :
- l'effort : F_0 = 39 MN correspond à l'écrasement de l'étrave
- et la pseudo-rigidité : r_1 = 1,62 MN/m à la force nécessaire pour amener l'écrasement supplémentaire d'une tranche courante de longueur-unité.

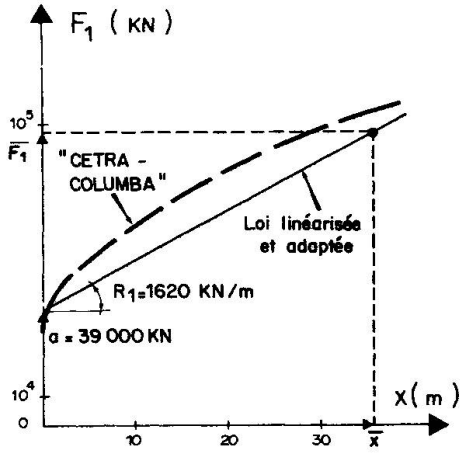

Fig. 3

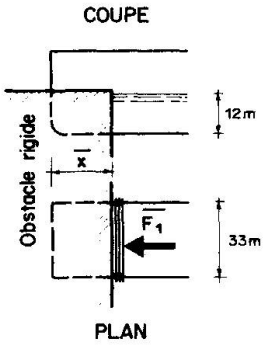

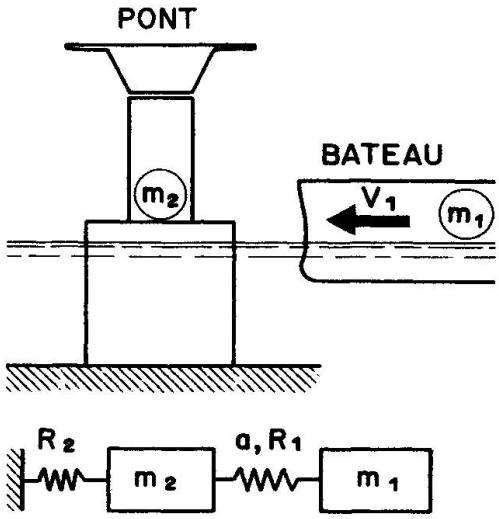

Fig. 4

II. CHOC DIRECT DU BATEAU-TYPE (1) SUR UNE PILE DE PONT (2)

II.1 Le problème est simplifié comme à 2 degrés de liberté seulement (fig 4) :
- le déplacement $D_1(t)$ du centre de gravité du bateau
- et celui, $D_2(t)$, du point d'impact sur la pile (de masse m_2 et rigidité r_2) que nous mesurons à partir du début du choc (t=o).

Le bateau s'écrase donc sur la longueur : $x = D_1 - D_2$

Nous négligeons (c'est défavorable) les phénomènes d'amortissement. Seules les forces d'inertie (de la forme : $-m_i D_i''$) (1) peuvent donc compenser le déficit entre les forces extérieures appliquées aux2 corps. D'où l'équilibre :

- du bateau : $F_1(t) + m_1 D_1'' = 0$ ①
- de la pile : $F_2(t) - F_1(t) + m_2 D_2'' = 0$ ②

II.2 Si la pile est indéformable (r_2 infini ; $D_2 = 0$; $D_1 = x$) et si la loi du bateau $F_1(D_1)$ est monotone, l'effort commun subi par la pile et le navire est maximum ($\bar{F}_1$) avec D_1, c'est-à-dire quand sa vitesse D'_1, s'annule. Alors son énergie cinétique s'est dissipée en travail de déformation, soit pour le "bateau type" considéré :

$$\frac{1}{2} m_1 V_1^2 = \int F_1(x)\,dx = \frac{1}{2 r_1}\left(\bar{F}_1^2 - F_o^2\right)$$

$$\bar{F}_1 = \sqrt{F_o^2 + r_1 m_1 V_1^2} = 96,2\ MN \quad ④$$

le bateau s'écrase sur la longueur : $\bar{x} = \frac{1}{r_1}(\bar{F}_1 - F_o) = 35,3\ m$ ⑤

Ces valeurs montrent bien qu'on ne peut considérer le bateau comme rigide ; on peut en revanche négliger la part élastique de sa déformation.

II.3 Pour une pile élastique ($F_2(t) = r_2 D_2(t)$), il faut distinguer 2 phases successives dans la percussion par le "bateau-type" :

II.3.1 Au début ($0 < t \leqslant t_o$ tel que $F_1(t) \leqslant F_1(t_o) = F_o$) : le bateau entraîne la pile ($D_1 = D_2 = D$) qui reste élastique. L'équilibre s'écrit :

$$(m_1 + m_2)\, D'' + r_2 D = 0$$

(1) L'accent désigne la dérivée par rapport au temps t.

Par ailleurs, comme le bateau se comporte comme un solide rigide ($x(t) = D_1(t) - D_2(t) = 0$), il y a conservation de la quantité de mouvement globale au moment du choc. Les conditions aux limites ($t = +0$) sont donc :

$$D_1(0) = D_2(0) \qquad \text{et} \qquad D_1'(0) = D_2'(0) = \frac{m_1}{m_1+m_2} V_1$$

D'où, avec : $\Omega^2 = \frac{r_2}{m_1+m_2}$: $D_1(t) = D_2(t) = \frac{m_1 V_1}{m_1+m_2} \frac{\sin \Omega t}{\Omega}$

$$F_2(t) = r_2 D_2(t) = m_1 V_1 \Omega \sin \Omega t \quad ; \quad F_1(t) = \frac{m_1}{m_1+m_2} F_2(t)$$

Malheureusement, en pratique, aucune pile n'est assez souple et lourde pour qu'on en reste là. Cette première phase s'achève donc à l'instant t_0 où le bateau commence à s'écraser. Alors :

$$D_1(t_0) = D_2(t_0) = \underline{D_0} = \frac{F_0}{r_2} \frac{m_1+m_2}{m_1} \quad ; \quad D'(t_0) = \underline{D_0'} = \frac{m_1 V_1}{m_1+m_2} \sqrt{1 - \frac{F_0^2}{r_2 m_1 V_1^2} \left(\frac{m_1+m_2}{m_1}\right)^3}$$

II.3.2 Ensuite ($t_0 < t$) le bateau s'écrase : $F_1(t) = F_0 + r_1 [D_1(t) - D_2(t)]$

(2) et (3) s'écrivent : $\begin{bmatrix} m_1 & 0 \\ 0 & m_2 \end{bmatrix} \begin{Bmatrix} D_1''(t) \\ D_2''(t) \end{Bmatrix} + \begin{bmatrix} r_1 & -r_1 \\ -r_1 & r_1+r_2 \end{bmatrix} \begin{Bmatrix} D_1(t) - D_0 \\ D_2(t) - D_0 \end{Bmatrix} = F_0 \begin{Bmatrix} -1 \\ +1 \end{Bmatrix}$

D'où par l'analyse modale :

- les pulsations propres ω_K par :

$$\omega^4 - \omega^2 \left(\frac{r_1}{m_1} + \frac{r_1+r_2}{m_2}\right)^K + \frac{r_1 r_2}{m_1 m_2} = 0 \qquad (\omega_1 < \omega_2)$$

- les vecteurs propres, normés par rapport au masses :

$$d_1^K = \left[m_1 + m_2 \left(1 - \frac{m_1 \omega_K^2}{r_1}\right)^2\right]^{-1/2} \quad ; \quad d_2^K = d_1^K \left(1 - \frac{m_1}{r_1} \omega_K^2\right)$$

D'où, compte tenu des conditions aux limites ($t = t_0$) et en posant :

$$A_K = F_0 \frac{m_1}{r_1} \left(d_1^K\right)^2 \; ; \quad B_1 = D_0' \frac{\omega_2^2}{\omega_1 (\omega_2^2 - \omega_1^2)} \; ; \quad B_2 = -B_1 \left(\frac{\omega_1}{\omega_2}\right)^3$$

$$\begin{Bmatrix} D_1(t) - D_0 \\ D_2(t) - D_0 \\ F_1(t) - F_0 \\ F_2(t) - r D_0 \end{Bmatrix} = \begin{bmatrix} 1 & 1 \\ 1 - \frac{m_1}{r_1} \omega_1^2 & 1 - \frac{m_1}{r_1} \omega_2^2 \\ m_1 \omega_1^2 & m_1 \omega_2^2 \\ r_2 \left(1 - \frac{m_1}{r_1} \omega_1^2\right) & r_2 \left(1 - \frac{m_1}{r_1} \omega_2^2\right) \end{bmatrix} \begin{Bmatrix} -A_1 (1 - \cos \omega_1 (t - t_0)) + B_1 \sin \omega_1 (t - t_0) \\ -A_2 (1 - \cos \omega_2 (t - t_0)) + B_2 \sin \omega_2 (t - t_0) \end{Bmatrix}$$

II.3.3 Exploitation numérique:

En pratique, la première phase a une durée t_0 très courte. Dans la deuxième, les termes en ω_K atteignent leurs valeurs maximales à des temps t_K voisins de :

- t_1 tel que $\operatorname{tg} \omega_1 (t_1 - t_0) = \frac{D_0'}{F_0} \sqrt{r_1 m_1}$ pour $K = 1$
- $t_2 \simeq t_0 + \frac{\pi}{2} \sqrt{\frac{m_2}{r_2}}$ $K = 2$

C'est donc très vite (à peu près à t_2) que la pile va recevoir une gifle magistrale, en subissant son effort maximal :

$$F_{2M} \simeq \overline{F_2} = F_0 \frac{m_1+m_2}{m_1} + D_0' \sqrt{r_2 m_2}$$

Le bateau est alors presque intact. Ce n'est que bien plus tard (vers t_1, et alors que la vibration de la pile s'est pratiquement amortie) que le bateau finirait de s'écraser sous un effort :

$$F_{1M} \simeq \overline{F_1} = \sqrt{F_0^2 + r_1 m_1 V_1^2}$$

et sur une longueur de : $x_M \simeq \overline{D_1} = D_0 + \overline{x_c}$

Par exemple, pour une pile (courante) : $r_2 = 10^6$ kN/m, et m_2 = 2 000 t, on obtient, avec V_1 = 7,72 m/s :

a - t_0 = 0,005 sec, temps où D_0 = 0,04 m et D_0' = 7,5 m/s

b - la pile subit son effort maximal: F_{2M} = 377 MN, à t_2 = 0,075 sec, en étant déplacée de D_2 = 0,38 m seulement

c - ce n'est qu'à $t_1 \simeq 8$ sec que le bateau finirait de s'écraser, sous F_{1M} = 94 MN, et sur $x_M \simeq 34$ m

Mais en réalité, compte-tenu de l'énormité de l'effort F_{2M} qui lui a été appliqué, la pile se sera rompue (ou aura basculé) avant t_2, c'est-à-dire très peu après le début du choc, et alors que le bateau est encore très peu abimé comme on le constate le plus souvent dans les accidents réels.

II.3.4 Conclusions :

Le balayage des plages (m_2 et r_2) des piles envisageables en pratique montre qu'aucune n'est capable de résister isolément au choc du bateau type à considérer.

Augmenter sa résistance fait croître parallèlement sa raideur et sa masse, et donc l'effort F_{2M} à supporter, sans espoir de convergence (action - résistance) dans le cadre technico-économique actuel.

Nous en avons conclu que, compte tenu de la profondeur limitée du fleuve, la seule solution sûre et réaliste pour protéger chacune des 2 piles principales du pont est de l'abriter au sein d'une île artificielle destinée à diffuser l'impact, jusqu'à ne plus agresser la fondation que de façon tolérable.

III. CHOC DE BATEAU SUR UN TALUS (berge naturelle ou île artificielle)

III.1 Essai d'analyse :

Lors du choc, le bateau pénètre dans le talus, dont il refoule le sol par butée. Pour être assuré de la stabilité de la pile qui y est enterrée, il est prudent de respecter les 2 conditions géométriques suivantes (fig 5) :

- le sommet, non écrasé, de son étrave, ne doit pas heurter la pile
- la fondation de celle-ci doit rester hors zones de sol en butée

La masse m_2 de sol mise en mouvement reste assez faible par rapport à celle, m_1 du bateau, pour sembler permettre, en première approximation, de négliger aussi bien la force d'inertie ($-m_2 D_2''$) du sol que la redistribution des vitesses au début du choc.

Dès lors (2) et (3) fusionnent en : $F_1(t) = F_2(t) = -m_1 D_1''(t)$

L'effort maximal F_{2M} subi par le talus restera donc inférieur à la valeur maximale $\overline{F_1}$ (4).

D'autre part, les maximaux des 2 déplacements D_K et forces F_K subis par le bateau (K=1) et le talus (K=2) sont obtenus simultanément, quant s'annulent les vitesses D_K'. L'énergie cinétique initiale du bateau s'est alors transformée en travail de déformation W_K, soit (fig 6) :

$$\frac{1}{2} m_1 V_1^2 = W_1 + W_2 = \frac{\overline{F}^2 - F_0^2}{2 r_1} + \int_0^{D_2} F_2 \cdot dD_2$$

$$W_2 = \int_0^{D_2} F_2(D_2)\, dD_2 = \frac{1}{2 r_1} (\overline{F}^2 - F_0^2)$$

D'où le maximum F_M de l'effort commun bateau - talus, à l'arrêt dans le sol (puis D_2 et D_1).

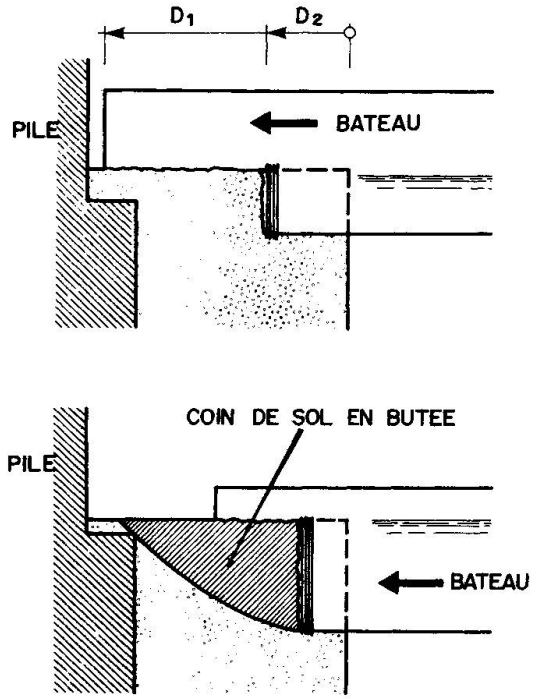

Fig. 5

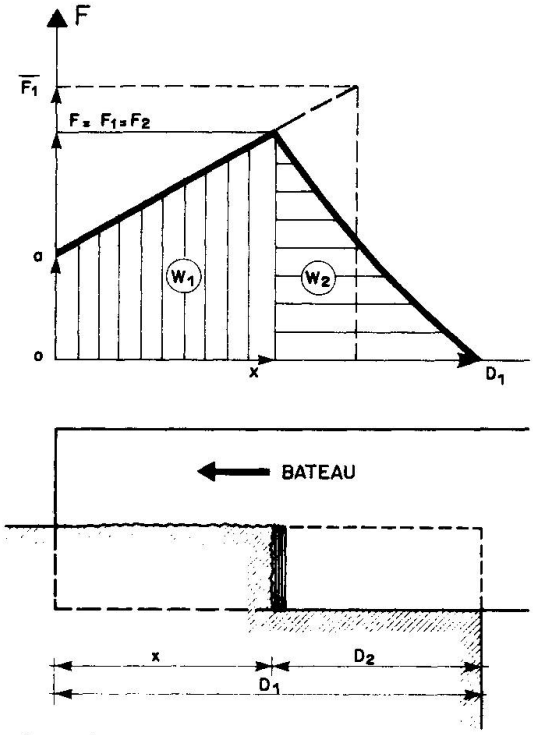

Fig. 6

III.2 Application au projet du Verdon

III.2.1 Ce qui précède n'est qu'approximatif (négligence des effets dynamiques dans le sol ; conditions aux limites). Mais nous manquons cruellement à cet égard de résultats expérimentaux, surtout pour estimer la loi F_2 (D_2) du talus, car on ne connait pas le faciès d'attaque du bateau, variant à mesure que celui-ci s'écrase.

Dans le cas du Verdon, nous avons fait l'hypothèse (certainement trop conservatrice) que le bateau avait une géométrie indéformable, et qu'il repousse, devant sa paroi frontale (barge à front plat) ou ses 2 parois d'étrave, un (ou 2) coins de terre (butée de Coulomb), normalement à ces parois.

II.2.2 D'où notre solution d'iles artificielles, allongées suivant l'axe du chenal (fig 7), pour :

a - faciliter l'écoulement du fleuve, et donc limiter les affouillements
b - s'adapter à la puissance des chocs à redouter :
  - les plus à craindre sont évidemment ceux de bateaux à pleine vitesse V_1, s'écartant assez peu de l'axe du chenal pour frapper quasiment de front les petits pans de l'ile.
  - ses longs pans sont menacés par les bateaux connaissant, peu avant leur passage sous le pont, une panne de barre en position de rotation, qui les rend ingouvernables. Mais en ce cas, l'eau dans laquelle tourne le bateau le ralentit, et le fait attaquer les longs pans sous vitesse initiale réduite.

Le coût des 2 iles (à talus de 5/1 et de 2/1) représente environ 10% du prix total de l'ouvrage. Une variante réduite, car à parements verticaux, réalisés par remplissage en sable de grands sacs en plastique, voire par un procédé inspiré de la "terre armée", reste néanmoins en compétition.

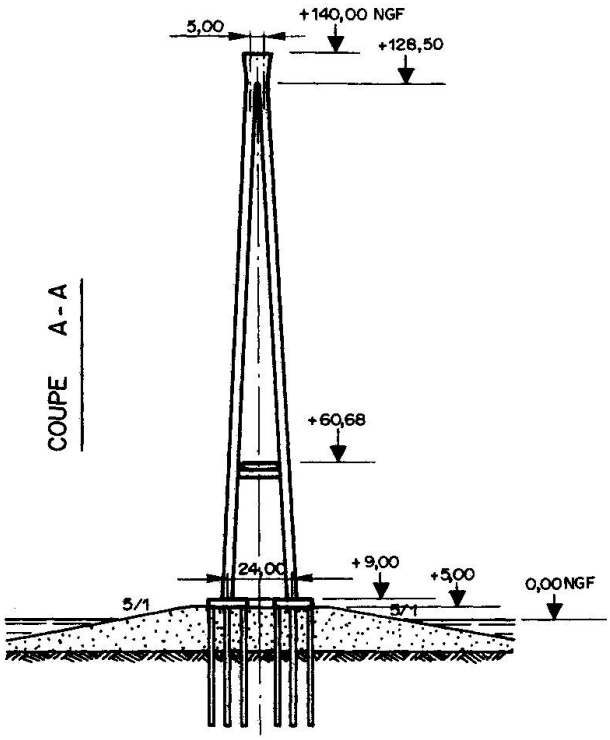

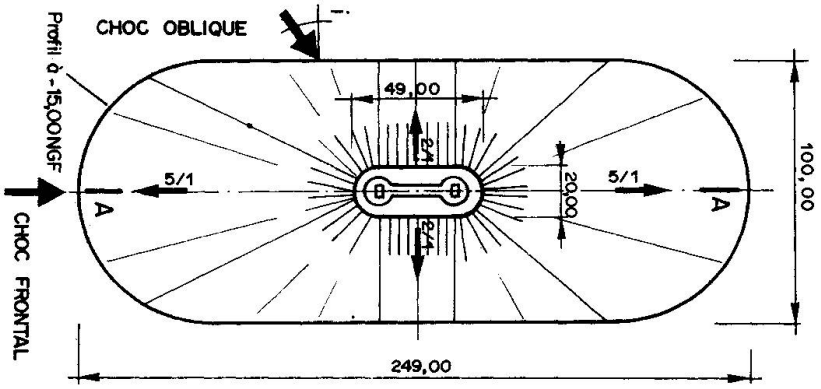

Fig. 7

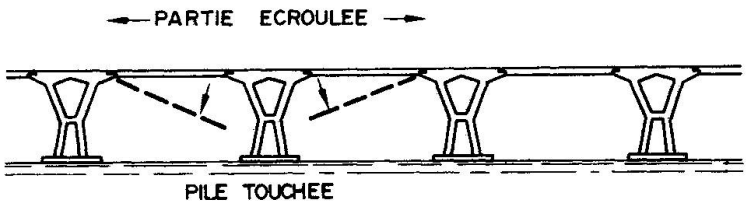

Fig. 8.1

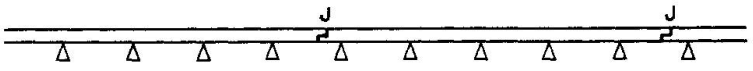

Fig. 8.2

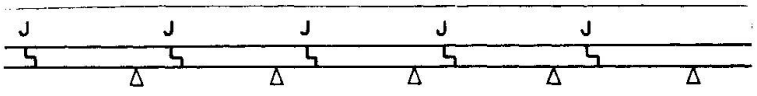

Fig. 8.3

IV CONSEQUENCES DU RISQUE DE CHOC DE BATEAUX POUR LE PROJET DU PONT DU VERDON

IV.1 Généralités - Partie centrale, sur chenal

C'est cette question qui a déterminé l'architecture générale du projet. Pour laisser le chenal (de 300 m) libre à la navigation en toute circonstance, de façon à ne pas asphyxier, en amont, le port de Bordeaux, nous avons choisi :

a - de concentrer la protection sur les 2 piles principales encadrant la passe, en les enterrant dans 2 iles artificielles, dont l'encombrement a fait porter la travée centrale à 400 m.
b - de limiter les conséquences qu'entrainerait la rupture, par choc, de toute autre pile du pont. On ne peut en effet économiquement envisager de toutes les protéger par des iles (qui , d'autre part, barreraient l'écoulement de la Gironde) Pour assurer la stabilité de l'ouvrage, même en cas de rupture d'une de ses 2 piles-culées d'extrêmité (n'empêchant donc plus le soulèvement du tablier) chacune des 2 travées de rive à dû être allongée à environ 200 m .

IV.2 Viaducs d'accès à l'ouvrage principal

Leur schéma statique est "cantilever" pour que la rupture éventuelle d'une pile courante n'entraîne que la chute du tronçon qu'elle porte, et des 2 travées indépendantes adjacentes, sans risque de propagation en chaîne à l'ensemble du tablier.

Un tel dispositif (cf les "fusibles" de nos installations électriques) a prouvé son efficacité lors de la rupture d'une pile du pont de Maracaïbo (1964, pétrolier, m_l = 47 000 T) (fig 8.1) et de 2 piles du pont de Hobart (1975, minéralier m_l = 17 000 t).

Les conséquences de la rupture d'une pile d'un pont continu (fig 8.2) seraient bien plus graves, puisqu'elle entraînerait l'effondrement de plusieurs centaines de mètres de tablier, et la nécessité d'en réparer le reste (mais comment?).

A l'inverse, la conception la moins admissible est évidemment celle d'un tablier isostatique sans "coupe-circuit" (fig 8.3) dont la rupture d'une seule pile entrainerait inéluctablement l'effondrement en chaîne de l'entière longueur du tablier.

REFERENCES

[I] J. FAUCHART : Choc de bateau sur un obstacle déformable : essai d'analyse pour l'étude de "faisabilité" du pont du Verdon sur la Gironde (Travaux, janvier 1982)

[II] DERUCHER et HEINS : Bridge and pier protective systems and devices (Dekker-New York - 1979)

[III] N. JONES : A litterature Survey on the collision and grounding protection (SCC 283 - United States coast guard - Washington - 1979)

[IV] J. FAUCHART : Choc de bateau sur obstacle déformable (présent congrès)